VNIVERSITAT DE VALÈNCIA

Facultat de Medicina i Odontologia
Programa 3139 Departament de Medicina

Mecanismos de resistencia primaria y secundaria a tratamiento antiHER2 en cáncer gástrico HER2 positivo

Tesis Doctoral presentada por:
Valentina Gambardella

Directores:
Prof. Andrés Cervantes Ruipérez
Dra. Josefa Castillo Aliaga

Enero, 2018

This thesis has been supported by the founding received by Valentina Gambardella form the INCLIVA Biomedical Research Institute and the grant awarded by the European Society of Medical Oncology.

To those who can read beyond the lines.

Index

3.3 Assess potential mechanisms related to acquired resistance among the resistant generated cell lines. **(Aim 3)**

3.3.1 Protein expression assessment analysed by Western Blot

3.3.2 Protein phosphorilation analysis performed by ELISA Pathscan Array

3.3.3 Mutational Analysis by Sequenom MassArray

3.3.4 Epithelial Mesenchymal transition evaluation

3.3.5 Evaluation of stem cells characteristics

3.3.6 Identification of differentially expressed genes by transcriptome analysis

3.4 Perform a functional analysis of the alterations identified in acquired resistant models. **(Aim 4)**

3.4.1 Pharmacological inhibition

3.4.2 RPS6 gene silencing by small interfering RNA transfection

3.5 Translation of findings *in vivo* using immunodeficient mice models. **(Aim 5)**

3.6 Confirm if the described alterations can play a role in resistance in gastric cancer patients. **(Aim 6)**

4. **Conclusions**

5. **Summary**

6. **References**

7. Supplementary material

Abbreviations

AKT	Protein kinase B
CSC	Cancer stem cells
CT	Chemotherapy
DMSO	Dimethyl sulfoxide
EBV	Epstein Barr Virus
EGFR	Epidermal growth factor receptor 1 , HER1
EGJ	Esophago-gastric junction
EMT	Epithelial Mesenchymal Transition
ERK	Extracellular Signal-regulated Kinase
FACs	Fluorescence activated cell sorting
FBS	Fetal Bovine Serum
GC	Gastric Cancer
HER 2	Human Epidermal Growth Factor receptor 2
HER3	Human Epidermal Growth Factor receptor 3
HR	Hazard Ratio
IGFR	Insuline growth factor receptor
IHC	Immunehistochemestry
JM	Justa Membrane
MET	Tyrosine-protein kinase Met or hepatocyte growth factor receptor (HGFR)
MSI	Microsatellite Instable
MSS	Microsatellite Stable
MTT	MTT 3-(4,5-dimethylthiazol-2-yl)-2,5-diphenyltetrazolium bromide
NCI	NCI N87
OE	OE 19
OS	Overall Survival
PBS	Phosphate-Buffered Saline
PFS	Progression Free Survival
RPS6	Ribosomial protein S 6
RT-qPCR	Quantitative reverse transcriptase-PCR assays
TBS	Tris-buffered saline
TTBS	Tween-Tris-buffered saline
TyK	Tyrosine Kinase

INTRODUCTION

1.1 Background

Gastric cancer (GC) is a global health issue and the third leading cause of cancer related death worldwide. Over one million of new cases are diagnosed each year and more than 70% occurs in developing countries, especially in East Asia. Gastric Cancer incidence is higher in men rather than in women (2:1). The typical age at diagnosis is ~60 years, but recently the incidence in younger population has increased (1).

In 2012, GC was diagnosed in approximately 951,000 individuals and led to deaths of 723,000 people worldwide. This disease is characterized by a relevant global variation in incidence with a peak in Japan and South Korea while the lowest incidence is observed in the United States, Canada, India and a few Middle Eastern countries. The reasons for such differences are multiple and complex and include genetic susceptibility, strains of *H. pylori* and dietetic factors. Due to the high incidence, in Japan, screening strategies proposed to high-risk populations, were adopted and they have resulted in a dramatic shift in stage at diagnosis and a reduction in GC-related mortality. Nevertheless, in the Western Countries, no screening program are widely available and the incidence of cardia GC has increased dramatically (2,3). *H. pylori* infection plays a relevant role in the incidence of this tumour and about 10% of patients with GC presents an Epstein Barr Virus (EBV) infection (4).

Several non-infectious factors, such as salty food intake; consumption of poorly preserved, smoked or chronically pickled foods; consumption of foods contaminated with aflatoxin, nitrates and fungi; pernicious anemia; and smoking are associated with GC (5,6).

Gastric cancer high mortality can be attributed to both the absence of significant symptoms in the early stages and the lack of validated screening programs in Western countries. As consequence, most of the cases are diagnosed at an advanced stage, which related with a poor prognosis.

Chemotherapy (CT) remains the main treatment for advanced disease but, despite new advances, median overall survival (OS) is about 12 months (7).

Thus, there is an urgent need for new treatments and strategies to improve outcomes. However, although multiple targeted agents are under investigation, so far, only trastuzumab and ramucirumab have demonstrated efficacy in advanced GC and have a regulatory approval (8,9).

Classic pathologic classification

During the 60's Lauren classified gastric adenocarcinoma into two main subgroups, intestinal and diffuse, according to different microscopic features. (**Fig.1**) (10).

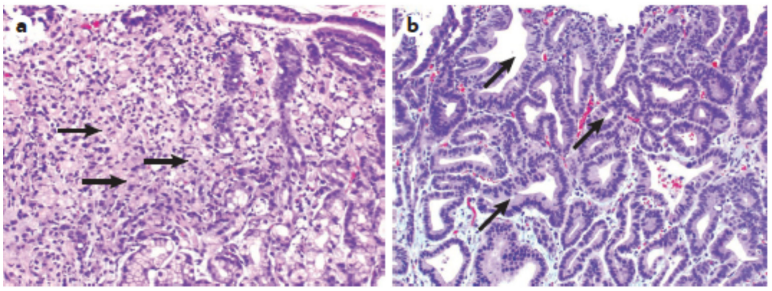

Figure 1. Histological classification of gastric adenocarcinoma. a. Diffuse-type gastric adenocarcinoma. **b.** Intestinal-type gastric adenocarcinoma. *Ajani, J. A. et al. Gastric adenocarcinoma. Nat. Rev. Dis. Primers 3, 17036 (2017).*

Nowadays, the recommended WHO pathological classification for GC considers several subtypes, basing on optical microscopy features, identifying tubular, papillary, mucinous and poorly cohesive (including signet ring cell carcinoma), plus uncommon histologic variants (11). These classifications, although commonly used in pathology reports, do not have any predictive value.

1.2 Molecular classification of Gastric Cancer

Despite the introduction and validation of new combination regimen of

chemotherapy, prognosis of patients diagnosed with advanced disease is very poor. For this reason, the identification of specific targets which could be susceptible for drug inhibition, is urgent. Personalized medicine represents up to know probably the only approach to try to control cancer progression. During last years among all solid tumors many efforts have been done to identify molecular alterations to evaluate new treatment strategies.

In an elegant analysis, 22 recurrent genomic alterations were firstly identified in GC samples. A part from the detection of already known deregulated pattern, such as ERBB2 and FGFR2, amplification of relatively not explored proteins, like KLF5 and GATA6, were also identified. In this experiment, FGFR2, KRAS, ERBB2, EGFR and MET were observed to be frequently amplified in a mutually exclusive manner (12). (**Fig.2**)

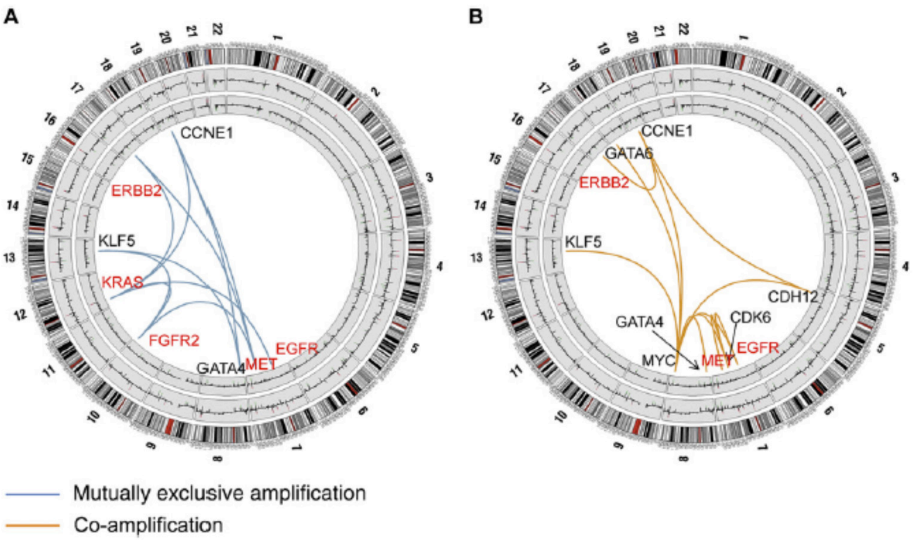

Figure 2. Mutually exclusive and co-amplified genomic. (A) Focal regions exhibition mutually exclusive patterns of genome amplification. (B) Focal regions exhibiting patterns of genomic co-amplification. Orange lines indicate pairs of focal regions (genes) exhibiting significant patterns of genomic co-amplification identified by DRP analysis ($p<0.05$). *A comprehensive survey of genomic alterations in gastric cancer reveals systematic patterns of molecular exclusivityand co-occurrence among distinct therapeutic targets Niantao Deng, et al., GUT 2012*

A relevant contribution concerning the comprehension of gastric cancer biology was given by the Comprehensive Genomic Analysis of GC developed by The Cancer Genome Atlas Research Network (TGCA) (13). This analysis focused on gene mutations, somatic copy number alterations, structural variants, epigenetic and transcriptional changes involving mRNAs and noncoding RNAs, as well as proteomic changes were studied with the aim to propose different molecular patterns. The ATLAS TGCA according to the underlined characteristics, proposed GC to be classified into four major subgroups: Epstain Barr (EBV)-infected, MSI tumours, genomically stable and chromosomally unstable tumours (CIN) according to the detectable prevalent alteration.

The EBV subgroup was so defined due to the evidence of high EBV burden and showed extensive DNA promoter hypermethylation. The second group was defined for being enriched for MSI and characterized by elevated mutation rates and hypermethylation, including hypermethylation at the MLH1 promoter. The third group, defined by the lack of molecular alterations was defined as genomically stable. Lauren diffuse subtype seems to belong prevalently to this group. The fourth group included chromosomally unstable tumours and could be recognized by the presence of extensive somatic copy-number aberrations.

According to mutational analysis, in the EBV group was detected a strong presence of PIK3CA ARID1A and BCOR mutations and only rare TP53 mutations. In hypermutated tumors, several mutated genes, including TP53, KRAS, ARID1A, PIK3CA, ERBB3, PTEN and HLA-B were identified. Among non-hypermutated tumours, several mutated genes were observed such as TP53, ARID1A, KRAS, PIK3CA and RNF43, but also genes involved in the b-catenin and TGF-β pathway. CDH1 somatic mutations were enriched in the genomically stable or diffuse subtype.

Evaluating targetable mutations is possible to conclude that EBV-positive tumours emerged to express PIK3CA mutations and recurrent JAK2 and ERBB2

amplifications. Mutations in PIK3CA, ERBB3, ERBB2 and EGFR, with many mutations at 'hotspot' sites were underlined also in MSI tumours. In CIN tumours, genomic amplifications of RTKs, many of which are amenable to blockade by therapeutics in current use or in development were detected. Recurrent amplification of the gene encoding ligand VEGFA was notable given the gastric cancer activity of the VEGFR2 targeting antibody. The strength of IL-12 mediated signalling signatures in EBV-positive tumours suggests a robust immune cell presence. When coupled with evidence of PD-L1/2 overexpression, this finding adds rationale for testing immune checkpoint inhibitors in EBV-positive gastric cancer.

The Asian Cancer Research Group (ACRG) proposed a similar analysis in more than 200 GC samples, to derive a new classification of molecular subtypes able to predict prognosis (14). Two different GC group, Microsatellite Instable (MSI) and Microsatellite Stable (MSS) tumors, were firstly identified. The MSS group was further divided into two subtypes: MSS/EMT (with epithelial-mesenchymal transition features), defined by a lower number of mutations, and the MSS/epithelial. This last group was also divided into TP53 mutant and TP53 wild type. TP53 no mutant tumors had a high prevalence of APC, ARID1A, KRAS, PIK3CA and SMAD4 mutations. When these molecular features were correlated with clinical characteristics, it was observed that MSS/EMT tumors occurred at younger age and correlates with Lauren diffuse type. On the other hand, the MSI subtype was frequently located in the antrum, more than the half of patients had an intestinal histology and early stage predominated at diagnosis (I/II). EBV infection was mainly seen in the MSS/TP53 mutant group. When a survival analysis was performed, there were substantial differences among the four groups. In particular, MSI subtype had the best prognosis, followed by MSS/TP53 mutant and MSS/TP53 wild type, while the MSS/EMT subtype was related to the worst survival. When the first site of relapse was investigated, it was also revealed that peritoneal metastases were more frequent in patients diagnosed with MSS/EMT group, while a high percentage of liver limited metastasis was detected in patients belonging to the MSI subgroup. According to these data, this model moreover establishes a prognostic stratification of GC. (**Fig.3**)

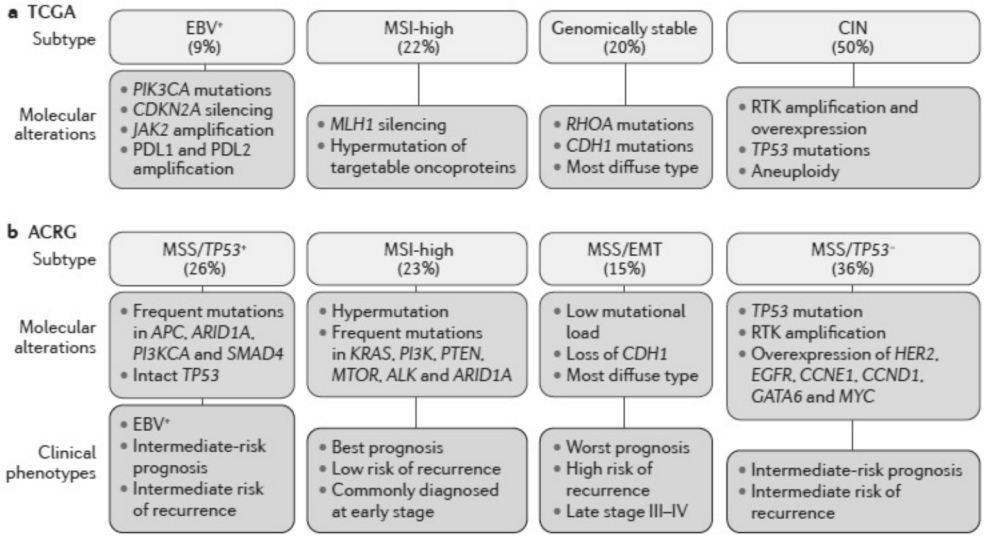

Figure 3. Molecular classification of gastric adenocarcinoma. a. The Cancer Genome Atlas (TCGA) Research Network analysis identified four molecular subtypes of gastric adenocarcinoma (GAC) -Epstein-Barr virus-positive (EBV^+) tumours; microsatellite instability (MSI)-high tumours; genomically stable tumours; and tumours with chromosomal instability (CIN). **b.** The Asian Cancer Research Group (ACRG) identified four subtypes of GAC that also provided useful clinical information. *Ajani, J. A. et al. Gastric adenocarcinoma. Nat. Rev. Dis. Primers 3, 17036 (2017).*

Despite being inspiring and trying to better define gastric cancer, these important molecular classifications cannot still be used as clinical practice to personalize treatment. The identification of molecular features of GC led to the discovery of specific intracellular pathways and driver genes that contribute to carcinogenesis. As in other solid tumours, the use of targeted agents that block these signaling pathways has recently emerged as a strategy for the treatment of advanced GC. Targeted agents may be used either alone or in combination with cytostatic drugs. Unfortunately, despite the evidence of such alterations, up to now, only HER2 and angiogenesis were detected as target for treatments.

The anti HER2 antibody trastuzumab and the anti VEGF ramucirumab have been shown to improve survival in advanced GC patients (8,9).

1.3 HER2 evaluation

HER2 amplified gastric cancer account for about 7-14% of all advanced gastric cancers. The frequency of overexpression of HER2 is slightly greater for cancers localized at the gastroesophageal junction rather than the stomach. HER2 amplification changes among the different histologic types and it seems to be related even with grading of differentiation, in particular HER2 amplified tumors are almost all well or moderately differentiated intestinal type (10).

HER2 is the only validated biomarker routinely tested in mGC, and trastuzumab in combination with doublet platinum-based chemotherapy represents the gold standard for patients with IHC 3+ or 2+/ISH+ tumors (8). Significant increases in progression-free survival, time to progression and objective response were reported in patients who received trastuzumab. An exploratory post-hoc analysis showed that the overall survival benefit was substantially higher among patients with high HER2 expression (defined as immunohistochemistry 2+ and a FISH-positive result, or immunohistochemistry 3+, regardless of FISH status) versus low (immunohistochemistry 0 or 1+ and FISH-positive) (16).

Even if trastuzumab has significantly improved the outcomes of HER2-positive mGC patients, primary and acquired resistance to treatment are relevant challenges narrowing its therapeutic index. In HER2-positive breast cancer, the molecular mechanisms of trastuzumab resistance have been extensively investigated. However, up to know, no treatment able to revert resistance has been introduced in clinical practice. Nevertheless, HER2-positive gastric and breast cancers should be considered different diseases for several reasons. From a biological point of view, HER2 positivity is more heterogeneous in GC at both intra- and inter lesional level (15) and HER2 amplification may also be coupled with other co-existing oncogenic drivers. Of note, in silico studies and analyses carried out in retrospective patient series showed that oncogene amplifications are not mutually exclusive as it was thought initially (12), but HER2 gene may be co-amplified with EGFR or MET.

Receptor co-amplifications and several other putative mechanisms of primary resistance to trastuzumab - such as PI3K/PTEN and MET/HER3 mutations - have been found in HER2-positive primary GC patients' samples and were preclinically validated. Therefore, HER2 addicted GCs might be easily identified not only by the presence of an intense and relatively more homogeneous HER2 staining, but also by the concomitant absence of other relevant oncogenic drivers. From a clinical point of view, HER2 addiction entails a potential long-lasting benefit from trastuzumab, whereas primary resistance to "pure" HER2 targeting only leaves potential sensitivity to chemotherapy alone. This spectrum may explain the relatively limited median OS absolute gain conferred by trastuzumab in both metastatic HER2-positive breast and gastric cancers (17).

1.4 HER Family and HER2 receptor

Human Epidermal Growth Factor Receptor 2 (HER2), also known as ErbB2, c-erbB2 or HER2/neu, is a 185 kDa protein with an intracellular tyrosine kinase domain and an extracelluar ligand binding domain. In humans, Epidermal Growth Factor Receptors (HER) family includes four members, HER1 (ErbB1, EGFR), HER2 (ErbB2), HER3 (ErbB3) and HER4 (ErbB4).

HER2 plays an important role in cell growth, survival and differentiation in a complex manner. It is well described to be the preferred partner to create heterodimer with other HER members and it is the most potent signal transduction pathway among all dimmers formed by the HER family.

HER2 is transmembrane glycoprotein composed of three distinct regions: an extracellular domain, N-terminal, a single α -helix transmembrane domain and an intracellular tyrosine kinase domain. The extracellular domain contains approximately 600 residues (90~110 kD) and can be divided into four subdomains (I–IV) with different functions. Domains II prevalently, and IV are involved in the homodimerization and heterodimerization. Subdomain IV is the critical binding

site for trastuzumab while pertuzumab binds to the dimerization arm of HER2 and prevents the dimerization of HER2 with other HER family members, leading to the transformation signal blocking. According to the different configuration assumed by domains II and IV, the extracellular domain can assume two different configurations one, the closed or inactive and the open or active. In the closed configuration inhibits the dimerization and so the activation. Crystallographic data indicates that most of HER2 receptors exist in the open configuration, suggesting that the dimerization arm of HER2 is always ready to dimerize with other receptors. This might be the mechanistic explanation for HER2's role as a preferred partner for other members in the HER family (18).

The transmembrane domain is a single α -helix comprised of 23 amino acids, among them there are two highly conserved motifs, one, the Sternberg-Gullick motif is presented in all HER members. A point mutation (Val-664→ Glu) in the Sternberg-Gullick motif of rat neu oncogene is known to induce oncogenic transformation. The G***G motif is found in the TM domain of HER1, HER2 and HER4, but not HER3. The intracellular domain is approximately 500 residues and comprised of a cytoplasmic juxtamembrane (JM) linker, a tyrosine kinase (TyK) domain and a carboxyl-terminal tail. TyK domain contains several important loops which form the enzyme active site, and it represents the target of the tyrosine kinase inhibitors, such as lapatinib. The carboxyl-terminal tail has six tyrosine residues which are available for transphosphorylation, and serve as the docking site for signalling molecules containing Src homology 2 (SH2) or phosphotyrosine binding (PTB) domain. No ligand has been actually identified (19). **(Fig.4)**

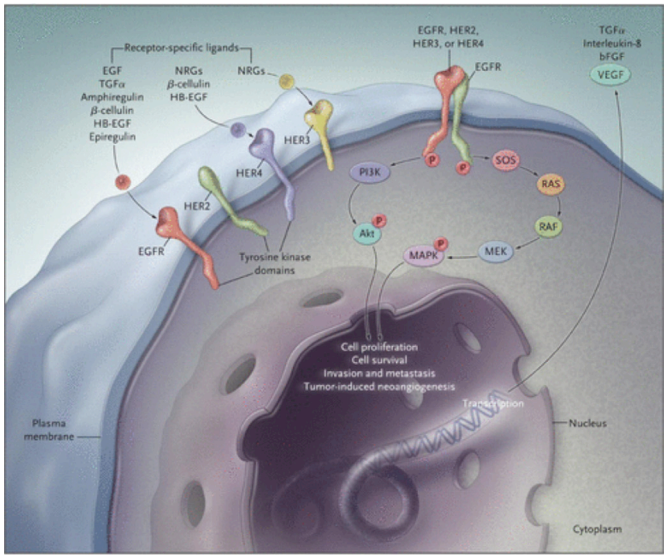

Figure 4. *HER Family, Ciardeillo NEJM 2008.*

1.5 HER2 Signalling Pathway

After dimerization, HER2 can signal through several downstream pathways including PI3K and MAPK pathways, both key factors to promote cell proliferation and prevent apoptosis.

In HER2 driven cancers, HER3 is an important heterodimer partner because it potently activates the phosphatidylinositide-3 kinase (PI3K)/AKT survival pathway via its six docking sites for the p85 regulatory subunit of PI3K. Although HER2 potently activates ERK signalling, it does not bind p85 nor directly activate PI3K/AKT. Thus, HER2-mediated activation of HER3 is essential for stimulation of the PI3K/AKT pathway.

HER2 amplified tumours have a strong dependence on PI3K/AKT signalling, as sustained blockade of this pathway appears to be required for the antitumor effect of HER2 antagonists. Comprehensive cancer cell line panels screened for sensitivity to pan-PI3K, p110α-specific, and AKT inhibitors have consistently shown preferential

activity of these drugs against *HER2*-amplified breast cancer lines (20). Further, genetic ablation of p110α has been shown to abrogate ERBB2-induced mammary tumour formation in transgenic mice. Importantly, mechanisms of *de novo* and acquired resistance to HER2 and EGFR directed therapies involve persistence or reactivation of PI3K/AKT signalling via alternate amplified RTKs and/or mutations in the PI3K pathway (21). Other downstream signalling pathways such as Src kinases, JAK/STAT and WNT are also activated by ERBB receptors (22, 23). **(Fig.5)**

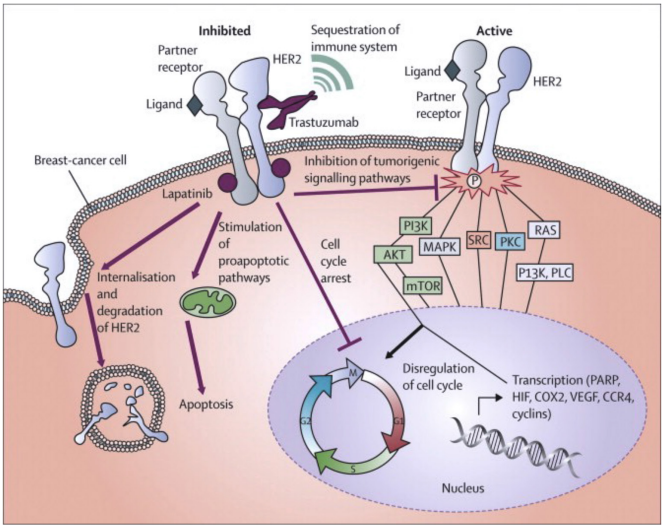

Figure 5. Mechanisms of action of trastuzumab and lapatinib Evolving novel antiHER2 strategy. *KL Jones - 2009 Lancet Oncology*.

1.6 HER2 inhibition in HER2 amplified gastric cancer patients.

HER2 amplification is present about in 7-15% of all locally advanced and metastatic gastric cancer. As demonstrated in a randomized phase III clinical trial, trastuzumab, a monoclonal antibody inhibiting HER2 activation, when added to platinum based chemotherapy was able to improve OS (13.8 versus 11.1 months) but, despite the observed clinical benefit, many patients presented a primary resistance to this treatment and all patients finally progressed, suggesting that there are some molecular events that act form the beginning or that develop during treatment responsible for resistance to this approach. (8)

Another anti HER2 blockage was tested using lapatinib, a duel HER1HER2 Tyrosine Kinase inhibitor added to platinum based chemotherapy for patients diagnosed with locally advanced or metastatic HER2 amplified gastric cancer. In a phase III randomized clinical trial, the addition of lapatinib to capecitabine and oxaliplatin (CapOx) did not increase OS in patients with HER2 amplified gastroesophageal adenocarcinoma (OS: 12.2 vs 10.5 months, HR, 0.91; 95% CI, 0.73 to 1.12; P = .3492). In a multivariate analysis, clear differences in the effect of lapatinib depending on region and age were found. In particular a multivariable Cox regression analysis of progression free survival (PFS) and OS revealed statistically significant effects of region (favouring Asian patients), age (favouring younger patients), pylorus status (favouring pylorus intact), histology (favouring non-diffuse histology), and treatment (favouring lapatinib), as well as an interaction between age and treatment). In these multivariable analyses, the effect of lapatinib treatment on PFS had an hazard ratio (HR) of 0.176 (95% CI, 0.062 to 0.495; P = .0010) and on OS had an HR of 0.304 (95% CI, 0.099 to 0.936; P = .0379). No correlation was observed between IHC status and OS benefit from lapatinib in this FISH-positive population. OS HR for IHC 0 to 1+ was 0.91 (95% CI, 0.55 to 1.51; P = .7082) and for IHC 2 to 3+ was 0.86 (95% CI, 0.68 to 1.09; P = .2105).

The absence of efficacy of lapatinib + CapOx in the overall population is no longer clear (24)

Basing on the really positive results demonstrated among HER2 amplified breast cancer patients, combination of trastuzumab and pertuzumab, a monoclonal antibody able to prevent HER2 from dimerizing with other ligand-activated HER receptors, most notably HER3, associated with platinum based chemotherapy, was also tested for HER2 amplified gastric cancer. After a median follow-up of approximately 2 years, median overall survival was 17.5 months in the experimental arm and 14.2 months in the standard treatment arm (HR = 0.84; *P* = .0565). Although a 3.3 month increase in survival was achieved, the study narrowly failed to meet the primary endpoint in the general population. (25)

Despite the use of a combination of trastuzumab with a platinum based chemotherapy, overall survival of patients diagnosed with HER2 amplified gastric cancer should be considered poor.

Clinical benefits are usually transitory, suggesting a high incidence of acquired resistance.

The importance of the HER2 blocking towards progression was explored in clinical trials and finally two different randomized trials have explored the use of lapatinib and TDM-1 beyond progression to a first line therapy.

The TyTAN study, a phase III randomized trial including only Asiatic patients, showed modest activity of second-line lapatinib plus paclitaxel for HER2- positive advanced gastric cancer, but did not demonstrate longer overall survival compared with patients treated with paclitaxel alone. Median OS was 11.0 months with lapatinib plus paclitaxel versus 8.9 months with paclitaxel alone (P = .1044), with no significant difference in median PFS (5.4 v 4.4 months) or TTP (5.5 v 4.4 months). ORR was higher with lapatinib plus paclitaxel versus paclitaxel alone (odds ratio, 3.85; P < .001). A Better efficacy with lapatinib plus paclitaxel was demonstrated in IHC3+ compared with IHC0/1+ and 2+ patients and in Chinese compared with Japanese patients. These results suggest that this approach cannot be considered and further investigation in order to better select patients whom could benefit from it are in need. (26)

Another anti HER2 drugs, TDM-1 was also tested beyond first line progression. Trastuzumab emtansine (T-DM1), is an antibody–drug conjugate, comprised of trastuzumab linked by a stable linker to the tubulin inhibitor emtansine.18 Intracellular release of cytotoxic emtansine-containing catabolites in HER2-positive breast cancer cells induces mitotic arrest and apoptosis.18 Like trastuzumab, trastuzumab emtansine inhibits HER2- mediated signalling and shedding of the HER2

extracellular domain, and mediates antibody-dependent cellular cytotoxicity.19,20. Its efficacy was proven in HER2 positive breast cancer patients, and it represents a clinical standard for these setting of patients beyond progression. The randomised phase 2/3 GATSBY study did not show overall survival superiority in patients treated with trastuzumab emtansine 2·4 mg/kg weekly compared with taxane therapy in patients with previously treated HER2-positive advanced gastric cancer. In addition, no clinical or biomarker subgroups were identified that showed an overall survival bene t with trastuzumab emtansine. The results of the secondary efficacy endpoints (progression-free survival, objective response rate, duration of response, and patient-reported outcomes) were consistent with the primary endpoint, even though the secondary endpoints might have been confounded by the effect of the open-label study design on investigator assessment of tumour response and disease progression. (27)

1.7 Possible mechanisms of resistance

Resistance to anti HER2 agents can develop from many alterations occurring to receptor structure, interaction with other transmembrane receptors or downstream effectors.

1.7.1 Intrinsic HER2 alterations

Some resistance mechanisms affect the capacity for HER2 inhibitors to directly engage HER2, as the presence of mutations in the receptors. p95-HER2 is a truncated form of HER2, lacking the trastuzumab binding region, which may arise from alternate transcription initiation sites in HER2.This form of HER2 retains kinase activity, and tumours with p95-HER2 may still be susceptible to kinase inhibition with a tyrosine kinase inhibitor such as lapatinib. (28)

A splice variant that eliminates exon 16 in the extracellular domain of the HER2 receptor has also been identified in HER2+ primary breast cancers and cell lines. Due to this alteration, the disruption of HER2 upon binding by trastuzumab does not

happen, resulting in trastuzumab resistance in cell lines. The Δ16 isoform was found to interact directly with Src.

HER2 mutations have been found in a small proportion of gastric cancers (29). These mutants of HER2 are resistant to lapatinib and trastuzumab but sensitive to the covalent HER2 TKI neratinib.

Alterations of other HER family members

Re-activation of EGFR and HER3 can also serve as a mechanism of resistance to ERBB inhibitors. In laboratory models of *HER2*-amplified breast cancer treated with trastuzumab, increased levels of EGFR and ERBB ligands led to an increase in active EGFR/HER3 and EGFR/HER2 dimers to promote resistance. This is consistent with data showing that trastuzumab is unable to block ligand-induced HER2-containing heterodimers. Several studies reported that in gastric cancer HER3 is a predictor of prognosis. Its activity is related downstream signaling PI3K/AKT. HER3 was found to be responsible for resistance in many solid tumors, among them, gastric cancer. (30)

Expression of other membrane-associated receptors

Activation of MET by its ligand hepatic growth factor (HGF) was also sufficient to promote resistance through activation of downstream signalling MET has also been implicated in trastuzumab resistance. HGF-induced signalling through MET was shown to abrogate the action of trastuzumab.

Further, gene amplification of MET and HGF was reported in a cohort of HER2+ patients who did not respond to trastuzumab and chemotherapy (31).

Similarly, activation of TGFβ receptors can increase ERBB ligand production and cleavage, particularly TGFα, amphiregulin and heregulin, via activation of the TACE/ADAM17 sheddase; this results in activation of HER3 and PI3K and

promotes drug resistance. Further, a gene signature of TGFβ activity was developed and shown to correlate with resistance to trastuzumab and poor clinical outcome in patients (32, 33).

IGF-I receptors have also been implicated in driving resistance to HER2 inhibitors. Overexpression of IGF-1R or an increase in levels of IGF-1R/HER2 heterodimers can potently activate PI3K/AKT signalling and confer resistance to trastuzumab in laboratory studies. Inhibition of IGF-1R with a neutralizing antibody or a small molecule TKI, or targeting the HER2 kinase with lapatinib was found to overcome IGF-1R- mediated resistance to trastuzumab (34).

The EphA2 receptor has been shown to confer resistance to trastuzumab in cell lines, and EphA2 expression was shown to predict poor outcome patients with HER2+ breast cancer (35).

The erythropoietin (Epo) receptor was found to be co-expressed in cell lines and primary tumours that overexpress HER2. In these cell lines, concurrent treatment with recombinant erythropoietin conferred trastuzumab resistance. In patients with HER2+ breast cancer, the concurrent administration of erythropoietin and trastuzumab correlated with a shorter progression-free and overall survival compared to patients not receiving erythropoietin (36).

In lapatinib-resistant HER2-amplified breast cancer cells, levels of the AXL RTK were markedly increased. Targeting AXL was able to re- sensitize some of these resistant cancers to the original TKI. (37)

Aberrant activation of PI3K/AKT/mTOR pathway

PI3K was identified as one of the most relevant mechanisms of resistance among several solid tumors. In gastric cancer many preclinical evidences suggested its role in resistance to anti HER2 inhibitors (38).

PI3K pathway consists of PI3Ks are a unique family of intracellular lipid kinases that phosphorylate the 3′-hydroxyl group of the inositol ring of phosphatidylinositides (PtdIns) and are divided into three classes. The most studied is class I PI3K, which stimulates the conversion of membrane-bound phosphatidylinositol-(4,5)-bisphosphate to phosphatidylinositol-(3,4,5)-trisphosphate .PIP3 acts as a secondary messenger, facilitating the recruitment and activation of kinases that possess the pleckstrin homology (PH) domain, such as PI3K-dependent kinase-1 (PDK1). The signalling duration of PIP3 is subject to regulation by phosphatase and tensin homolog (PTEN), which acts to oppose PI3K activity. The serine/threonine kinase AKT, also known as protein kinase B (PKB), possesses a PH domain, and is recruited to the plasma membrane along with PDK1. Phosphorylation of amino acid residues T308 and S473 by PDK1 and mTORC2, respectively, is essential for full AKT activation. Following activation, AKT can phosphorylate many target proteins, most notably glycogen synthase kinase 3 (GSK3), tuberous sclerosis 2 (TSC2), caspase 9 and PRAS40 (AKT1S1), which explains its relatively wide spectrum of downstream effects in promoting cell proliferation, differentiation, apoptosis, angiogenesis and metabolism. mTOR is an evolutionarily conserved serine/threonine protein kinase that belongs to the PI3K-related kinase family (PIKK). The accessibility of the mTOR active site is governed in part by mTOR-associated proteins that form two distinct complexes: mTOR complex 1 (mTORC1) and 2 (mTORC2). These complexes differ in their composition, mode of activation and rapamycin sensitivity. Activation of mTORC1 is regulated by multiple intracellular and extracellular cues, such as growth factors, nutrients, energy status and stress. Upon activation, mTORC1 regulates many cellular functions, such as cell growth, protein synthesis and autophagy via S6 kinase (S6K; RPS6K), eukaryotic translation initiation factor 4E-binding protein 1 (4E-BP1; EIF4EBP1) and ULK1, respectively. The downstream effectors of mTORC2 identified thus far are mainly members of the AGC kinase family, including AKT, protein kinase C (PKC) and serum and glucocorticoid induced kinases (SGKs), which modulate cytoskeleton organisation, cell survival, lipid homeostasis and metabolism (39).

Somatic alterations in the PI3K/AKT pathway are the most frequent in breast cancer, occurring in approximately 30% of HER2+ tumours. These include mutation and/or amplification of the genes encoding the PI3K catalytic subunits p110α (*PIK3CA*) and p110β (*PIK3CB*), the PI3K regulatory subunit p85α (*PIK3R1*), the PI3K effectors AKT1, AKT2, and PDK1, and loss of the lipid phosphatases PTEN and INPP4B. It is generally accepted that the antitumor activity of HER2 inhibitors depends on inhibition of PI3K-AKT downstream of HER2. Thus, one would expect that activating mutations in the PI3K pathway would confer resistance to HER2 inhibitors.

Constitutive activation of PI3K, via overexpression of *PIK3CA* mutants, conferred resistance to the trastuzumab in laboratory studies (40). Patients with 'hot spot' *PIK3CA* mutations and undetectable or low PTEN measured by IHC, exhibited a poorer outcome after treatment with chemotherapy and trastuzumab compared to patients without those alterations.

Ribosomal protein S6 (RPS6) is a downstream effector of PI3K. It is a key regulator of 40S ribosome biogenesis, and its phosphorylation is closely related to cell growth capacity. In a previous experiment, high level of phosphorylated-ribosomal protein S6 (p-S6) (immunohistochemistry score Z5) and an increased ratio of p-S6/S6 (immunohistochemistry score Z0.75) were significantly associated with shortened disease-free survival in patients with esophageal squamous cell carcinoma. S6 and S6 kinase 1 knockdown resulted in attenuation of viability by suppressing cyclin D1 expression in esophageal cancer cells. Furthermore, depletion of S6 and S6 kinase resulted in a reduction in esophageal cancer cell migration and invasion (41).

Aberrant activation of RAS/RAF/MEK/MAPKK pathway

The ERK pathway plays an important role of integrating external signals from the presence of mitogens such as epidermal growth factor (EGF) into signalling events promoting cell growth and proliferation in many mammalian cell types.

In a simplified model, the presence of mitogens and growth factors trigger the activation of canonical receptor tyrosine kinases such as EGFR leading to their dimerization and subsequent activation of the small GTPase Ras. This then leads to a series of phosphorylation events downstream in the MAPK cascade (Raf-MEK-ERK) ultimately resulting in the phosphorylation and activation of ERK. The phosphorylation of ERK results in an activation of its kinase activity and leads to phosphorylation of its many downstream targets involved in regulation of cell proliferation. In most cells, some form of sustained ERK activity is required for cells to activate genes that induce cell cycle entry and suppress negative regulators of the cell cycle (42).

MAPK and PI3K pathways. ERK, RSK, AKT, and S6K often act on the same substrate, sometimes in concert, to promote cell survival, proliferation, metabolism, and motility (43).

Other molecules downstream of HER2

Src family kinase signalling has been implicated by several studies in promoting resistance to HER2 inhibitors. In HER2+ breast cancer cells with acquired resistance to lapatinib, up-regulation of Src activity was observed in several resistant cell lines. Resistance was associated with recovery of PI3K/AKT signalling despite inhibition of HER2. Src is thought to mediate resistance in part via phosphorylation and inhibition of PTEN, leading to constitutive PI3K signalling. (44) In an elegant previous experiment conducted *on vitro*, HER2 positive gastric cancer cell lines treated with lapatinib finally developed Src mutations that was considered as possible mechanism of resistance (45).

Signal transducer and activator of transcription 3 (STAT3) protein is a member of a family of latent cytoplasmic transcriptional factors that convey signals from the cell surface to the nucleus upon activation by cytokines and growth factors. Engagement of cell surface receptors by polypeptide ligands induces tyrosine phosphorylation

of STAT3 protein by Janus kinases, growth factor receptor tyrosine kinases, and, in some cases, Src family tyrosine kinases. STAT3 has been shown to regulate genes that control fundamental biological processes including cell proliferation, survival, and development. STAT3 expression was observed to be activated in both lapatinib and trastuzumab resistant breast cancer models. (46, 47).

Epithelial Mesenchymal transition

The epithelial-mesenchymal transition (EMT) was first described as a developmental process during which epithelial cells acquire a motile mesenchymal phenotype. EMT is now recognized as a critical event during carcinoma metastasis and play a relevant role in inducing drug resistance among solid tumors. Indeed, this process results in degradation of the surrounding matrix, which leads to invasion and intravasation and facilitates the reestablishment of cancer cell colonies at distant sites (48). Recent studies have suggested that cancer stem cells (CSCs) intrinsically possess characteristics that are associated with mesenchymal cells, with critical functions in tumour initiation, growth, metastasis and resistance to drugs (49, 50).

The most common biochemical change associated with EMT is the loss of E-cadherin expression.

Epithelial cells express high levels of E-cadherin, whereas mesenchymal cells express those of N-cadherin, fibronectin and vimentin. Thus, EMT entails profound morphological and phenotypic changes to a cell.

Many transcription factors (TFs) that can repress E-cadherin directly or indirectly can be considered as EMT-TF (EMT inducing TFs). SNAI1/Snail 1, SNAI2/Snail 2 (also known as Slug), ZEB1, ZEB2, TCF3 and KLF8 (Kruppel-like factor 8) can bind to the E-cadherin promoter and repress its transcription. (51).

The Snail family of zinc-finger transcription factors consist of Snail1 (Snail), Snail2 (Slug) and Snail3 (Smuc), which shares an evolutionary conserved role in mesoderm formation in vertebrates

Snail plays an important role in cell cycle and survival. Snail also confers resistance to cell death induced by serum depletion or TNFα administration by activating the MAPK and PI3K survival pathways (52, 53).

Alterations in apoptosis and cell cycle control

Alterations in the normal apoptotic process can also induce resistance to HER2-targeted therapies. Levels of the pro-apoptotic BH3-only Bcl2 family member, BIM, are predictive of response to lapatinib in HER2-amplified breast cancers (54).

Survivin, a member of the inhibitor of apoptosis protein family that inhibits the activity of caspases, was demonstrated to be a point of convergence of several pathways that can lead to resistance to HER2 inhibitors as observed in some preclinical models (55).

The amplification of cyclin E, was even described as potential mechanisms of anti HER2 inhibition. Such alteration was observed in preclinical model and confirmed among HER2 positive breast cancer patients (56).

1.8 Aims:

- To analyse potential mechanisms related to primary resistance to antiHER2 inhibition in HER2 positive commercial gastric cancer cell lines selected with specific characteristics.

- To develop of *in vitro* models of acquired resistance to trastuzumab and lapatinib.

- To assess potential mechanisms related to acquired resistance among the resistant generated cell lines.

- To perform a functional analysis of the alterations identified in acquired resistant models.

- To reproduce our findings *in vivo* using immunodeficient mice models.

- To confirm if the described alterations can play a role in resistance in gastric cancer patients.

MATERIAL AND METHODS

2.1 Cell lines, cell culture and reagents

To explore possible mechanisms responsible for primary and secondary resistance to anti HER2 treatment nine human gastric cancer cell lines were used, including five established commercial gastric cancer cell lines and four resistant models generated in our laboratory. The cell lines AGS, SNU 484, SNU 216, NCI N87 were obtained from the American Type Culture Collection (ATCC) while OE 19 were purchase from the European Collection of Authenticated Cell Cultures (ECACC)-Sigma. Those cells were both HER2 amplified, SNU216, NCI N87 and OE 19, and HER2 negative, SNU 484 and AGS. Thirteen lapatinib-conditioned HER2 overexpressing gastric cancer cell lines were obtained in our laboratory. Among them three lapatinib resistant lines, the LR1-OE and the LR2-OE, derived from OE 19 parental cell line and the LR-NCI, deriving from NCI N87 were used for this investigation. At the meantime, twelve trastuzumab-conditioned HER2 overexpressing gastric cancer cell lines derived from NCI N87 were also obtained. One of them, the TR-NCI, was finally used for this study. The medium growth conditions and the origin of these cell lines are described in **Table 1**. The resistant cell lines were culture with the appropriate conditioning medium unless the experiment required a withdrawal of drugs for at least 48h before to perform it.

Cells were grown at 37ºC in a humid atmosphere containing 5% CO_2. For cell maintenance, subcultures were prepared from 1:5 dilution when confluence was near the 90%. This procedure was performed by aspirating the medium and washing with phosphate-buffered saline (PBS); the cells afterwards peeled off with 0,25% trypsin-EDTA 1x (Gibco) and suspended in the medium. To the cryopreservation cells were suspended in FBS with 10% of dimethylsulfoxide (DMSO) (sigma). Cells were then stored in cryovials and placed at -80ºC for 1 day in a container with isopropanol before being placed in a liquid nitrogen tank for long term storage.

Cell line	Complements	Origin
AGS	10% FBS + 1% Glutamine + 1% Penicillin/streptomycin	Female patient diagnosed with gastric adenocarcinoma
SNU 484	10% FBS + 1% Glutamine + 1% Penicillin/streptomycin	Gastric adenocarcinoma
SNU 216	10% FBS + 1% Glutamine + 1% Penicillin/streptomycin	Peritoneal metastasis from gastric adenocarcinoma of a young asian female patient
NCI N87	10% FBS + 1% Glutamine + 1% Penicillin/streptomycin	Peritoneal metastasis from gastric cancer of a male patient
OE 19	10% FBS + 1% Glutamine + 1% Penicillin/streptomycin	Adenocarcinoma of gastric cardia/oesophageal gastric junction of a male patient
LR1 OE	10% FBS + 1% Glutamine + 1% Penicillin/streptomycin + lapatinib	Cell line derived from OE19 conditionating with lapatinib
LR2 OE	10% FBS + 1% Glutamine + 1% Penicillin/streptomycin + lapatinib	Cell line derived from OE19 conditionating with lapatinib
LR NCI	10% FBS + 1% Glutamine + 1% Penicillin/streptomycin + lapatinib	Cell line derived from NCI N87 conditionating with lapatinib
TR NCI	10% FBS + 1% Glutamine + 1% Penicillin/streptomycin + trastuzumab	Cell line derived from NCI N87 conditionating with trastuzumab

Table 1. Medium Growth condition and cell line origin.

Lapatinib, Pimasertib, GSK2126458 (Omipalisib), saracatinib, everolimus, was purchased from Selleck Chemicals. (**Tab.2**) Stock solution were prepared in DMSO and aliquots were stored at -20ºC. Trastuzumab was obtained from Roche. The doses of drugs used in each experiment were indicated in the Results section. Vehicle treated cells (<0,1%DMSO) were used as controls.

	Mechanism of action
Herceptin Trastuzumab	Trastuzumab consists of two antigen-specific sites that bind to the juxtamembrane portion of the extracellular domain of the HER2 receptor and that prevent the activation of its intracellular tyrosine kinase. The remainder of the antibody is human IgG with a conserved Fc portion. Several possible mechanisms by which trastuzumab might decrease signaling include prevention of HER2-receptor dimerization, increased endocytotic destruction of the receptor, inhibition of shedding of the extracellular domain, and immune activation.
Lapatinib tyverb	Lapatinib is a reversible dual TKI that selectively targets and inhibits HER2 and EGFR with proven effectiveness in clinical trials. In vitro studies showed that lapatinib inhibited the activation of the three main EGFR and HER2 downstream signaling pathways, MAPK, PI3K-AKT and PLCγ, through decreased phosphorylation of target receptors and the Raf, ERK, AKT, and PLCγ1 proteins. Additionally, this TKI increased p38 expression, a stress-induced member of the MAPK pathway that is involved in apoptosis, the subG1 phase of the cell cycle (a hallmark of apoptosis), and the cyclin-dependent kinase inhibitors p21 and p27.
Pimasertib (AS703026)	Pimasertib selectively binds to and inhibits the activity of MEK1/2, preventing the activation of MEK1/2-dependent effector proteins and transcription factors, inhibiting growth and tumor cell proliferation. MEK1/2 (MAP2K1/K2) are dual-specificity threonine/tyrosine kinases that play key roles in the activation of the RAS/RAF/MEK/ERK pathway and are often upregulated in a variety of tumor cell types.
Omipalasib (GSK2126458, GSK458)	Omipalasib is a highly selective and potent inhibitor of p110α/β/δ/γ, mTORC1/2. It causes a significant reduction in the levels of pAkt cells. It leads to a G1 cell cycle arrest and produces the inhibitory effect on cell proliferation in a large panel of cell lines.
Everolimus	Everolimus (Afinitor®, RAD-001 (40-O-(2-hydroxyethyl)-rapamycin) is a rapamycin analog (rapalog) that is being developed as an antitumor agent. Like rapamycin, everolimus binds the cyclophilin FKBP-12, and this complex binds the serine/threonine kinase, mTOR (mammalian target of rapamycin) when it is associated with raptor and mLST8 to form a complex (mTORC1), and inhibits signaling downstream.
Saracatinib	ZD0530 (saracatinib) is a potent orally bioavailable v-src sarcoma (Schmidt-Ruppin A-2) viral oncogene homolog (avian) inhibitor. Src is a non-receptor protein tyrosine kinase that is involved in the regulation of numerous cellular functions such as growth, adhesion, migration and embryonic development and has been linked to the development of numerous cancers.

Table 2. Mechanisms of action of the drugs tested.

2.2 Authentication of cell lines

To guarantee the continued quality of the cell lines used in this study a Short Tandem Repeat (STR) DNA profiling of all the cells were performed, including newly developed lapatinib and trastuzumab-resistant cell lines. Genomic DNA was extracted in different steps of the study and Bioidentity, a biotechnology company of genetics analysis, monitored the identity of the cells. These analyses are able to confirm the identity of the cell lines and complying with international standards of authentication (ANSI/ ATCC).

2.3 Generation of Lapatinib-resistant clones from OE19 and NCI N87 cells *in vitro*

To explore possible mechanisms responsible for acquired resistance to anti HER2 treatment two lapatinib-sensitive HER2 amplified cell lines were selected, OE19 and NCI N87. For the resistance generation assay cells were seed at a 60-70% confluence and exposed to an initial IC50 dose (OE19: 0,16 μM; NCI N87 0,01μM). Lapatinib dose was progressively increasing every 2-3 weeks over a period of 4-5 months until resistant clones emerged. The media and compound was replenished every 3 days. The final lapatinib concentration reached was 1uM and 1,5uM for the OE19 cells and 0,05μM for the NCI N87 cells. Each single clone was picked with cloning cylinders (Sigma) and expanded in culture medium containing their specific resistant dose. The remaining cells in the plate were recovered and named as pool-LR cells, frozen but not used in this study. The effects of lapatinib conditioning on the cells were examined by monitoring cell morphology and sensitivity to lapatinib and at the end thirteen lapatinib-resistant cell clones were selected to be frozen, generating a little library of lapatinib-resistant cells. For further characterization in this study it was selected two clones derived from OE19 cells, named LR1-OE (1μM lapatinib-resistant) and LR2-OE (1,5μM lapatinib-resistant) and one 0,05μM lapatinib-resistant clone from NCI N87 based in their phenotypic characteristics.

2.4 Generation of Trastuzumab-resistant clones from NCI N87 cells *in vitro*

The generation of trastuzumab-resistant model was performed using NCI N87 cells, the unique gastric cancer cells of our panel that present a clear sensitivity to this drug. Cells seeded at 50% of confluence were exposed to increasing concentration of trastuzumab beginning with the IC50 dose over a period of 5 months, reaching a final concentration of 1000ug/ml at the end of this period. Single clones were picked, generating a little library of eleven trastuzumab-resistant cells, as it was described above. One 1000μg/ml trastuzumab-resistant clone named TR NCI was selected for further characterization in this study.

2.5 Cell growth assay (MTT)

Cells ($4x10^3$ cells) were seeded in 96-well plates and allow adhering overnight at 37ºC. Cells were treated with the appropriate media supplemented with or without lapatinib, trastuzumab, pimasertib and GSK. Drugs were administered using different growing doses as is indicated in each experiment in the results section, while controls were treated with the same proportion of vehicle used to prepare each drug. Following treatment of cells 72 hours, MTT reagent (3-(4,5-Dimethyl-2-thiazolyl)-2,5-diphenyl-2H-tetrazolium bromide; Sigma) was added and incubated for 4 hours at 37ºC. The medium was removed; DMSO was added to each well, mixed and incubated for 30 minutes at room temperature. Cell viability was determined measuring absorbance at the length of 570 nm and 690 λ respectively. Proliferation or inhibition of proliferation was calculated relative to untreated controls. Each assay was carried out at least in triplicate. The results were finally analyzed with Excel and Graphpad to calculate viability and IC50.

2.6 Genomic DNA extraction from cultured cells

Genomic DNA extraction was extracted using a protocol based on a popular method described by Sambrook et al. (1989). Cells ($3x10^6$) were lysed in 500ul of digestion buffer (10mM Tris-HCl pH 8,0; 100mM NaCl; 0,5% SDS (p/v); 25mM EDTA pH 8,0; 100ug/ml Proteinasa K) and incubated a 50ºC under stirring for 15h.

For purification of DNA, 1volume of phenol:chloroform:isoamyl alcohol (25:24:1) was added and centrifuged 10 min at 1700g. The aqueous phase was transferred to a new tube and the DNA was precipitated with 1/2 volume of 7,5M ammonium acetate and 2 volumes of 100% ethanol, washed with 70% ethanol, dried and resuspended in deionized sterile water. Total DNA isolated was quantified in the Nano-Drop 2000 Spectrophotometer.

2.7 RNA extraction from cultured cells

RNA isolation from cells was performed using the "High Pure RNA Isolation Kit" (Roche) following the manufactured protocol that included a DNase Incubation step to ensure safe, complete removal of contaminating DNA from any RNA sample. Total RNA isolated was quantified in the Nano-Drop 2000 Spectrophotometer measuring absorbance values at 260/280 nm wavelength to estimate protein contamination level. Each sample ratio was in an optimal (1.8-2.0) interval. RNA degradation was also measured by estimating RIN factor on Bioanalyzer 2100 (Agilent Technologies).

2.8 Quantitative reverse transcriptase-PCR assays (RT-qPCR)

A total of 500ng of RNA were retrotranscribed to cDNA using The "High-capacity cDNA Reverse Transcription Kit" (Applied Biosystems) following the company protocol. The samples were then stored at 4 °C, for immediate use, or at -20 °C until required.

A real time PCR (qPCR) was performed using iTaq Universal SYBR Green Supermix (Bio-Rad) on the "QuantStudio 5 Real-Time PCR System" (Applied Biosystems). All reactions were performed in triplicate. A commercial primer were used to analyse RPS6 gene expression (qHsaCID0038051, Bio-Rad). Rest of the primers were obtained from the PrimerBank database (57), a public resource for PCR primers and are shown in **table 3**. GAPDH was used as a reference gene. The amplification cycle for qPCR was: 20 s 95 °C followed by 40 cycles of 3 s 95 °C,

30 s 60 °C, and a melting curve analysis to verify the amplification product. RNA expression levels were calculated using 2^-ΔCt method where ΔCt was the Ct value of the sample minus the Ct value of the endogenous control.

Gene	Forward	Reverse
ABCC2	TCTCTCGATACTCTGTGGCAC	CTGGAATCCGTAGGAGATGAAGA
ABCC5	AGTCCTGGGTATAGAAGTGTGAG	ATTCCAACGGTCGAGTTCTCC
AKR1B10	TCAGAATGAACATGAAGTGGGG	TGGGCCACAACTTGCTGAC
AKR1C1	CAATTGGATTATGTTGACCTCTAC	ACTTCTCCACGGCCTCCCAC
AKR1C2	AAGTAAAGCTCTAGAGGCCGT	GCTCCTCATTATTGTAAACATGT
AKR1C4	CGACATAAACTATGGGTGGACC	CTGGGGTTCGTTTGTGTTTCT
AQP5	CGGGCTTTCTTCTACGTGG	GCTGGAAGGTCAGAATCAGCTC
CAPN9	AGAGGCACCCTGTTTGAGGAT	CCCCTGGTCGTTTCCACAC
CDKN1A	TGTCCGTCAGAACCCATGC	AAAGTCGAAGTTCCATCGCTC
E-CADHERINA	GTCAGTTCAGACTCCAGCCC	AAATTCACTCTGCCCAGGACG
FBP1	CTACGCCAGGGACTTTGACC	GGCCCCATAAGGAGCTGAAT
GAPDH	CCAAGGTCATCCATGACAAC	TGTCATACCAGGAAATGAGC
IL17RE	AAGGGACTTCGCTCTAAAAGGA	TCAGGCAGCAAATCAAAGGAG
PGC	TGCTTGGAAGTACCGCTTTGG	TGGAGTCCCGATGCTGATCT
SLUG	TGTTGCAGTGAGGGCAAGAA	GACCCTGGTTGCTTCAAGGA
SNAIL	ACCACTATGCCGCGCTCTT	GGTCGTAGGGCTGCTGGAA
TINAG	GGTACTCGATTCAAAAGAGCCA	GCCGCATAGAACTCAGTGACA
TWIST	GGAGTCCGCAGTCTTACGAG	CCAGCTTGAGGGTCTGAATC

Table 3. PCR primers selected.

2.9 Protein extraction

Sub confluent cells (70-80%) were used for protein analyses. Cells were washed with PBS and lysed in RIPA buffer (50 mM Tris-HCl pH 7.5, 150 mM NaCl, 0.1% SDS, 1% Triton x-100, 0,5% deoxycholic acid sodium salt (w/v)) supplemented with 2ul/ml Protease Inhibitor cocktail (Sigma) and 10ul/ml phosphatase inhibitor cocktail (Sigma). Samples were incubated on ice for 15 minutes, sonicated with 1 pulse of 10 seconds at an amplitude of 37% on a Ultrasonic homogenizer (Fisherbrand Model 120 Sonic Dismembrator) on ice and centrifuge at 14000xg speed for 20min at 4ºC. The supernatants were recovered and quantified using the "Pierce BCA Protein Assay Kit" (Thermo Scientific) following the manufactured protocol.

2.10 Immunoblot Analysis

Samples containing equal amount of protein (30 µg) were diluted with loading buffer (Bio-Rad). Proteins were resolved by sodium dodecyl sulfate-polyacrylamide gel electrophoresis (SDS-PAGE) followed by transfer onto nitrocellulose membranes (Bio-Rad) using the Mini-protean II system (Bio-Rad). The membranes were blocked for 1h at room temperature in 5% (w/v) BSA-containing TTBS (20mM Tris-Hcl pH 7.6; 137mM NaCl, 0,1% Tween 20) on a shaking platform and incubated overnight at 4ºC with the primary antibodies. The antibodies and blotting conditions used in this study are described in (**Tab.4**) Specific bands were recognized using peroxidase-conjugated secondary antibody (DAKO). Inmunoblots were visualized using the "ECL Western Blotting detection kit" reagent (GE Healthcare) and the ImageQuant LAAS 400 (Healthcare Bio-Sciencies) system. Protein levels were normalized by β-actin expression or GAPDH expression.

ANTIBODY	DILUTION	SUPPLIER	REFERENCE
AKT	1/500	Cell signaling	4691
CD44	1/500	Cell signaling	3570
E-Cadherin	1/1000	Cell signaling	3195
EGFR	1/1000	Cell signaling	2232
ERK	1/1000	Santa Cruz Biotechı	sc-93
HER2/ErB2	1/1000	Cell signaling	2165
HER3/Erb3	1/500	Cell signaling	12708
IGFR-1R	1/500	Cell signaling	9750
NRF2	1/500	Abcam	ab62352
p-HER3/Erb3	1/500	Cell signaling	2842
pAKT	1/500	Cell signaling	9271
pEGFR	1/500	Cell signaling	3777
pERK	1/1000	Santa Cruz Biotechı	sc-7383
pHER2/ErbB2	1/500	Cell signaling	2243
pS6 Ribosoma	1/1000	Cell signaling	4858
pSRC	1/500	Cell signaling	6943
pSTAT3	1/500	Cell signaling	9134
S6 Ribosomal	1/1000	Cell signaling	2217
SRC	1/1000	Cell signaling	2109
STAT3	1/500	Cell signaling	9139

Table 4. Antibodies and blotting conditions.

2.11 ELISA: PathScan RTK Signaling Antibody Array

To monitor differences in cell signaling events in the antiHer2 resistant clones *versus* parental cells an RTK signaling antibody array kit (Cell signaling, 7982) was used. It allowed interrogating 8 samples for 28 receptor tyrosine kinases and 11 important signaling nodes when phosphorylated at tyrosine or other residues. In this kit specific capture antibodies, each validated for human, are spotted in duplicate on glass slides that provide a sturdy base. Briefly, cells were washed with cold PBS and lysed. Cell lysates (250 μg) were incubated on the slide, followed by a biotinylated detection antibody cocktail and chemiluminescence detection method according to the manufactured protocol. ImageQuant LAAS 400 (Healthcare Bio-Sciencies) was used as digital imaging system. Spots were quantified using Image J software (NIH).

2.12 Flow cytometric analysis of apoptosis

Twenty-four hours after treatment the cells culture medium was collected, the cells were trypsinised and recovery in a volume of medium necessary to adjust a concentration of $5x10^5$cells/ml. They were pelleted and washed with PBS. Cells were then treated with Annexin V Alexa Fluor 488 (Inmuno step, ANXFK-100T) to identify apoptotic cells and with 7-ADD (Inmuno step, BB10x) to identify dead cells, followed by flow cytometric analysis on Beckman GalliosTM. These analyses were performed in the Central Service for Experimental Research in the University of Valencia. Each experiment was repeted at least three times for triplicate.

2.13 Flow cytometric analysis of cell cycle distribution

To evaluate cell cycle changing related to the exposure to different drugs, cells were trypsinised, centrifuge, adjusted to 1x106 cells/ml concentration in Hypotonic propidium iodide solution (1mg/ml Trisodium citrate, 0,1% Triton x-100, 50ug/ml Propidium Iodide, 1mg/ml RNase) and incubated at 4ºC for 12 hours. A flow cytometry was performed using the appropriate protocol for each cell type. Cell cycle analysis were performed using a Beckman GalliosTM. The distribution of cells in different cell cycle phases was calculated using FlowJo software (TOMY

Digital Biology, Tokyo, Japan). Each experiment was repeated at least three times for triplicate.

2.14 Depletion of RPS6 by synthetic small interfering RNAs

RPS6-specific siRNAs (Qiagen SI00708008) was utilized for RPS6 silencing. A validated Universal Negative Control (Qiagen 1027310) was used as a control for transfection. One day prior to transfection 3x105 cells were seeded in 6-well plates in a medium without antibiotics to reach an optimal confluence of 50-60%. Cells were transfected using 20nM RPS6-siRNA or control siRNA and Lipofectamine transfection reagent RNAiMAX (Invitrogen). The siRNA-Lipofectamine mixture was prepared according to the manufaturer's instructions and was uniformly added into each well containing cells and medium. The plate was shaken for mixing. The cells were then cultured at 37ºC in the incubator and where collected after 48h of culture.

2.15 Sequenom MassARRAY somatic mutation genotyping

Mutational status was investigated by using a MassARRAY system (Sequenom, San Diego, CA, USA) and an OncoCarta Panel v1.0 (Agena Bioscience; http://agenabio.com/oncocarta-panel) following the manufacturer's protocols. The panel consists of 24 multiplexed assays that detect 238 mutations in 19 oncogenes. This procedure is a rapid and cost effectiveness method of identifying key cancer driving mutations across a large number of samples. The amount of DNA added to the polymerase chain reaction was 20ng per reaction. DNA was amplified using OncoCarta PCR primer pools, and unincorporated nucleotides were inactivated using shrimp alkaline phosphatase (SAP); a custom mixture of nucleotides was used. A single base extension reaction was performed using extension primers that hybridize immediately adjacent to the mutations being studied. Salts were removed by adding a cation-exchange resin. The multiplexed reactions were spotted onto SpectroCHIP II arrays, and DNA fragments were resolved by MALDI-TOF on a compact mass spectrometer (Sequenom, San Diego, CA). An additional customized mutation

panel was used. This second panel was designed in collaboration with the Cancer Genomics Group at the Vall d'Hebron Institute of Oncology (Barcelona, Spain) and includes, in 9 multiplexes, a total of 86 somatic mutations in 14 genes. This second panel includes 28 additional positions in 5 additional genes. Therefore, a total of 266 different positions in 24 oncogenes were checked.

2.16 Wound healing migration assay

Cell lines were plated to confluence in 6-well plates 24 hours prior to scratches with a sterile P10 micro-pipette tip. The scratch was photographed with an inverted microscope (LEIKA MC170) over a 3 days period after medium was refreshed to observe any healing migration.

2.17 *In vitro* Tumorsphere formation assay

To estimate the percentage of cancer stem/progenitor cells in a population of tumor cells, the capability of cells to create spheres was tested. Cells were cultured until the confluence reached 80% and detached using 1× trypsin–EDTA. Cells free from serum were suspended in a medium supplemented with 1x B27 (Thermo Scientific), 20 ng/mL Epidermal growth factor EGF (Invitrogen) and 20 ng/mL basic fibroblast growth factor bFGF (Invitrogen). Cells were subsequently cultured in ultra-low attachment 6-well plates at a density of $0{,}1x10^6$ cells per well, and were incubated at 37 °C with 5 % CO2. After one-week incubation, tumorspheres formation was analyzed under a inverted microscope (LEIKA MC170) using the 10x magnification lens.

2.18 Gene expression Microarray Analysis

The Clariom^{TM} S Assay for human (Affimetrix Thermofisher) containing up to 20,000 well-annotated transcripts was used for microarray analysis. Cells RNA was obtained as previously described and it was processed in the Multigenic analysis section of the Central Unit for Research in Medicine of the University of Valencia. Data were analyzed and statistically fitered using Partek Genomics Suite v6.6

software. Input files were normalized with the robust multi-chip average (RMA) algorithm for gene array. To narrow the list of relevant genes, it was applied a restrictive filtering algorithm using a combined criterion, which required both a fold change absolute value of 2 or higher and a statistical significance of $p<0,005$ between subgroups. A Benjamini-Hochberg step-up false discovery rate procedure was also used with a final maximum FDR value of 0,005.

Functional Annotation Clustering of differentially expressed genes were also performed using the Pathway Studio v10 (Elsevier).

2.19 Xenograft models

6 week-old female inmunodeficient mice SCID (nufl/nufl) mice were purchased from Charles River Laboratory. The research protocol was approved (2017/VSC/PEA/00108) and mice were maintained in accordance with the institutional guidelines of the University of Valencia Animal Care and Use Committee. Animal care was in compliance with Spanish and European Community (E.C. L358/1 18/12/86) guidelines on the use and protection of laboratory animals. Mice were acclimatized at the University of Valencia Medical School Animal Facility for 2 weeks before being injected with cancer cells and then caged in groups of five under controlled conditions (12–12 hours light dark cycle; room temperature 20 22C; humidity 55%–60%). A total number of 3 x 10^6 NCI N87, TR-NCI N87, LR NCI N87, OE 19, LR1OE 19, LR2OE 19 cells in 300 µL of Matrigel (BD Biosciences): PBS (1:1) were subcutaneously injected to the dorsal flank of mice.

Tumor size and body weight were measured twice weekly, and the tumor volume (V) /2 (L, long diameter of the tumor; W, short diameter of the tumor). Each mouse was marked to make it recognizable according to the veterinarian indication. When maximum diameter permitted was achieved, mice were euthanized, each tumor was exported to obtain paraffine and frozen samples. Plasma of each mouse was also collected.

2.20 Immunostaining

Immunohistochemistry was performed on a formalin-fixed paraffin-embedded tissue of 32 gastric cancer patients. Two different antibodies were used: anti-RPS6 (1:100, Cell signaling) and anti-pRPS6 (1:400, Cell signaling). 2um tissue sections were cut into coated slides, deparaffinised with xilol and rehydrated through 90%, 80% and 70% ethanol. After washing in water, the slides were autoclaved for 3 min at 1,5 atmospheres in sodium citrate buffer (pH=6) for antigen retrieval. Endogenous peroxidase activity was blocked with hydrogen peroxidase for 5 min at room temperature. After rinsing with tris buffered saline 1X (TBS), the sections were incubated with primary antibodies for 30 min, washed with TBS 1X and incubated with secondary antibody for 30 min (K5007, DakoReal EnVision HRP Rabbit/ Mouse, Dako, Glostrup, Denmark). Diaminobenzidine (DAB) and haematoxylin chromogen (Dako) method was used. The sections were subsequently examined by light microscopy and the intensity of staining relatively qualified in the Department of pathology at the University of Valencia.

For the immunofluorescent staining of culture cells, 15x103 cells were seeded per well in μ-slide VI plate (Ibidi). After 24 h cells were fixed with a freshly solution of 4% formaldehyde in PBS during 12 min at room temperature, washed three times with PBS and blocked/permeabilized with 0,5% Triton X-100 in PBS. Then cells where incubated with a 1/500 dilution of Nrf2 antibody in blocking/permeabilization solution overnight at 4ºC. An anti-rabbit IgG Alexa Fluor 488 (Invitrogen) was used as a secondary antibody at 1/400 dilution. To visualize the nuclei and preserved signals generated, the cells were stained with Mounting Medium with DAPI (Qiagen). The fluorescent images were captured using appropriate filters in a confocal Espectral Leica SP2 microscope (leica Microsystems Heidelberg GmbH).

2.21 Patient population

From 2012 to 2017, 32 patients diagnosed with locally advanced or metastatic HER2 amplified gastric cancer, were evaluated at the Hospital Clinico of Valencia.

HER2 evaluation was performed according the updated guidelines. To be considered positive and susceptible of treatment with trastuzumab, tumours may have presented IHC +++ for HER2 or IHC ++ with a FISH amplification. Pathology records were analysed in the Division of Medical Oncology of the Hospital Clinico of Valencia, Spain. Reports were all reviewed. Clinical data were extracted from electronic medical records and reviewed retrospectively to collect age, comorbidities, classical prognostic factors such as T, nodal invasion and site of metastasis. IHC assay to verify the presence of the alteration observed in preclinical models were performed.

2.22 Statistics

Analysis of the difference of comparisons in protein levels and response to treatment was performed using the Student t-test (two-tailed with unequal variance). The cut-off for statistical significance was set as $p \leq 0.05$. To evaluate the meaning of alterations detected by Affimetrix Clarion S analysis a ANOVA was performed with GraphPad. To evaluate biomarkers relating to survival, Kaplan Meier curve was performed by STATA.

RESULTS AND DISCUSSION

3.1 Potential mechanisms related to primary resistance to antiHER2 inhibition in HER2 positive stablished gastric cancer cell lines selected with specific characteristics. (Aim 1)

3.1.1 Cell lines characterization

To better evaluate possible mechanisms involved in the development of primary resistance to antiHER2 drugs, a panel of gastric cancer cell lines were typified. In particular, five different gastric cancer cell lines were selected: three known to be HER2 amplified as SNU 216, OE 19, NCI N87, and two, known to be HER2 negative, AGS and SNU 484.

Mutational analysis:

To understand the molecular mechanisms which could lead to resistance to anti HER2 drugs, a Sequenom MassArray was performed by using an Oncocarta 2.1 to detect any mutations. KRAS and PI3K mutations were present in AGS, a HER2 negative cell line, while no HER2 amplified cells harboured any mutations according to the panel used. (**Tab.1**)

Cell lines	Somatic Mutations	HER2
AGS	KRAS: G12D; PIK3CA E453K	negative
NCI N87	WT	positive
OE 19	WT	positive
SNU 216	WT	positive
SNU 484	WT	negative

Table 1. Sequenom MassArray analysis

Protein expression analysis

By Western Blot analyses, overexpression of HER2 was demonstrated among all HER2 positive cells, especially in the NCI N87, soon followed by the OE 19. Phosphorylation of HER2 was also higher in NCI N87. This data confirmed the HER2 amplification of our model.

To better investigate possible mechanisms responsible for primary resistance, a protein evaluation of the others members of the HER family was performed by Western Blot analysis.

EGFR was expressed among all cell lines a part from SNU 484, where it was not detectable. Its phosphorylation was not evaluable in AGS and SNU484 cell lines, while it was clearly observed among all the HER2 lines.

HER3 was present among all cell lines with higher expression in the NCI N87 and OE 19. Activation of HER3 as a consistent finding of activation was also noted in the same cells. (**Fig.1**)

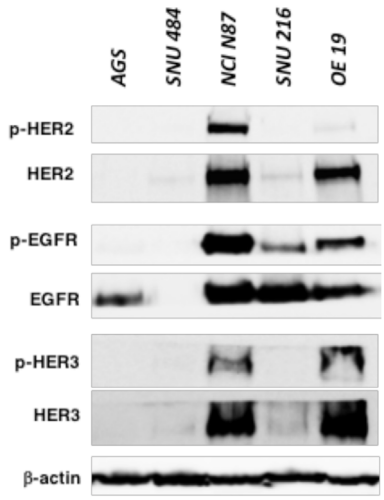

Figure 1. Western Blot Analysis of HER family expression in a panel of GC cell lines. β Actin is used as loading control.

When exploring MAPK and PI3K pathways, it was possible to detect that both ERK and AKT were expressed in all cell lines, suggesting a relevant role of these proteins already considered downstream effectors of HER2. Nevertheless, the activation of AKT was higher in the AGS cells probably due to the known mutation

of PIK3CA and KRAS, able to constitutively activate such pathway. Both ERK expression and activation are widely present, without any significant differences. (**Fig.2**)

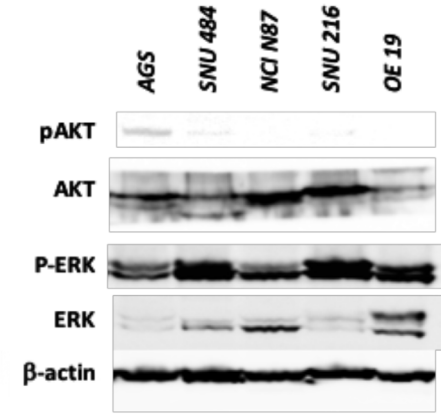

Figure 2. Western Blot Analysis showing the phosphorilation of ERK and AKT signaling molecules in a panel of GC cell lines. β Actin is used as loading control.

To complete the characterization of mechanisms of resistance, MET and AXL were also evaluated. Finally MET was expressed in all cell lines a part from the SNU 484. MET activation was not evaluable. SNU 216 cell line was known to be MET amplified and this data was confirmed in our analysis. In this cell line was also possible to see the hyperexpression of AXL. (**Fig.3**)

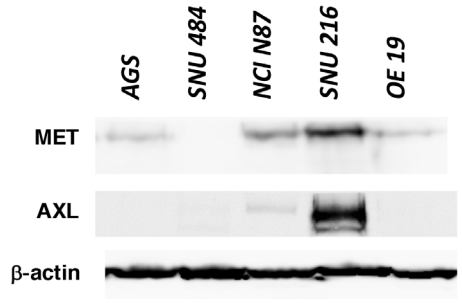

Figure 3. Western Blot Analysis showing the expression of the transmembrane receptors MET and AXL in a panel of GC cell lines. β Actin is used as loading control.

RPS6 was activated in the AGS cell line as shown in our immunoblotting. This observation is in line with the presence of PIK3CA mutation harboured by these cells. (**Fig.4**). The two cell lines characterised to have the more relevant expression of HER2, OE 19 and NCI N87, do not present an activation of RPS6.

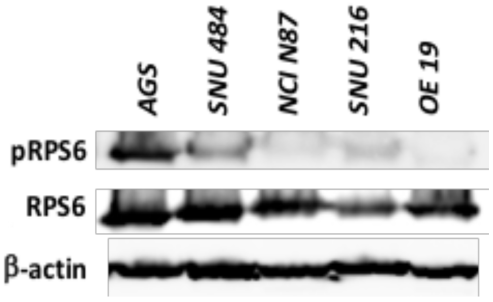

Figure 4. Western Blot Analysis showing the phosphorylation of RPS6 in a panel of GC cell lines. β Actin is used as loading control.

3.1.2. Pharmacological sensitivity assays

The results obtained from both, the mutational analysis and Western Blot, suggested the relevant role of PI3K and MAPK activation in cell proliferation. All cell lines were treated with a panel of specific inhibitors to verify the potential inhibition of cell growth.

Trastuzumab and lapatinib were used in all cells to effectively confirm the absence of response of the HER2 not amplified cell lines and to analyse the sensitivity in SNU 216, OE 19 and NCI N87 cell lines. MTT analyses were performed finally showing no response among HER2 not amplified cells; instead, a different sensitivity among the HER2 amplified cells were detected. In particular, NCI N87 cell lines were detected to be really sensitive to both trastuzumab, (IC50: 50 μg/ml), and lapatinib, (IC50 0,01 μM), (**Tab.2**). Despite being HER2 amplified, OE 19 cell line showed less sensitivity to trastuzumab. Nevertheless, lapatinib was able to block cell growth achieving an IC50 of 0,16 μM (**Tab.2**) very similar to the ones already published

in other experiences. SNU 216 were found to be less sensitive to both trastuzumab and lapatinib, possibly because of the presence of MET amplification which can be considered a mechanism of primary resistance.

IC 50	Trastuzumab	Lapatinib
NCI N87	50 μg/ml	0,01 μM
OE 19	> 1000 μg/ml	0,16 μM
SNU 216	> 1000 μg/ml	> 2 μM

Table 2. IC50 NCI N87 and OE 19 treated with increasing doses of trastuzumab and lapatinib. OE 19 were found to be resistant to trastuzumab.

Based upon the results of WB analysis, showing hyperphosphorilation of ERK, Pimasertib, a potent MEK1/2 inhibitor was used to confirm the involvement of the MAPKK pathway in cell proliferation. At the same time, being AKT y RPS6, a downstream effector o mTOR, significantly activated, the inhibition of PI3K pathway was also considered to evaluate if it could be related with resistance. Treatment with Omipalisib (GSK458), a highly selective and potent dual inhibitor of PI3K p110α/β/δ/γ and mTORC1/2 was administered.

Cell lines and their response to the different treatments selected were further studied by FACs, to evaluate the capacity of these drugs, on causing apoptosis or cell cycle inhibition after 24 hours from treatment. This experiment was performed at least three times for triplicate.

Treatments were tested as single agent or as combination. The rational of combination was to evaluate the capability of such drugs in improving the effect of anti HER2 inhibitors. Apoptosis assays (**Fig.5**) and Cell Cycle (**Fig.6**) assays suggested that adding GSK to both lapatinib and trastuzumab was able to improve apoptosis and lead to a decrease of the S phase of cell cycle underlying an anti-proliferative effect of GSK 458 when combined with trastuzumab and lapatinib. GSK 458 when used as single agent was also able to induce apoptosis and to decrease the proportion

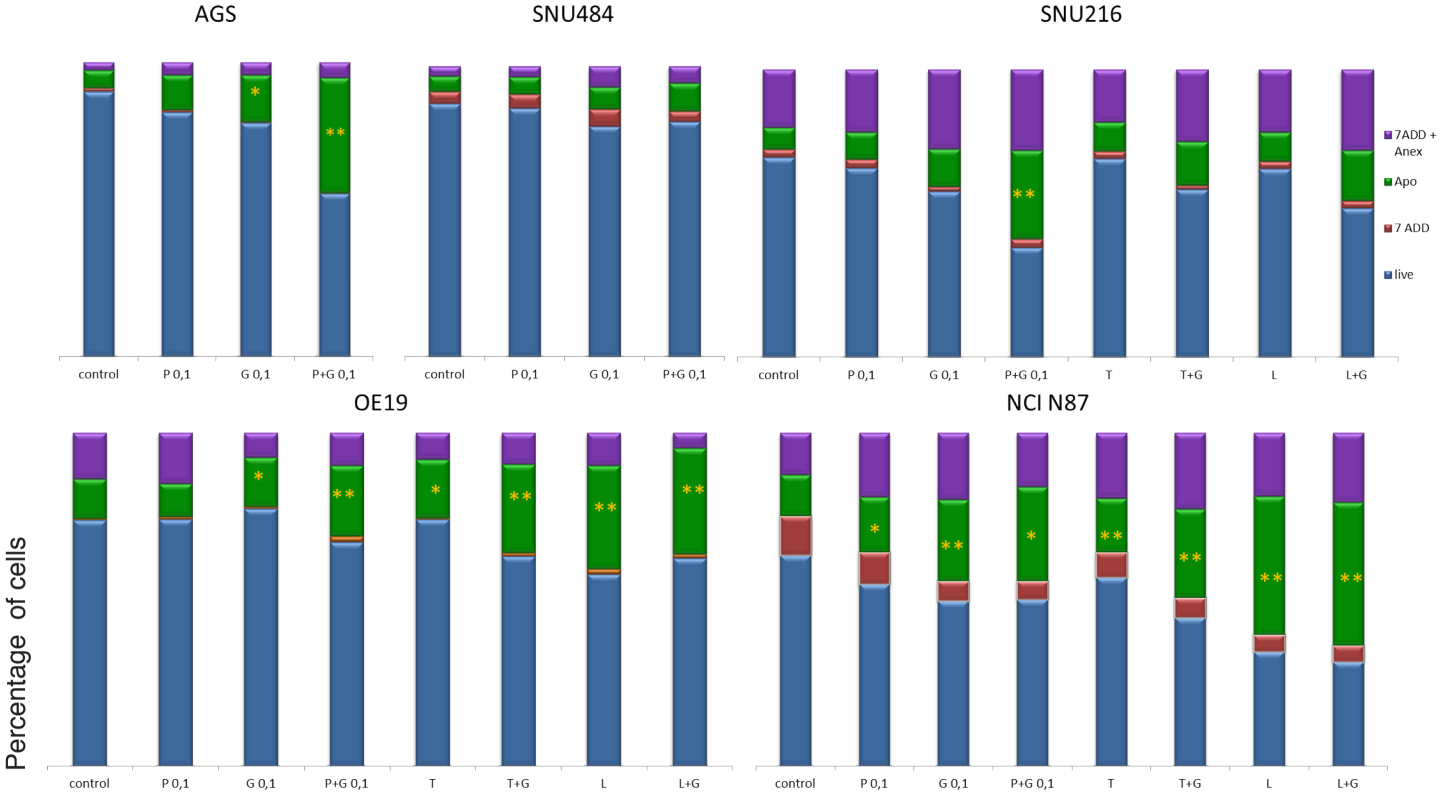

Figure 5. Apoptosis Assay in a panel of gastric cancer cell line treated with Pimasertib (P) 0,1 µM; GSK 458 (G) 0,1 µM; Trastuzumab (T) 100 µg/ml, Lapatinib (L) 0,1 µM, as single agent or combination.

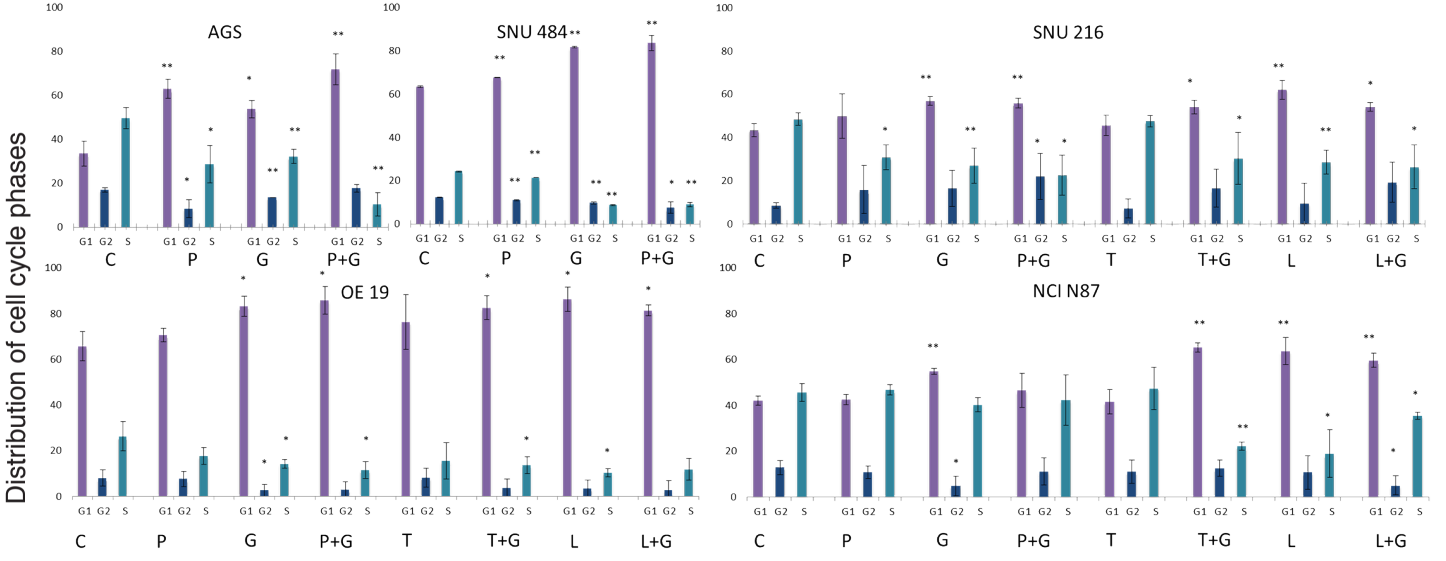

Figure 6. Cell Cycle Assay in a panel of gastric cancer cell line treated with Pimasertib (P) 0,1 μM; GSK 458 (G) 0,1 μM; Trastuzumab (T) 100 μg/ml, Lapatinib (L) 0,1 μM, as single agent or combination.

of cells in the S phase of cell cycle in AGS. Pimasertib reduces S phase of AGS cell line when used as single agent or in combination with GSK 458. No relevant effect was observed among HER2 positive gastric cancer cell lines.

Discussion

To evaluate potential mechanisms of primary resistance we selected a panel of gastric cancer cell lines known to be HER2 amplified or negative. All cell lines were analysed in order to verify common alterations or differences which could improve our understanding on the mechanisms related to primary resistance. To better characterise our cells, a mutational analysis was performed to verify the presence of such mutations which can lead to resistance. As results, only one of the HER2 negative cell line, the AGS, was found to harbour both *KRAS* and *PI3K* mutations, while according to the selected panel, no others mutations among the other cell lines were described.

Protein expression analysis by Western Blot was also used to explore the widely known pathways implicated in primary resistance in others HER2 positive models. Impressively, AKT and ERK, downstream effectors of MAPKK and PI3K were both hyerexpressed and activated among our cell lines. Their activation was impressively relevant in AGS cell lines, probably due to KRAS and PIK3CA mutations. When downstream effectors were analysed, RPS6 was detected to be expressed among all cell lines, and its activation was relevant in the AGS cells according to their molecular profile while its activation was less relevant among the HER2 positive cell lines, OE 19 and NCI N87.

To test the sensitivity to anti HER2 drugs, trastuzumab and lapatinib were both used to evaluate viability in all our cells. HER2 negative cells did not respond to these treatments while HER2 positive cells experienced a decrease in cell growth as expected. Nevertheless, NCI N87 were found to be sensitive to both trastuzumab and lapatinib while OE 19 were sensitive to lapatinib but not to trastuzumab.

According to the hyperexpression of ERK, AKT and RPS6 revealed with Western Blot analysis treatment with pimasertib and GSK 458 were also tested as single agent or in combination with trastuzumab and lapatinib.

Finally, it was possible to conclude that GSK 458 when used as single agent decreases cell growth decreasing the percentage of cells in the S phase of cell cycle. When this drug was tested in combination with antiHER2 inhibitors a positive effect against cell growth was detected confirming the primary role of PI3K/AKT/mTOR in HER2 resistance (21). This phenomenon has been already described in other HER2 positive models, such as breast cancer, where PI3K was associated to resistance to trastuzumab and lapatinib. Nevertheless, the role of RPS6 is not widely explored.

3.2 Development of *in vitro* models of acquired resistance to trastuzumab and lapatinib (Aim 2)

To explore possible mechanisms related to acquired resistance to anti HER2 inhibition, resistant cell lines deriving from NCI N87 and OE 19 were developed in our laboratory. According to the sensitivity to these drugs, we developed both lapatinib and trastuzumab model deriving from NCI N87 and a lapatinib resistant model deriving from OE 19 cell line. Trastuzumab was not used for OE 19 because of the lack of primary sensitivity. **Fig.1**

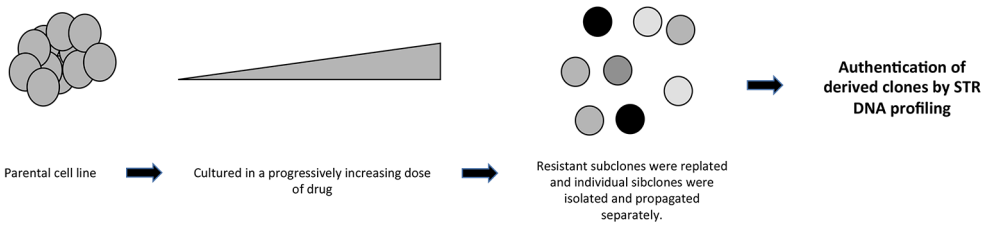

Figure 1. Schematic view of the development of resistance models, clone selection and authentication.

3.2.1 Development of a cell line model of acquired lapatinib resistance Lapatinib-conditioning of OE 19 cells.

OE 19 cells overexpress HER2 and are sensitive to lapatinib with an IC50 of 0,16 μM, obtained with MTT. The conditioning process lasted about 4-5 months. When cells become to growth, suggesting a resistance phenomenon, lapatinib dose was increased till 1 and 1,5 μM. single clones were isolated and expanded in culture. During all time, the morphology and the sensitivity of the cell lines to lapatinib was monitored. The morphology of OE 19 cells altered already during the first 2 months of lapatinib conditioning. The resistant cells also exhibited distinct morphological phenotype compared to the parental cell line, in some of them, it was possible to observe some morphological changes towards a mesenchymal phenotype. **Fig.2**

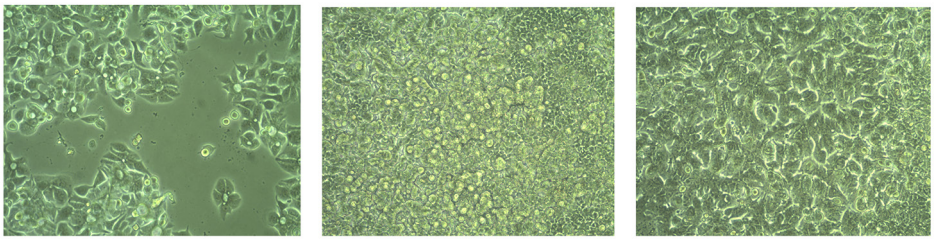

Figure 2. OE 19 treated with increasing doses of Lapatinib: morphological changes versus parental cell line.

After 5 months of conditioning, the sensitivity of the cells to lapatinib was tested. A total of 8 clones of lapatinib resistant cell lines were isolated, and two, LR1 OE and LR2 OE, were finally selected to continue the experiment due to their morphological phenotype and resistance. A viability assay by MTT was performed to evaluate resistance to increasing doses of lapatinib. **Fig.3**

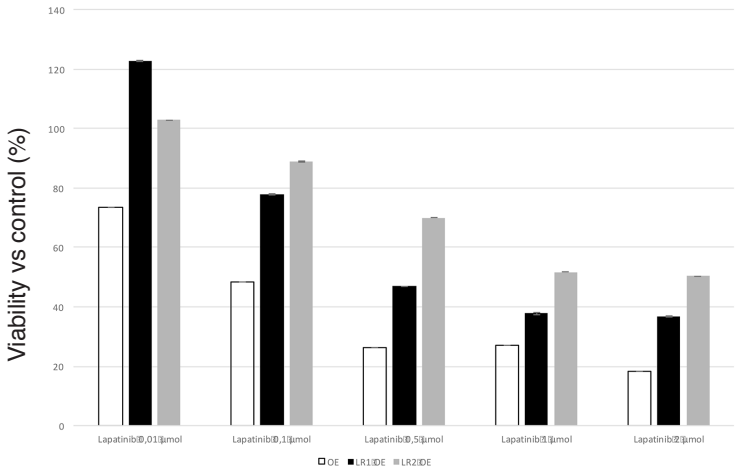

Figure 3. Viability of OE 19 cell line and its resistant clones, LR1 OE and LR2 OE, to increasing doses of lapatinib. Data are shown as means +/- standard error derived form three indipendent experiments.

Lapatinib-conditioning of NCI N87 cells.

NCI cells overexpress HER2 and are sensitive to lapatinib with an IC50 of 0,01 μM. A lapatinib dose which would result in 50% growth inhibition basing on viability results, was considered. NCI N87 cells were initiated with twice weekly treatments of 0,01 μM of lapatinib. When cells become to growth, suggesting a resistance phenomenon, lapatinib dose was increased till 0,05 μM. The conditioning process lasted about 4-5 months. Even in this case, the morphology of NCI N87 cells altered already during the first 2 months of lapatinib conditioning. The resistant cells also exhibited distinct morphological phenotype compared to the parental cell line, in some of them, it was possible to observe some morphological changes towards a mesenchymal phenotype as observed in the OE 19 derived clones. (**Fig.4**)

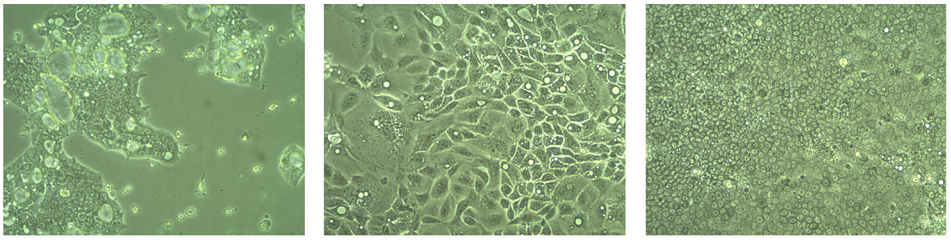

Figure 4. NCI N87 treated with increasing doses of Lapatinib: morphological changes versus parental cell line.

After 5 months of conditioning, the sensitivity of the cells to lapatinib was tested. A total of 5 clones of lapatinib resistant cell lines were isolated, but only one, LR NCI, was selected being the most resistant to further evaluations. A viability assay by MTT was performed to evaluate resistance to increasing doses of lapatinib, showing that this model was resistant also to higher doses of lapatinib. (**Fig.5**)

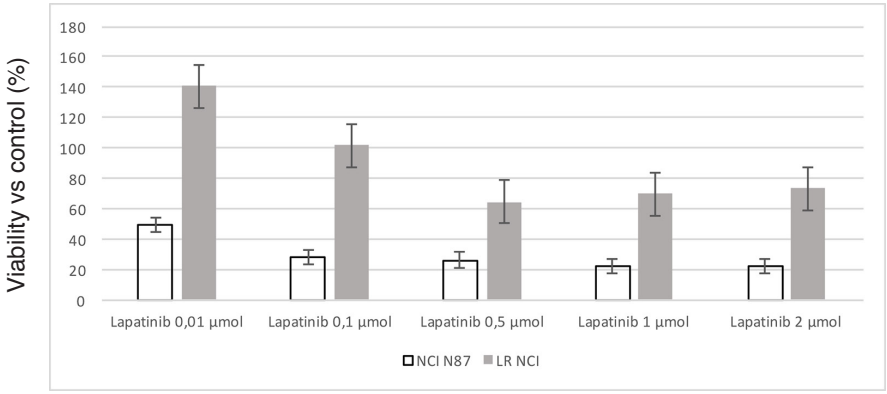

Figure 5. Viability of NCI N87 cell line and its lapatinib resistant clone, LR NCI , to increasing doses of lapatinib. Data are shown as means +/- standard error derived form three indipendent experiments.

3.2.2 Development of a cell line model of acquired trastuzumab resistance

Trastuzumab, a monoclonal antibody able to inhibit HER2 signalling combined with platinum based chemotherapy, represents the gold standard for HER2 positive locally advanced or metastatic gastric cancer. Despite the use of this personalized approach, clinical benefit deriving from this treatment is quite poor.

NCI N87 cells overexpress HER2 and are sensitive to trastuzumab with an IC50 of 50 µg/ml. A trastuzumab dose which would result in 50% growth inhibition basing on viability results, was considered. NCI N87 cells were initiated with twice weekly treatments according to the IC50 of trastuzumab. When cells become to growth, suggesting a resistance phenomenon, trastuzumab dose was increased. Finally, after the first 2 months, cells were all treated with a concentration of trastuzumab of 1000 µg/mL. The conditioning process lasted about 4-5 months. After 4 months of conditioning, the sensitivity of the cells to trastuzumab was tested. A total of 12 clones of trastuzumab resistant cell lines were isolated.

As for lapatinib resistant models, obtained resistant cells also exhibited distinct morphological phenotypes compared to the parental cell line. In some of them, even in this case, it was possible to observe some morphological changes towards

a mesenchymal phenotype. Moreover, it was possible to observe a heterogeneous growth consisting of the presence of at least two different patterns. **Fig.6**

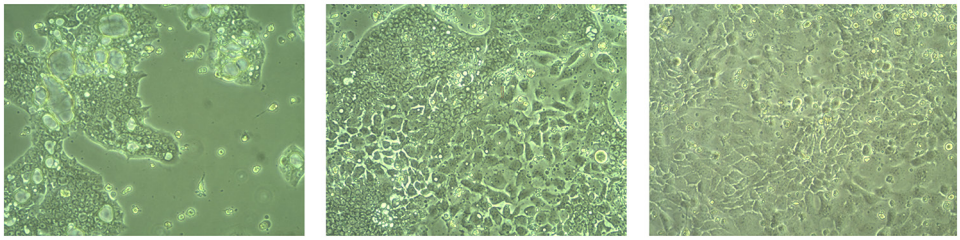

Figure 6. NCI N87 treated with increasing doses of Trastuzumab: morphological changes versus parental cell line.

After 5 months of conditioning, the sensitivity of the cells to trastuzumab was tested. A total of 12 clones of trastuzumab resistant cell lines were isolated, among them the most resistant line, TR NCI was selected to continue with the study. (**Fig.7**)

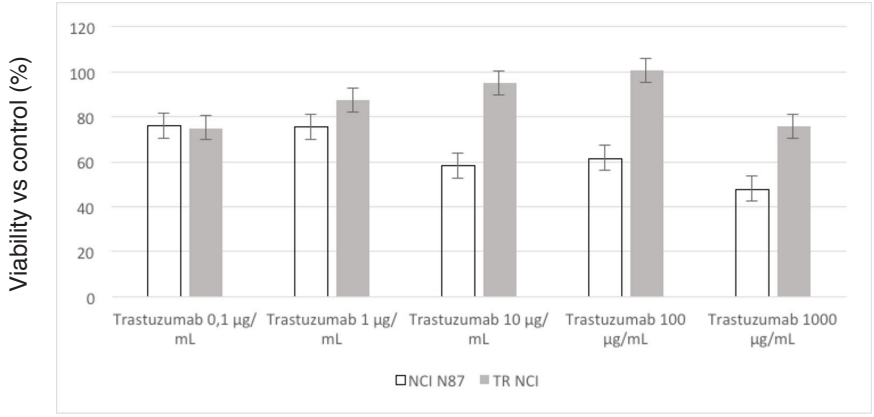

Figure 7. Viability of NCI N87 cell line and its rastuzumab resistant clone, LR NCI , to increasing doses of lapatinib. Data are shown as means +/- standard error derived form three indipendent experiments.

Finally, we were able to isolate 13 OE and NCI N87 derived lapatinib resistant clones and 12 trastuzumab resistant clones. Among them, to continue our experiment only 2 lapatinib resistant clones deriving from the OE 19 parental cell line (LR OE 1 and LR OE 19 2), one deriving from the NCI N87 parental cell line, LR NCI and one from trastuzumab resistant cell, TR NCI were chosen. The selection of these clones was based on morphologically features and proliferation assay, suggesting a more resistant phenotype.

3.2.3 Cell Lines Authentication

Genotyping analysis was performed, as previously described in session 2.2, to certify the origin and exclude possible contamination. All clones were confirmed to derive form the parental line, which were also tested to confirm their identity after being cultured during those months.

3.2.4 Assessing the stability of acquired lapatinib and trastuzumab resistance

To establish a reliable cell line model of lapatinib and trastuzumab resistance, the phenotype must be stable when the cell line is frozen and re-thawed. To asses this, OE 19 and resistant cells and the NCI N87 and resistant cells were frozen. After a minimum of seven days in liquid nitrogen, the frozen stocks were thawed and the viability of the stocks assessed by microscopy. The cells were then passaged a minimum of 3 times before lapatinib and trastuzumab sensitivity assays were repeated. Finally, it is possible to observe that resistance to both lapatinib or trastuzumab was maintained even if it decreased in a not relevant manner towards the not frozen lines. **Fig.8**

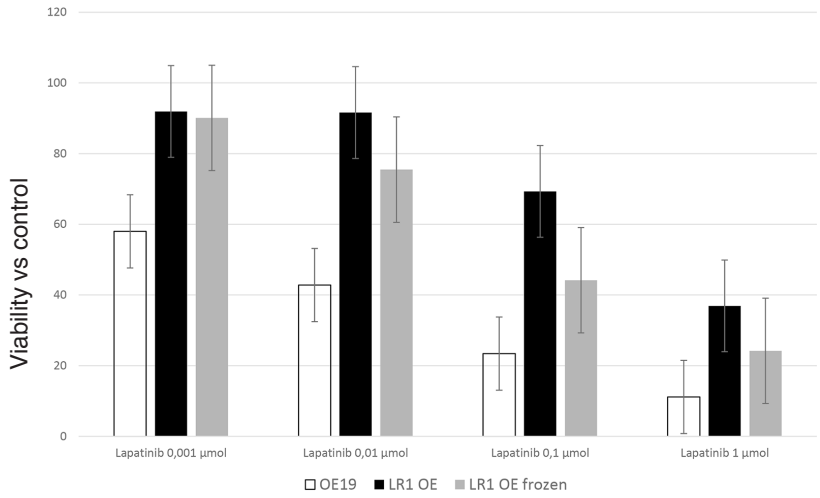

Figure 8. Assessment of the stability of acquired lapatinib resistant cells after being frozen. Data are shown as means +/- error standard form three independent experiments.

3.2.5 Cross resistance to lapatinib and trastuzumab among NCI N87 derived clones

Moreover, a test to verify cross resistance of lapatinib resistant cells to trastuzumab and vice versa was performed for NCI resistant clones. Finally, LR-NCI demonstrated quite resistance towards trastuzumab and the same was observed for TR-NCI, suggesting that probably mechanisms responsible for acquired resistance to lapatinib may coincide to the ones to trastuzumab. **Fig.9,10**

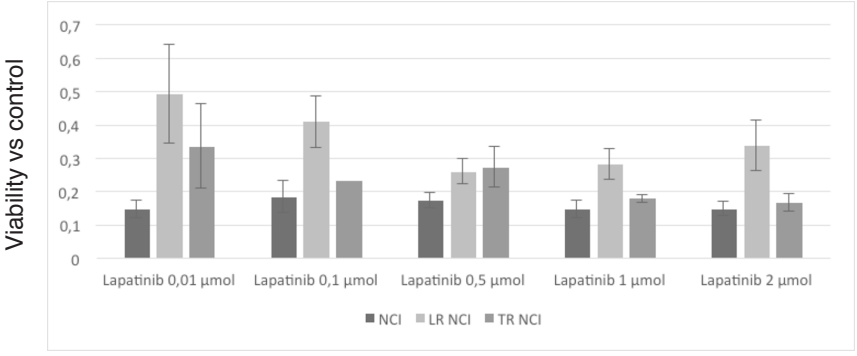

Figure 9. Evaluation of cross resistance to lapatinib among LR NCI, lapatinib resistant clone , TR NCI, Trastuzumab resistant clone and NCI N87. Data are shown as means +/- error standard form three independent experiments.

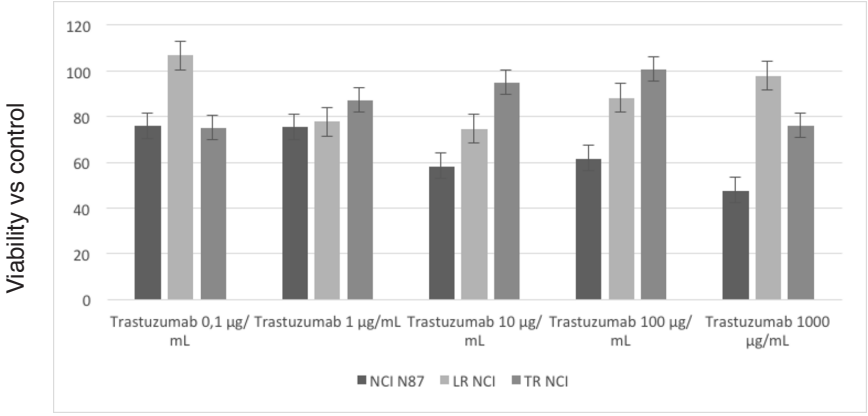

Figure 10. Evaluation of cross resistance to trastuzumab among LR NCI, lapatinib resistant clone , TR NCI, Trastuzumab resistant clone and NCI N87. Data are shown as means +/- error standard form three independent experiments.

Discussion

Resistance to targeted agents represents a relevant problem for cancer patients. To evaluate possible mechanisms related to acquired resistance to anti HER2 drugs in HER2 positive gastric cancer models, resistant cells lines were developed in our laboratory.

It is not possible to exclude that different mechanisms of resistance could emerge by starting the selection process from different HER2 positive gastric cancer models. To overcome this problem, that is clearly one of the major limitation of the published experiments, it was decided to select two different lines form which develop our resistant models. Moreover, it was planned to conduct this experiment using different clones deriving from the same parental line to better study tumour heterogeneity, being aware that resistance to the same drug may derive from several mechanisms. Eventually, we were able to obtain several stable resistant models to both lapatinib and trastuzumab to be used to explore mechanisms responsible for acquired insensitivity to anti HER2 drugs.

3.3 Assessment of potential mechanisms related to acquired resistance among the resistant generated cell lines. (Aim 3).

3.3.1 Protein expression assessment analysed by Western Blot.

The overexpression of several proteins has been shown in previously published cell line models of acquired lapatinib and trastuzumab resistance. To verify if such alterations were present even in our models, several Western Blot analyses were performed to detect the expression and the phosphorylation of this resistance associated proteins.

Expression of HER family members

To better understand mechanisms of acquired resistance, Epidermal Growth Factor Receptors Family expression and activation were explored in parental cell lines and resistant clones by Western Blot. (**Fig.1)**

HER2 was detectable in all cell lines, but its expression is slightly less present in both lapatinib resistant cell lines models. HER2 activation is increased in trastuzumab resistant line, suggesting a possible role in the acquired resistant phenotype. (**Fig.1)**

EGFR was widely and homogeneously expressed among all cell lines, nevertheless the activation of EGFR, similarly to what happened for HER2, was prevalent for the TR-NCI cell line. On the contrary, EGFR activation decreases in all OE lapatinib resistant models while this phenomenon was not observed for the LR NCI. (**Fig.1)**

HER3 was overexpressed in all lapatinib resistant clones deriving from OE 19, while it was not present on NCI lapatinib resistant clones. In the trastuzumab resistant model, no changes were detectable versus parental cell line. (**Fig.1)**

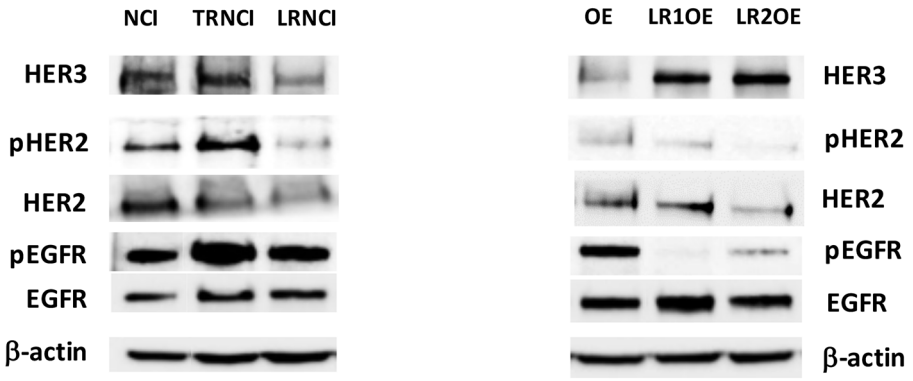

Figure 1. Western Blot Analysis of HER family expression in NCI N87 parental cell line and TR NCI, Trastuzumab resistant cone, and LR NCI lapatinib resistant clone and OE 19 parental cell lines, LR1 OE and LR2 OE, lapatinib derived resistant clones. β Actin is used as loading control.

Alterations in P13K/AKT/mTOR and MAPK signalling pathways

To explore the activation of pathways that are widely known to induce drug resistance, AKT and ERK expression and activation were both explored. AKT expression and activation was increased in the lapatinib resistant clones derived from OE 19 while it was not detectable in the resistant models derived from NCI N87. ERK activation was consistent in all lapatinib resistant cells. (**Fig.2**)

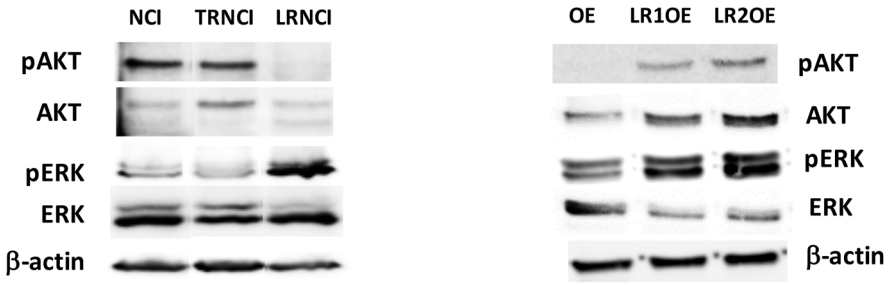

Figure 2. Western Blot Analysis showing the phosphorilation of ERK and AKT signaling molecules in NCI N87 parental cell line and TR NCI, Trastuzumab resistant clone, and LR NCI lapatinib resistant clone and OE 19 parental cell lines, LR1 OE and LR2 OE, lapatinib derived resistant clones. β Actin is used as loading control.

RPS6, downstream effector of PI3K/AKT/mTOR pathway, was observed to be expressed in all cell lines. The activation of this protein was consistently increased among all resistant clones. (**Fig.3**)

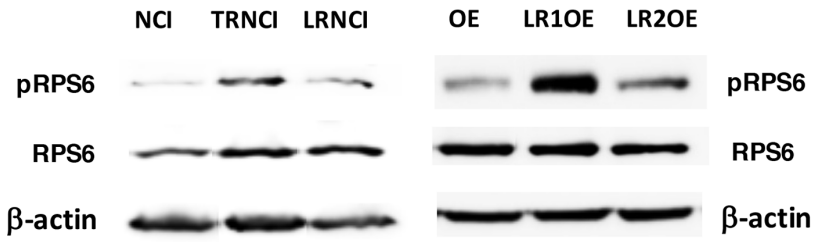

Figure 3. Western Blot Analysis showing the phosphorilation of RPS6 in NCI N87 parental cell line and TR NCI, Trastuzumab resistant clone, and LR NCI lapatinib resistant clone and OE 19 parental cell lines, LR1 OE and LR2 OE, lapatinib derived resistant clones. β Actin is used as loading control.

Other molecular pathways

To explore its implication in the acquired resistance of our models, many transmembrane receptors known to have a potential role in resistance were studied by Western Blot analysis. (**Fig.4**)

IGFR was identified in all cell lines and it was more expressed by the TR NCI and LR2 OE. Its activation was not evaluable. MET was explored and it was under the limit of detection among OE 19 and resistant clones. On the contrary, it was found to be expressed by the NCI and a little increase in its expression in resistant clones. STAT 3 was observed to be activated in TR NCI and in all OE lapatinib resistant clones. Despite differences in activation, STAT 3 expression was present in all cell lines with an increase in expression in lapatinib resistant clones. (**Fig.4**)

Among our cell lines, SRC was observed to be expressed in all our cells, and a relevant increment of its activity was observed among all lapatinib resistant clones. In the trastuzumab resistant cells, an increase of SRC expression was detected. (**Fig.4**)

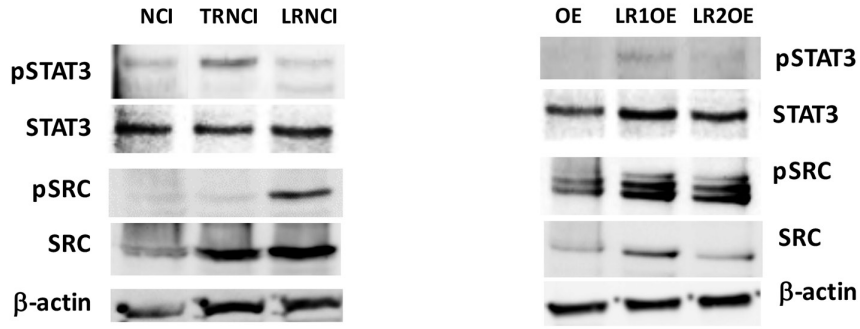

Figure 4. Western Blot Analysis showing the phosphorilation of STAT-3 and SRC in NCI N87 parental cell line and TR NCI, Trastuzumab resistant clone, and LR NCI lapatinib resistant clone and OE 19 parental cell lines, LR1 OE and LR2 OE, lapatinib derived resistant clones. β Actin is used as loading control.

3.3.2 Protein phosphorilation analysis performed by ELISA Pathscan Array

To complete the study to better explore new activated proteins that could be involved in resistance to both lapatinib and trastuzumab complementing the results of the WBs analyses, an ELISA path-scan array was performed. OE 19, LR1 OE, LR2 OE and NCI N87, LR-NCI and TR NCI cell lines were all considered for the evaluation. Among all the observed proteins, listed above in **tab 1**, RPS6 was notably hyperactivated in LR1 OE and LR2 OE according to previous WB; while in NCI N87 lapatinib and trastuzumab resistant, this alteration was less relevant. RP6S over-activation was also present in both OE 19 and NCI N87 parental cell lines.

List of phosphorilated proteins analised in PathScan Array (ELISA)			
FGFR1	TrkB/NTRK2	EphA3	Tie2/TEK
TrkA/NTRK1	PDGFR	Axl	S6RP
ALK	EphA2	p44/42 MAPK (ERK1/2)	Lck
EphA1	Tyro3/Dtk	Src	IGF-IR
EphB4	Akt/PKB/Rac	Stat3	Ret
Akt/PKB/Rac	Zap-70	Her3/ErbB3	M-CSFR/CSF-1R
IRS-1	Her2/ErbB2	InsR	EphB3
EGFR/ErbB1	FGFR4	Ron /MST1R	VEGFR2/KDR
FGFR3	Met/HGFR	FLT3/FIK2	c-Abl
Stat 1	c-Kit/SCFR	EphB1	

Table 1. List of phosphorylated proteins.

It was possible to see that even SRC was hyperactivated among all the resistant cells, a part from the trastuzumab resistant line. AKT and ERK were noted to be increased in all OE 19 resistant models, as expected according to the results already commented. Among the NCI N87 resistant models, its phosphorylation was less clear, however its expression was confirmed by Western Blot Analysis. A confirmation of the hyperactivation of STAT 3, as previously described, was even observed. Only in the trastuzumab resistant line it was not evident, despite the results observed on Western Blot. In this analysis, an increment of FGFR1 and FGFR3 was also detected in resistant lines. Interestingly, alterations in the Ephrin proteins, conferring a mesenchymal phenotype, were also observed. (**Fig.5,6,7**)

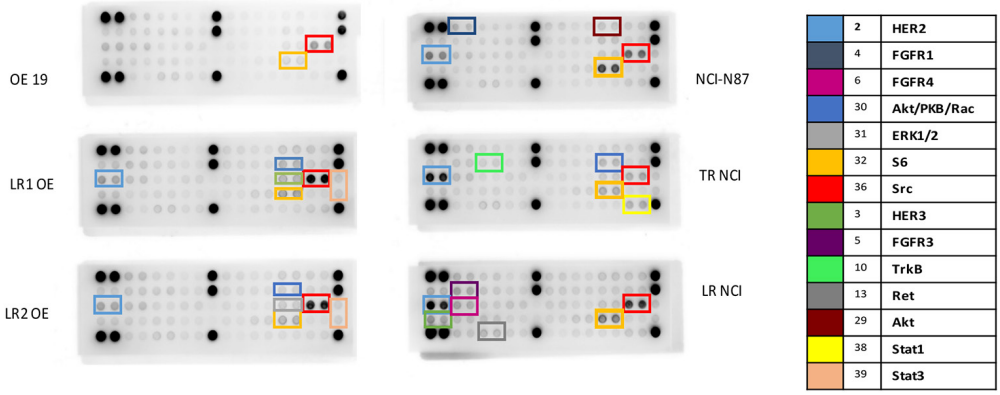

Figure 5. Hotspots of phophorilated proteins according to PathScan ELISA of the OE 19 parental cell lines, LR1 OE and LR2 OE, lapatinib derived resistant clones NCI N87 parental cell line and TR NCI, Trastuzumab resistant clone, and LR NCI lapatinib resistant clone.

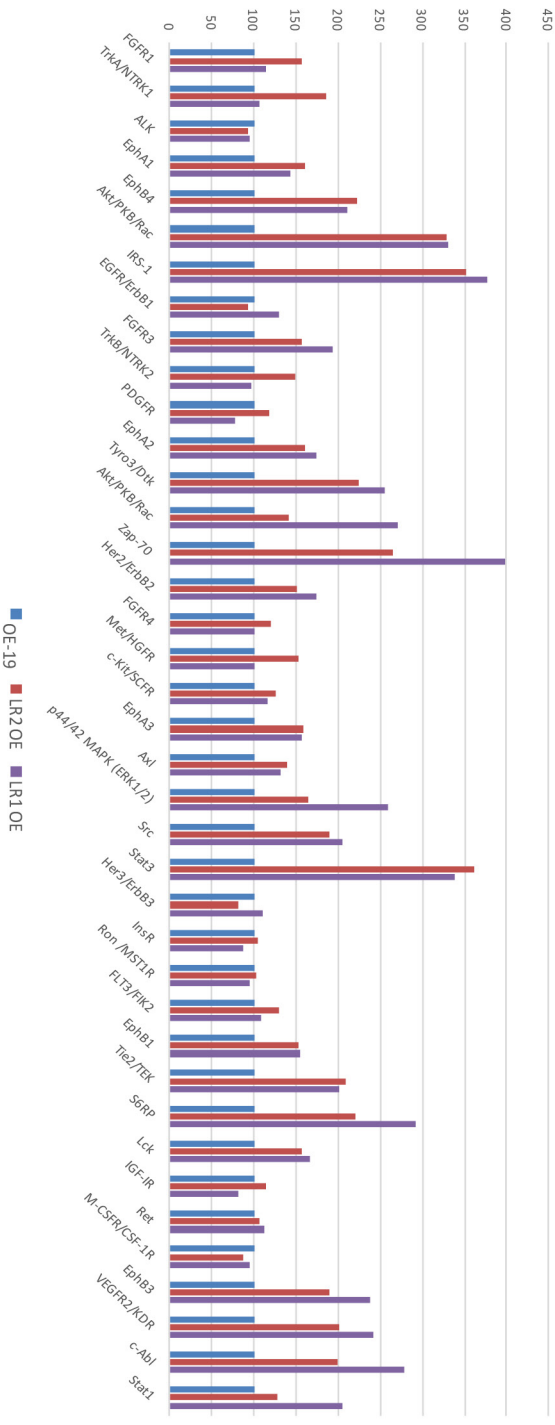

Figure 6. Quantification of the phosphorylated protein from the PathScan ELISA of the OE 19 parental cell lines, LR1 OE and LR2 OE, lapatinib derived resistant clones.

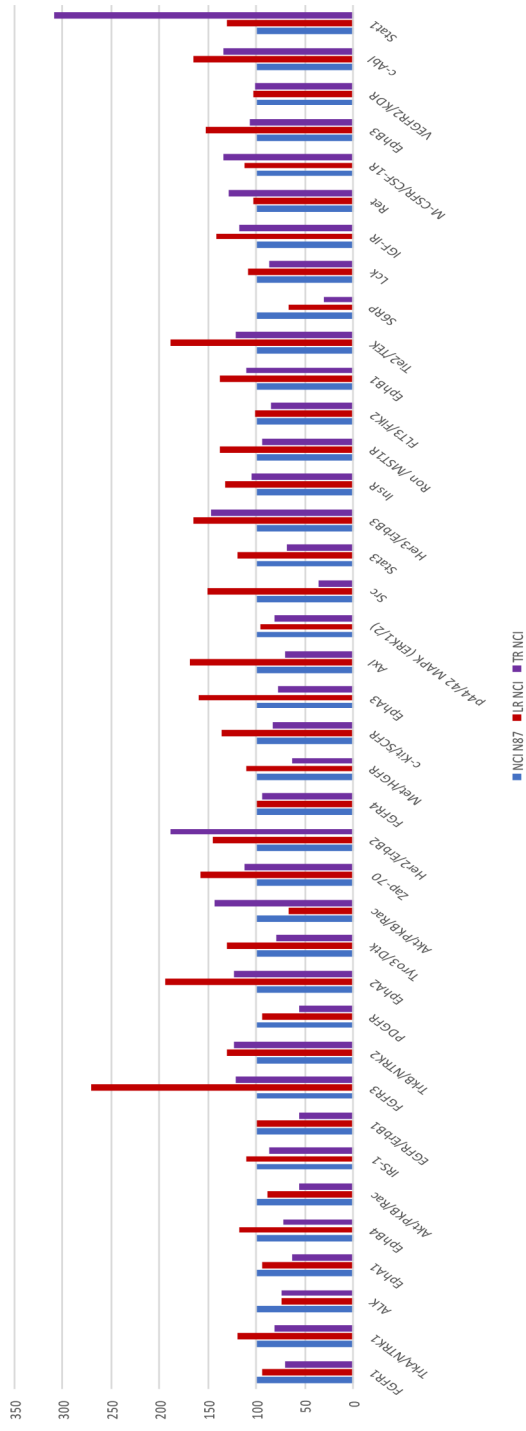

Figure 7. Quantification of the phosphorylated protein from the PathScan ELISA of the NCI N87 parental cell line and TR NCI, Trastuzumab resistant clone, and LR NCI lapatinib resistant clone.

3.3.3 Mutational Analysis by Sequenom MassArray

To complete the analysis of possible changes occurred due to drug exposure that can justify the presence of a secondary resistance, resistant cells were also studied with Sequenom MassArray to evaluate the possibility of secondary mutations. (**Supplementary material 1**)

It was possible to observe a E746_A750del deletion of EGFR in LR NCI cell line. EGFR T790M mutation was detected among LR1 OE cell line with a low percentage. An AKT3 mutation in the LR2 OE and in the TR NCI was also observed in a low percentage. (**Tab. 2; Fig. 8**)

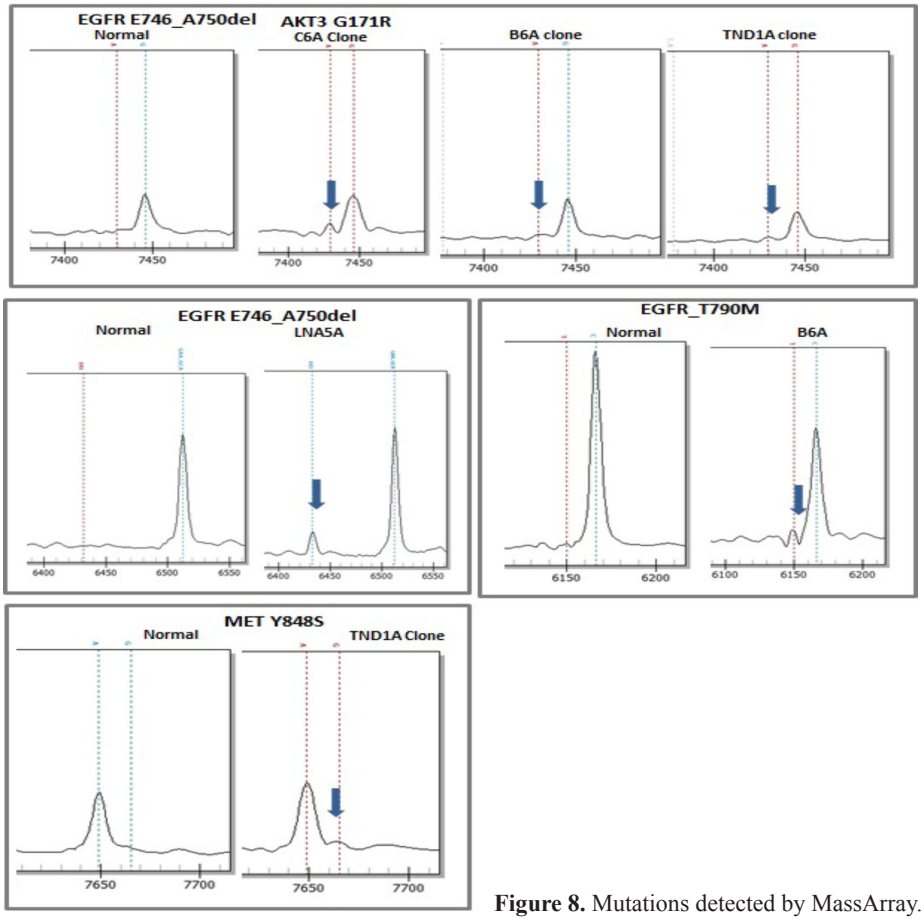

Figure 8. Mutations detected by MassArray.

	Gene	Mutation	WT Fr. (%)	Mut Fr. (%)	Z-score	Confidence
LR1 OE	EGFR	T790M	91,3	8,7	5,526	2.Medium
	AKT3	G171R	88,5	11,5	10	1.High
LR2 OE	AKT3	G171R	90	10	10	1.High
	MET	Y848S	89,8	10,2	5.95	1.High
	KIT	V560del	91,4	8,6	2,414	2.Medium
LR NCI	EGFR	E746_A750del	86,2	13,8	10	2.Medium
TR NCI	AKT3	G171R	88,1	11,9	10	1.High
	MET	Y1248_T3742	90,8	9,2	10	1.High

Table 2. List of mutations observed among derived resistant cells.

3.3.4 Epithelial Mesenchymal transition evaluation

Proteins known to be related with Epithelial Mesenchymal Transition (EMT) as FGFR, STAT 3 and SRC were detected in our resistant models as previously discussed. In our experiment, it was possible to observe that some of our developed cells clearly appear to have mesenchymal phenotype. This phenomenon, associated with the high activation in our models of PI3K/AKT/mTOR signalling pathway, known to have essential role in mediating EMT, lead to the investigation of the EMT. A Wound healing assay, a Western Blot analysis and a RT pPCR were performed to figure out the presence of mesenchymal markers.

The wound healing assay underlines that all resistant cell lines were able to migrate effectively more than the corresponding parental cell lines. (**Fig.9**)

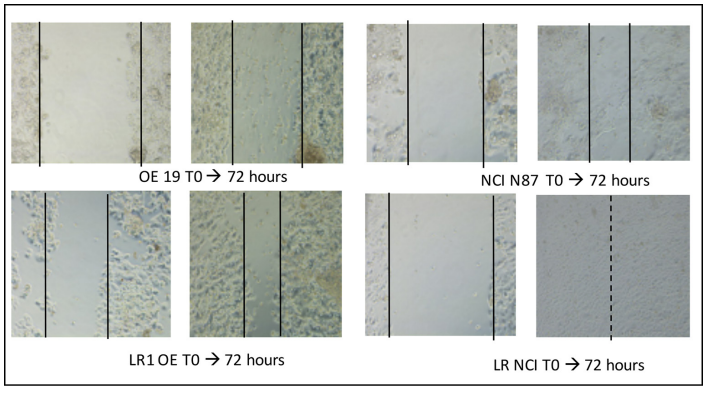

Figure 9. Some example of wound healing migration assay after scratching, confluence at 72 h. Migration of OE 19 versus LR1 OE lapatinib resistant clone; Migration of NCI N87 versus LR NCI, lapatinib resistant clone.

A RT-qPCR analysis was performed to explore if these cell lines were experiencing EMT. E-Cadherine, SNAIL and SLUG (Snail2) were studied. Finally, it was possible to underline a decrease of E-cadherine among resistant cell lines, independently form being resistant to lapatinib or trastuzumab. Snail and Slug were both hyperexpressed suggesting the possible role of the acquired mesenchymal phenotype. (**Fig.10**)

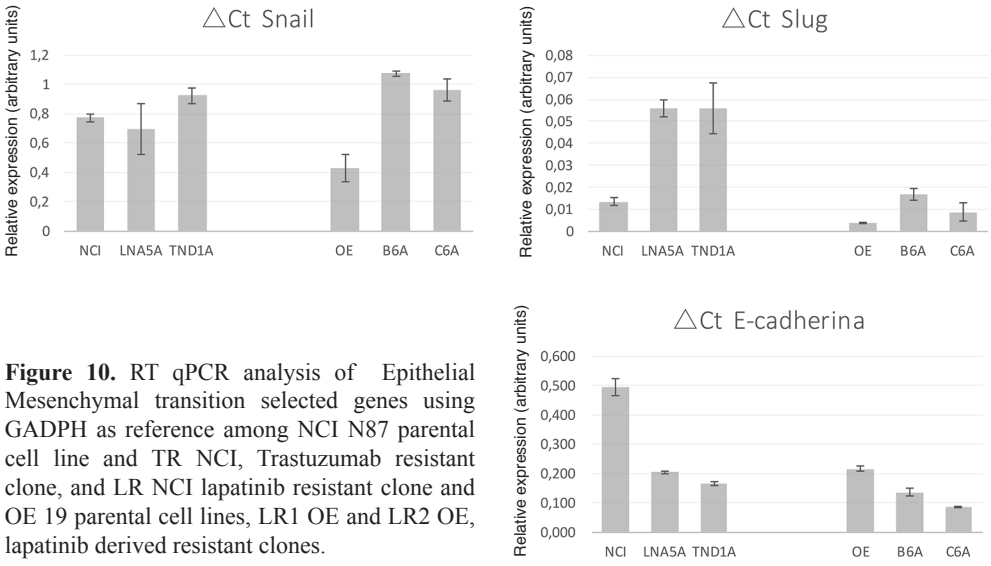

Figure 10. RT qPCR analysis of Epithelial Mesenchymal transition selected genes using GADPH as reference among NCI N87 parental cell line and TR NCI, Trastuzumab resistant clone, and LR NCI lapatinib resistant clone and OE 19 parental cell lines, LR1 OE and LR2 OE, lapatinib derived resistant clones.

By Western Blot it was possible to confirm in trastuzumab resistant model and in OE-lapatinib resistant cells a decrease of the expression of E-Cadherine suggesting the change towards a mesenchymal phenotype. **Fig.11**

Figure 11. Western Blot Analysis showing the expression of E-Cadherin in NCI N87 parental cell line and TR NCI, Trastuzumab resistant clone, and LR NCI lapatinib resistant clone and OE 19 parental cell lines, LR1 OE and LR2 OE, lapatinib derived resistant clones. β Actin is used as loading control.

3.3.5 Evaluation of stem cells characteristics

To evaluate if these cells have some characteristic of stem cells like, an experiment to verify if these cells were able to create oncospheres was conducted, due to the fact that stem cells are more able to create spheres in 3D culture.

In our experiment OE 19, LR1 OE, LR2 OE, NCI N87, LR NCI and TR NCI were all able at the condition previously described in session 2.18, to create spheroidal models. It was possible to develop oncospheres of all cell lines studied. Parental ones and lapatinib resistant clones have such characteristics that lead to this phenomenon, nevertheless, among them it was possible to observe that the trastuzumab resistant cell, had the best capability to produce them. (**Fig.12**)

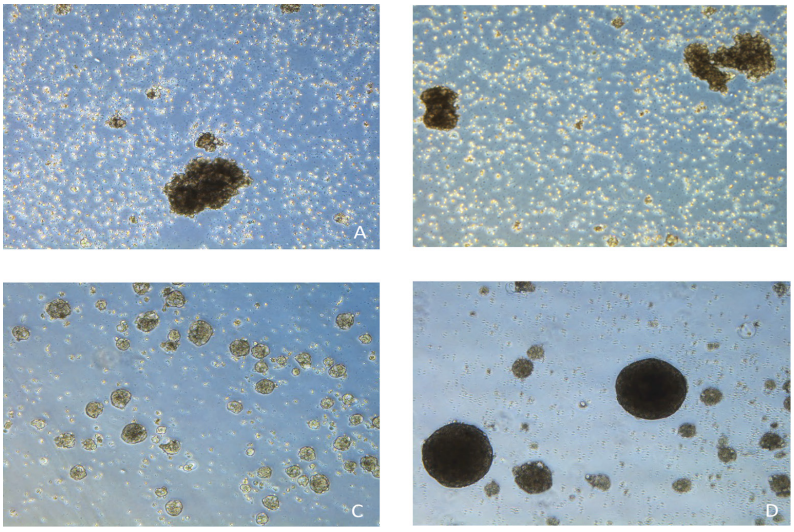

Figure 12. Spheres formation assay 3D. TR NCI acquired high ability to form spheres in suspension culture.

Due to this result, an assay to explore stem cells markers was performed with FACs technology and western blot. As stem cells markers, CD44 and Fibronectine were used. Finally, the FACs analysis did not show any relevant differences between resistant cell lines and the parental lines. CD44 was also studied with Wester Blot, but it was no longer possible to detect its expression.

3.3.6 Identification of differentially expressed genes by transcriptome analysis

Transcriptome analysis represents a very relevant advance in the knowledge of many biological processes. In our cells, Genome-wide expression profiles was evaluated by using Clarion S microarray. This analysis was planned to evaluate up to 20,000 well-annotated transcripts to find some specific characteristics leading to the analysis of common or different alterations present in these cell models to better explore possible mechanisms of resistance. OE 19 parental cell line and LR1 OE and LR2 OE were selected to conduct this study.

Data were analysed using Partek Genomics Suite v 6.6 software. Statistically significant mRNA changes between the different cell lines were identified using an analysis of variance model with a probability value (p-value) < 0,05 and with a probability a Fold Discovery rate (FDR)< 0,05. In order to get an overview of the differences in the mRNA expression profiles in resistant and parental cell lines, principal component analysis (PCA) was performed. PCA reduce the complexity of high-dimensional data and simplifies the task of identifying patterns of variability. The samples (three biological replicates of each cell line) are represented by the dots and grouped onto coloured ellipsoids in the three-dimensional plot. Samples that are near in the plot have a large number of variables in common. Similar mRNA expression profiles were observed for the LR1OE and LR2 OE cell lines versus parental cell line as shown by the strong grouping of the dots from each cell line. **Fig.13**

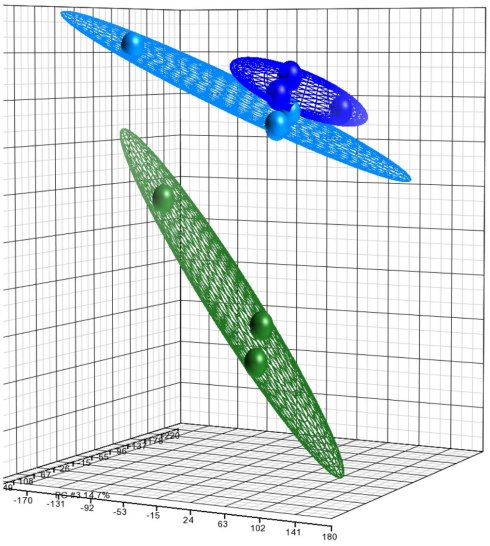

Figure 13. Principal component analysis (PCA) of the mRNAs profiles in parental (OE19) and its derived lapatinib resistant cell lines (LR1OE, LR2OE). The OE19 cell line profile is represented by green dots, LR1 OE cell line is represented by light blue dots and the LR2OE is represented by blue dots. The colored ellipsoids show a different directionality in each cell line based on similarities and differences. The axes correspond to principal components; PC1: x-axis, PC2: y-axis, and PC3: z-axis.

Unsupervised hierarchical clustering revealed again a robust classification between two different groups, showing that the resistant cell lines had different genes expressions compared to the parental cell line. (**Fig.14**)

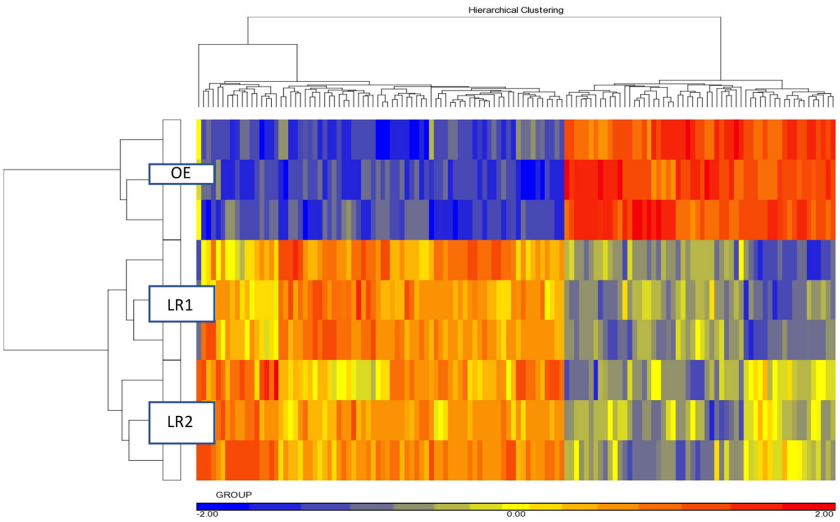

Figure 14. Heat map of the expression profile changes between parental (OE19) and its derived lapatinib resistant cell lines (LR1OE, LR2OE). 132 mRNAs were found to significantly change their expression in resistant clones versus parental line. The expression scale is shown under the heat map. Blue boxes represent low-expression while red boxes represent high-expression.

A Venn diagram showed differentially expressed mRNAs in each resistant cell line versus parental cell line and a comparison of each of the resistant cell lines. Impressively 132 genes were significant differentially expressed among two resistant clones versus parental line (ANOVA, FDR <0.05). Among them, 76 genes were upregulated and 56 were downregulated in the resistant clones. It is also observed that LR2 OE cell line, which is resistant to a major dose of lapatinib (1,5uM) presented a greater number of gene expression changes (476 genes) compared to parental cell line rather than LR1 OE resistant cell line (1uM) (189 genes). (**Fig.15**)

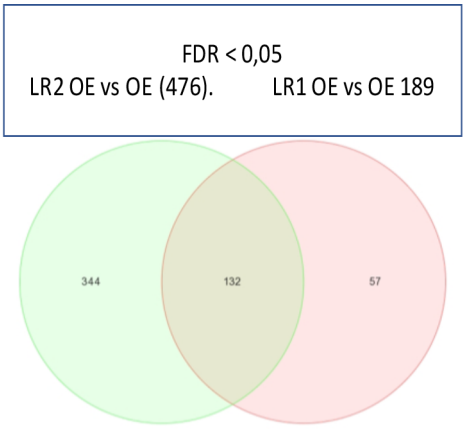

Figure 15. Venn diagram showing overlap of 132 genes differentially expressed among lapatinib resistant cell lines versus parental line (ANOVA, FDR<0,05).

A Functional annotation of the 132 overlapping genes using Pathway Studio v10 (Elsevier) identified an enrichment on the following biological process: metabolic process, response to drug, oxidation-reduction process and positive regulation of cell proliferation. (**Fig.16**)

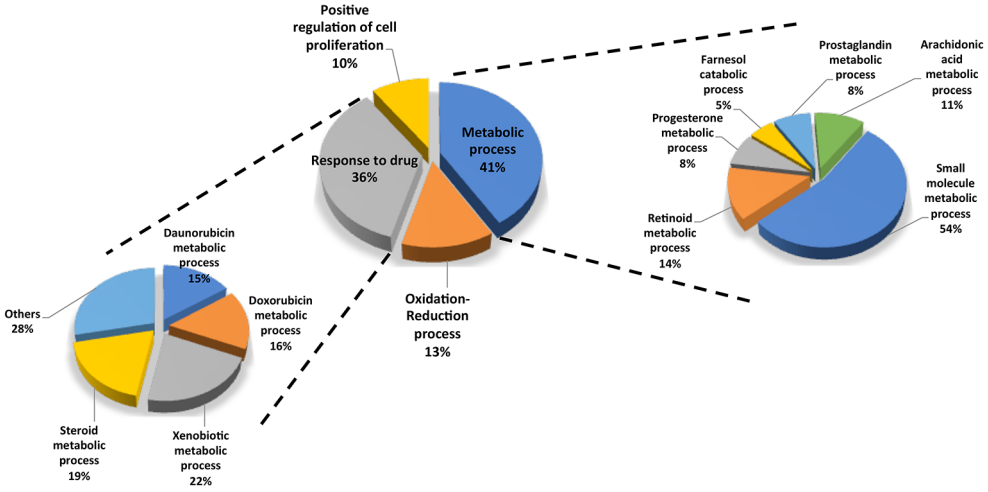

Figure 16. Functional annotation of genes using Pathway Studio database. Pie charts represent the percentage of significantly enriched biological process terms of 132 differentially expressed genes identified in lapatinib resistant cell lines.

A list, according to the folder changes, >2 times, was selected. (**Tab.3** + **Supplementary material 2**) The majority of them are related to cell metabolic function and are described to be implicated in resistance to chemotherapeutics agents conferring a "so called" drug resistant phenotype *in vitro*. Nevertheless, such alterations are no widely explored as mechanisms of resistance to tyrosine kinase inhibitors.

Name	Fold-Change (LR1 OE vs. OE)	Fold-Change (LR1 OE vs. OE) : pvalue		Name+Alias	Fold-Change (LR2 OE vs. OE)	Fold-Change (LR2 OE vs. OE) : pvalue
ABCC2	6,162	9,25E-05		ABCC2	5,1487	1,90E-04
TINAG	5,4589	9,84E-07		TINAG	5,6438	8,47E-07
CES1	5,1294	1,00E-05		m_Ces1e	2,3442	9,36E-04
AK8	4,9183	9,56E-06		AK8	3,8194	3,41E-05
CYP4F11	4,2496	9,82E-07		CYP4F11	3,2946	4,29E-06
r_LOC290704	3,6207	2,46E-07		r_LOC290704	3,7378	2,03E-07
AKR1C2	3,3861	1,16E-06		AKR1C2	3,3516	1,24E-06
LPAR1	2,9378	4,60E-05		LPAR1	4,3666	4,56E-06
ABCC5	2,8104	6,15E-07		ABCC5	2,6213	1,05E-06
GCLM	2,7677	2,33E-06		GCLM	3,0386	1,19E-06
NAT8	2,614	3,35E-04		NAT8	2,7804	2,20E-04
HRASLS2	2,4723	5,53E-06		HRASLS2	2,385	7,50E-06
IL17RE	2,2524	9,36E-06		IL17RE	1,5687	5,93E-04
PTGR1	2,1909	6,08E-07		PTGR1	1,9916	1,65E-06
AKR1C1	2,036	1,74E-07		AKR1C1	2,1113	1,18E-07
AKR1B10	1,9806	1,71E-04		AKR1B10	2,1398	8,12E-05
AKR1C4	1,9478	1,73E-04		AKR1C4	2,5724	1,43E-05
AGPAT9	1,8748	3,06E-05		AGPAT9	2,1868	6,05E-06
ZDHHC1	-1,3453	1,33E-04		ZDHHC1	-2,3621	4,38E-08
ECHDC1	-1,53	5,02E-05		ECHDC1	-2,222	4,43E-07
CDKN1A	-1,5351	3,35E-04		CDKN1A	-2,1468	5,34E-06
GABRR1	-1,5578	2,84E-04		GABRR1	-2,0527	8,99E-06
FAM214A	-1,5953	2,15E-04		FAM214A	-2,2788	3,53E-06
FUT6	-1,6028	2,65E-04		FUT6	-2,2805	4,76E-06
MUC5B	-1,656	8,57E-05		MUC5B	-2,395	1,48E-06
TNFAIP2	-1,8579	1,01E-04		TNFAIP2	-2,2308	1,57E-05
TCEA3	-1,8698	1,66E-04		TCEA3	-5,5026	9,13E-08
CRIP2	-2,0622	6,35E-05		CRIP2	-2,0871	5,65E-05
TMEM154	-2,0757	2,66E-05		TMEM154	-2,2981	1,02E-05
CTPS2	-2,0981	3,53E-06		CTPS2	-2,9318	2,01E-07
CAPN9	-2,1091	9,26E-07		CAPN9	-2,6105	1,32E-07
SIPA1L1	-2,1709	3,06E-04		SIPA1L1	-2,0592	4,88E-04
SEMA3E	-2,5166	5,44E-06		SEMA3E	-4,4035	1,43E-07
IFITM2	-2,6782	6,99E-05		IFITM2	-2,3522	1,88E-04
VSIG2	-2,7035	6,88E-06		VSIG2	-2,1232	5,31E-05
HS6ST2	-2,8055	2,40E-07		HS6ST2	-2,3152	1,18E-06
APBB1IP	-2,9098	1,10E-04		APBB1IP	-8,6301	5,95E-07
FNBP1	-3,3497	2,38E-05		FNBP1	-3,3733	2,28E-05
ABCA12	-3,4371	1,30E-05		ABCA12	-3,438	1,30E-05
ST6GALNAC3	-3,5543	7,46E-05		ST6GALNAC3	-3,764	5,44E-05
AQP5	-4,6357	6,47E-06		AQP5	-5,2803	3,50E-06
PGC	-6,9669	6,95E-05		PGC	-10,9417	1,53E-05
CST1	-8,6422	7,51E-05		CST1	-9,0702	6,42E-05

Table 3. List of gene commonly altered more than 2 fold in LR1 OE and LR2 OE versus parental line.

A validation of some of the selected genes was provided by RT qPCR and finally it was possible to confirm them in the examined cells. Interesting alteration in Caspase-9 and IL-17RE were also detected. Caspase-9 has a critical role in apoptosis and decrease of its expression was demonstrated to have a key role in acquiring resistance model. (58) Another alteration that was observed, was the increase of transcription of IL 17RE and its role in gastric cancer is emerging and not completely defined. (59) **Fig.17**

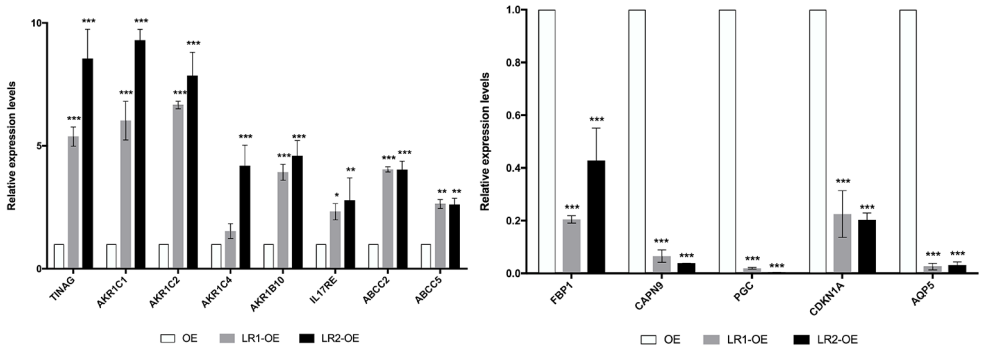

Figure 17. Validation by RT qPCR of results of Transcriptome analysis.
*: p<0,05; **:p<0,01; ***:p<0,001

When studied with details the altered pathways, basing on data already published in the literature, it was possible to identify in our model a large number of genes regulated by NFR2, a master transcriptional regulator that activates genes involved in oxidative stress response, detoxification, and drug resistance (60-63). Previous studies described that, in normal conditions, Keap1 sequesters NRF2 in the cytoplasm, and that translocation of NRF2 into the nucleus is essential for the transactivation of the targeted genes. Therefore it was investigated the level and subcellular localization of NRF2 protein.

3.6.7 Evaluation of NRF2 expression and activation among resistant cell lines

NRF2 expression was evaluated by Wester Blot analysis and it was overexpressed in all lapatinib resistant models. In TR NCI it was possible to observe an increase of the expression of NRF2, while in the LR NCI, a different protein size seen to be induced. (**Fig.18**)

Figure 18. Western Blot evaluation of NRF2 among NCI N87 parental cell line and TR NCI, Trastuzumab resistant cone, and LR NCI lapatinib resistant clone and OE 19 parental cell lines, LR1 OE and LR2 OE, lapatinib derived resistant clones. β Actin is used as loading control

An immunofluorescence assay was performed to evaluate the intracellular localization of NRF2. Finally, it was possible to see an increment of NRF2 protein expressio among both lapatinib and trastuzumab resistant cells and It was also possible to underline a clear nuclear translocation, suggesting a protein activation, in all the resistant models versus the parental lines. Such phenomenon was detected in both trastuzumab and lapatinib resistant cell lines. (**Fig.19**)

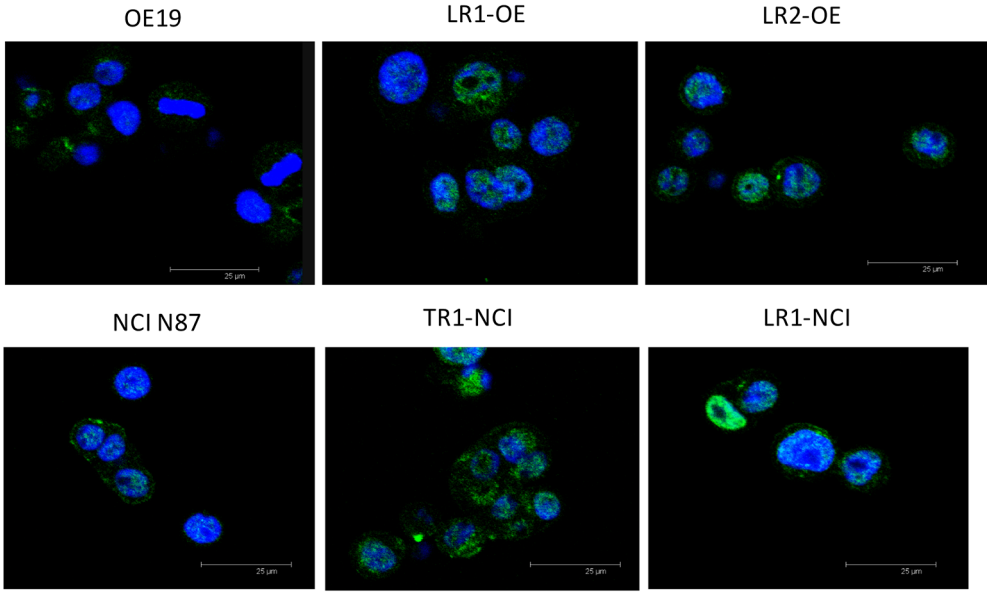

Figure 19. Immunofluorescence staining of NRF2. Cells were fixed and labeled with anti human NRF2 antibody and appropriate FITC- conjugated secondary antibodies. Cells were contrasted with DAPI for visualization of the nuclei. Slides were viewed using confocal microscopy.

Discussion:

To characterise our developed resistant clones, Western Blot analyses were performed. In our experiment, HER2 was detectable in all cell lines, but its expression was slightly less present in both lapatinib resistant models. On the contrary, HER2 activation is increased in trastuzumab resistant line, suggesting a role in the acquired resistant phenotype. This alteration was already described in HER2 positive breast cancer models, where resistance to trastuzumab was associated with an increase of the expression of HER2. (64). In our model, EGFR was widely and homogeneously expressed, especially in TR NCI while its activation was less relevant among lapatinib resistant clones, which, on the contrary, overexpress HER3. Re-activation of EGFR and HER3 have been already described as mechanisms of trastuzumab resistance in HER2-amplified breast cancer cells.

MAPK and PI3K pathways alteration were also investigated. ERK activation, well known to promote cell proliferation, was underlined in all lapatinib resistant cells. The role of PI3K activation, as mechanism of resistance in HER2 amplified both gastric and breast cancer is better defined. In our experiment, AKT expression and activation was increased in the lapatinib resistant clones derived from OE 19 while it was not detectable in the resistant models derived from NCI N87. The study of PI3K was further explored by analysing downstream effectors. RPS6 is a key regulator of 40S ribosome biogenesis, and its phosphorylation is closely related to cell growth capacity. High level of phosphorylated RPS6 and an increased ratio of pRPS6/RPS6 were significantly associated with shortened disease-free survival in patients with esophageal squamous cell carcinoma. (65) In our experiment, RPS6 was observed to be expressed in all cell lines, and its activation was impressively increased among all resistant clones. RPS6 activation can be considered a converging point of possible different causes of resistance. Moreover STAT 3 and SRC were even found to be overexpressed and hyperactivated in our model. In conclusion, despite the evidence of different alteration among our generated cell lines, supporting the hypothesis of the heterogeneity deriving from drug pressure, it is possible to conclude that there are multiple alterations commonly detectable that could justify the lack of response to antiHER2 drugs. In particular, SRC, STAT 3 and RPS6 were identified among those activated proteins.

To study a wider field of alterations, an ELISA assay was performed. In our experiment, RPS6 and SRC were notably altered. It was also possible to observe a relevant increase of many proteins able to induce epithelial mesenchymal transition such as FGFR and Ephrins, that can justify drug resistance. FGFR is a family of four tyrosine kinase receptors that contribute to carcinogenesis by stimulating tumour proliferation, survival, and neoangiogenesis by activating MAPKK and PI3K (66). Recent studies provide evidence for an increasing role or FGFR signalling as a key mediator of resistance to several anticancer therapies (67,68), including the dual HER2 and EGFR inhibitor lapatinib (69). FGFR3 was demonstrated to be overexpressed in

gastric cancer tumour models selected for resistance to trastuzumab. (70). It has been demonstrated that FGFR2 is a pivotal molecule for the survival of lapatinib resistant cells, suggesting that a switch of addiction from the HER2 to the FGFR2 pathway enable cancer cells to become resistant to HER2-targeted therapy (71). The other relevant alteration observed in the RTK analyses, was the increase in expression among resistant cells, of EphA2, EphA3, EphB1, EphB3 belonging to the family of the ephrin proteins. Eph receptors and ephrin ligands play critical roles in various biological functions and tumorigenesis. (72). In our experiment, it was possible to underline again the relevant role of Src, STAT 3 and RPS6 in acquired resistant model even if the activation of RPS6 was not so clear in NCI resistant cells. These data were not confirmed by Western Blot, allowing not to exclude RPS6 from the common mechanisms of developed resistance.

To further investigate molecular characteristics, a mutational analysis performed by Sequenom MassArray was performed. A E746_A750del deletion of EGFR in LR NCI cell line and EGFR T790M mutation was detected among LR1 OE cell line. Such alterations are related to resistance to tyrosine kinase inhibitors in lung cancer but their role in other models is not clear.

An AKT3 mutation in the LR2 OE and in the TR NCI was also observed in a low percentage. The presence of AKT mutation may contribute to PI3K pathway hyperactivation but the percentage of all the described mutation load present in our cells is in the limit of detection so the meaning of such alterations need to be further investigated.

We also studied if acquired resistance could be related to EMT and Stem cells. Migration assay confirmed the capacity of resistant cells to migrate more rather than parental lines. It was also possible to observe that cell lines were able to create sphere models, in particular trastuzumab resistant cells. Loss of E-Cadherine was confirmed among all resistant cells, supporting the hypothesis of a mesenchymal

transition. By RT qPCR it was also possible to detect an increase of Snail and Slug, transcriptional factors, directly related to mesenchymal transformation. Stem cells characteristics were not confirmed when stem cells markers, such as CD44, were tested with FACs or Western Blot.

The evaluation of other alterations responsible for acquired resistance was completed by a transcriptome analysis. For this analysis only one line and its derived lapatinib resistant cells were screened. It was possible to conclude that several genes implicated in metabolic function, oxidation and reduction and drug transporters were highly altered. By doing a deep analysis, we identified NFR2 as a possible convergent point of regulation of several of these processes. NRF2 binds to the antioxidant response element (ARE) in the promoter regions of its target genes to activate their transcription. Although NRF2 is constantly ubiquitinated by Kelch-like ECH-associated protein 1 (Keap1) under normal conditions, it is constantly stabilized in various human cancers and confers a growth advantage on cancer cells by enhancing cytoprotection and anabolism. Cancers with high NRF2 levels are associated with poor prognosis through various mechanisms. Recent reports have revealed that NRF2 promotes metabolic reprogramming of various metabolic pathways to maintain the aggressiveness of cancer progression, suggesting a role even in oesophageal squamous cell carcinoma. NRF2 was described to promote both the pentose phosphate pathway (PPP) and under the sustained activation of PI3K-Akt signalling, and this metabolic shift supported cell proliferation in addition to enhancing cytoprotection (73).

The expression of NRF2 was confirmed among all our resistant cells by Western Blot. Its activation was elegantly studied with immunofluorescence assay that confirm the activation of NRF2, due to its present in the nucleus of resistant models. This finding suggests an important role of this protein in acquired resistance.

3.4 Perform a functional analysis of the alterations identified in acquired resistant models. (Aim 4)

3.4.1 Pharmacological inhibition

To effectively verify the role of SRC, MAPK and PI3K/AKT/mTOR pathways, a pharmacological inhibition using respectively saracatinib, pimasertib, everolimus and GSK 458 was performed. OE 19, LR1 OE, LR2 OE, LR NCI and TR NCI were all tested by MTT analysis to test viability using increasing doses of each single drug, performed as previously described. Saracatinib when used at the concentration of 0,1 μM was not able to decrease viability in a significant manner. When it was used at the concentration of 1μM, an inhibition of cells proliferation was observed, but it was more evident for parental cell lines rather than resistant models. Everolimus when used at 0,1 μM was able to inhibit only the viability of NCI N87 while resistant clones were less sensitive to this drug. Among OE 19 cell line and its derived clones, viability inhibition was less clear. Nevertheless, GSK 458 was clearly able to inhibit viability of all analysed cells, showing a relevant inhibition in all resistant models. Pimasertib was also tested and no efficacy was underlined among NCI N87 cell line and its derived clones. Pimasertib was able to slightly decrease viability of both LR1 OE and LR2 OE, probably due to their hyperactivation of ERK. (**Fig.1,2**)

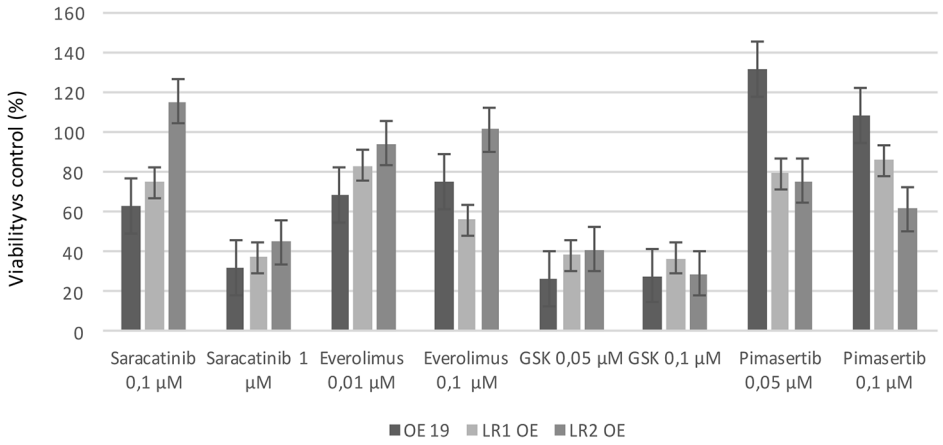

Figure 1. Viability of OE 19 cell line and its resistant clones, LR1 OE and LR2 OE versus control (%) to different doses of saracatinib, everolimus, GSK 458 and pimasertib. Data are shown as means +/- standard error derived from three indipendent experiments.

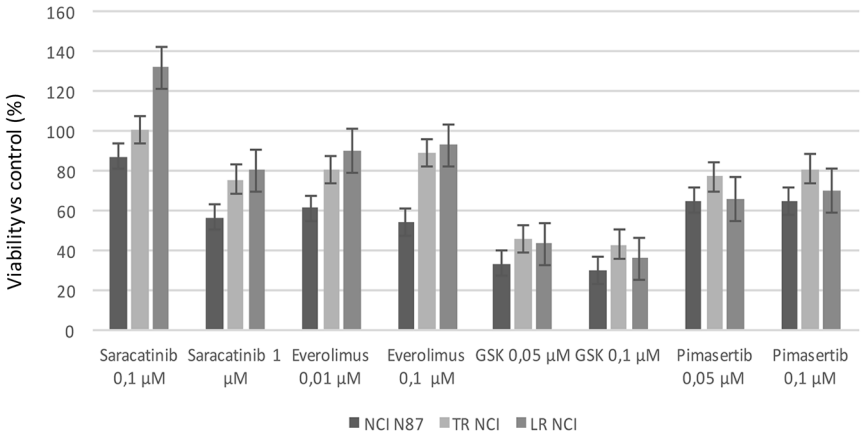

Figure 2. Viability of NCI N87 cell line and its lapatinib resistant clone, LR NCI versus control (%) to different doses of saracatinib, everolimus, GSK 458 and pimasertib. Data are shown as means +/- standard error derived from three indipendent experiments.

3.4.2 RPS6 gene silencing by small interfering RNA transfection

To evaluate specifically the relation of PI3K/AKT/mTOR/RPS6 pathway in cell growth, a silencing of RPS6 was performed by siRNAs, as previously described.

OE 19, LR1 OE, LR2 OE and NCI N87, LR NCI and TR NCI were all studied to evaluate the impact of the knockdown of this protein on their growth. Silencing of RPS6 was verified by RT qPCR.

Silencing RPS6 caused a considerable reduction of the viability of all cell lines tested, indicating a primary role in cell growth and survival. (**Fig.3**)

Knockdown cells were treated with lapatinib in order to check if knocking down RPS6 was able to restore sensitivity to this drug. It was possible to observe that after 72 hours, lapatinib succeeded in inhibiting viability among all cell lines. Among them the less relevant effect was observed for the LR2 OE cell line which a less activation of this protein. (**Fig.4,5**)

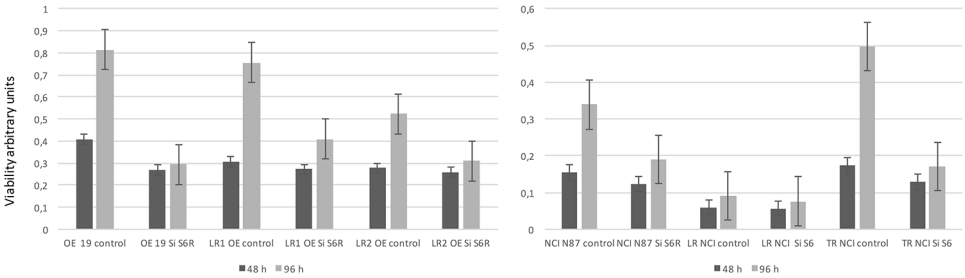

Figure 3. (A) Viability Assay of OE 19 cell line and its resistant clones, LR1 OE and LR2 OE after transient transfection at 48 and 96h with siRNA control (control) or siRNA RPS6 (Si S6R). (B) Viability Assay of NCI N87 cell line and its resistant clones, LR NCI and TR NCI after transient transfection at 48 and 96h with siRNA control (control) or siRNA RPS6 (Si S6R).

Discussion:

Functional tests were performed to verify the meaning of the alteration SRC, MAPK, PI3K pathways in cells with HER2 acquired resistance.

The results of our viability assays show no real benefit from the use of saracatinib, despite the overactivation of SRC observed in all resistant clones. It may be possible that resistance to this drug could derive form the alteration related to drug transporters or metabolic changes as observed in the transcriptome analysis. Nevertheless, a relevant inhibition with a dual PI3K/TORCH1/2 inhibitor in resistant cells, confirms the primary role of PI3K/AKT/mTOR pathway in the development of resistance. The use of a dual inhibitor achieved better results than everolimus suggesting a major activity perhaps for the inhibition of both PI3K and TORC1/2 and the greater specificity of this compound.

When a knockdown of RPS6 expression was performed, it was possible to block the function of this protein in these cells. Importantly knockdown of RPS6 alter growth of all resistant and parental cells. Moreover, it seems to be proportional to the level of expression of this protein in the different cell lines. Moreover, in

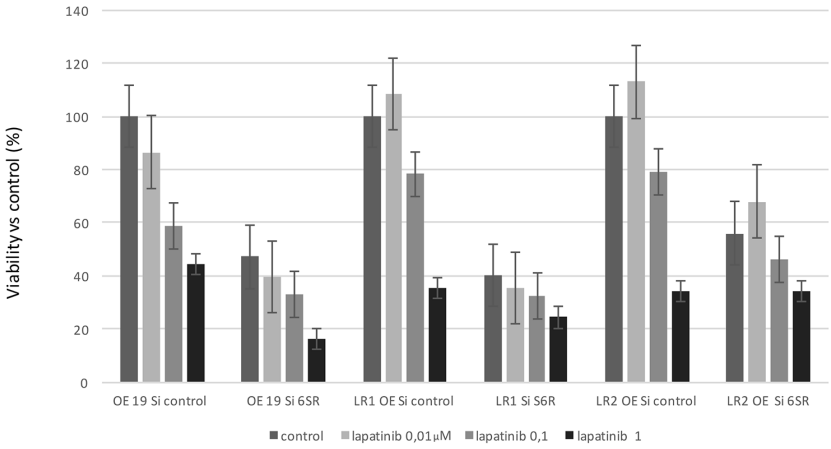

Figure 4. Viability Assay of OE 19 cell line and its resistant clones, LR1 OE and LR2 OE with siRNA control (Si control) or siRNA RPS6 (Si S6R). After 24 h of knockdown cells were treated with increasing doses of lapatinib. Viability was analysed after 72 h.

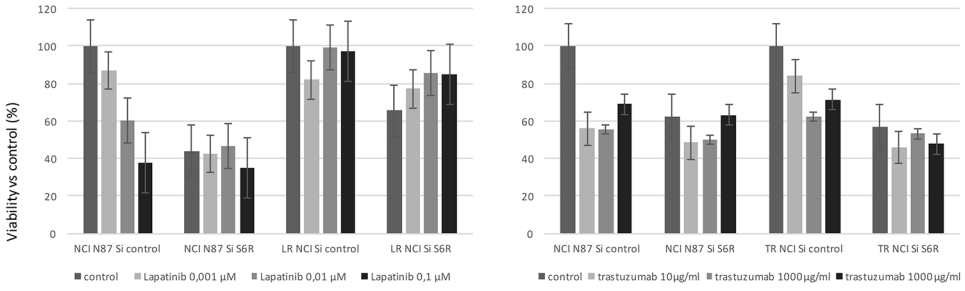

Figure 5. (A) Viability Assay of NCI N87 cell line and its resistant clone, LR NCI with siRNA control (Si control) or siRNA RPS6 (Si S6R). After 24 h of knockdown cells were treated with increasing doses of lapatinib. Viability was analysed after 72 h. (B) (A) Viability Assay of NCI N87 cell line and its resistant clone, TR NCI with siRNA control (Si control) or siRNA RPS6 (Si S6R). After 24 h of knockdown cells were treated with increasing doses of trastuzumab. Viability was analysed after 72 h.

knockdown cells, treatment with lapatinib and trastuzumab was able to reduce viability suggesting a possible role of the combination in restoring sensitivity. RPS6 should be considered a converging point of resistance.

The role of NRF2 in these models should be further investigated to better understand if its inhibition would restore sensitivity to anti HER2 drugs.

3.5 Translation of findings *in vivo* using immunodeficient mice models (Aim 5)

An *in vivo* experiment was conducted to verify if these cells were able to growth in immunodeficient mice SCID (nufl/nufl).

For this experiment, OE 19, LR1 OE, LR2 OE, NCI N-87, LR NCI and TR NCI were all used. Cells were injected in mouse flanks, as previously described, and tumour growth was measured twice a week. When tumour achieved a mean volume of 1cm^3, mice were euthanized according to the ethical procedures previously approved at the University of Valencia. Tumour samples were collected to be analysed. Part of the tumour was frozen directly and part formalin-fixed paraffin-embedded. Plasma deriving from each mouse was even collected. In our experiment, according to tumour growth, it was possible to observe that all cell lines were able to growth in xenografts and that the LR1 OE were characterised from the most rapid growth. (**Fig.1**)

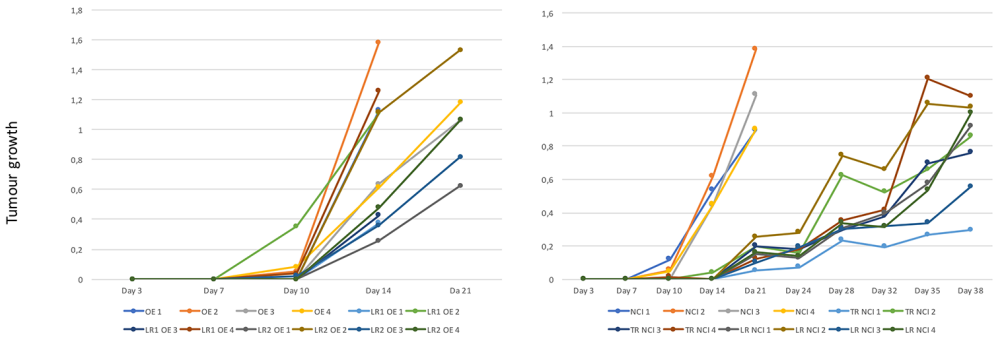

Figure 1. Xenograft models: tumor growth (A) OE 19 and resistant clones. (B) NCI N87 and resistant clones

A new pivotal trial was also conducted *in vivo*. LR1 OE were injected as previously described. On day 4, when tumour was not clinically evaluable, mice were randomly assigned to receive treatment with vector, lapatinib as single agent or lapatinib combined with GSK 458. Despite not being statistically significat due to the number of population, the use of combination of lapatinib and GSK 458 was able to decrease tumour growth. (**Fig.2**)

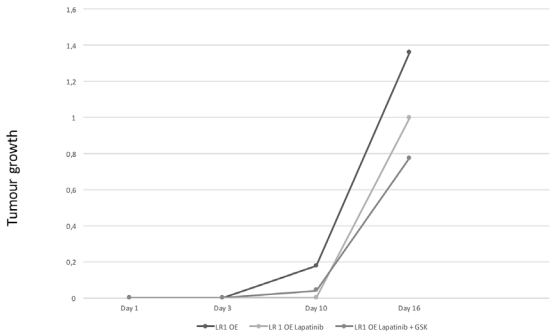

Figure 2. Tumor growth LR1 OE, avarege of tumours.

Immunohistochemistry was performed revealing a reduction of the expression of pRPS6 among the mouse treated with the combination of lapatinib and GSK 458 while no differences in RPS6 expression were observed among all mouse confirming the inhibition of PI3K pathway obtained by using GSK 458. (**Fig.3**)

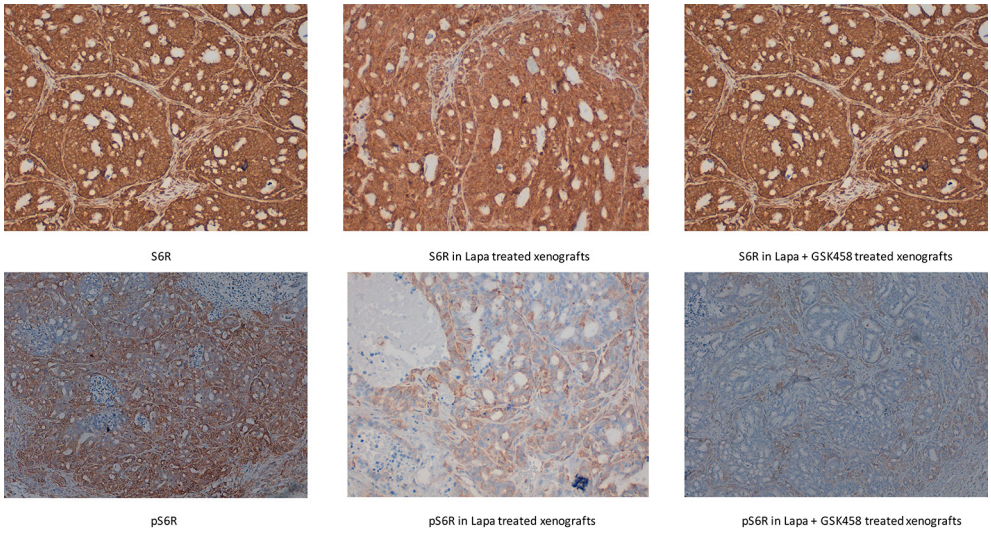

Figure 3. Immunostaining in xenograft tumours. A) RPS6 expression at baseline, post lapatinib treatment and post lapatinib + GSK 458. B) pRPS6 expression at baseline, post lapatinib treatment and post lapatinib + GSK 458.

Discussion:

We were able to induce tumour growth in *in vivo* models. All cells finally formed tumours in SCID mice and their growth was analysed in details When the pivotal trial was started to evaluate the correct dose to use of both lapatinib and GSK 458, it was possible again to demonstrate that all cells injected were able to produce tumour in mice. Treatment was active, and in LR1 OE model was possible to observe a decrease of tumour growth when the combination of lapatinib and GSK 458 was used. This result is only exploratory being no statistically significant due to the limited number of mice. A new experiment with a great population is in need. On tumour samples an IHC of pRPS6 was performed, confirming its inhibition by using GSK 458, that could even justify the decrease of proliferation.

3.6 Validation of the PI3K activation as an escape pathway for trastuzumab resistance in gastric cancer patients. (Aim 6)

To check on the clinical relevance of the previously studied mechanisms of resistance in gastric cancer patients, we retrospectively selected in our database 32 individuals diagnosed with HER2 amplified (IHC 3+) metastatic GC. All patients were diagnosed and treated at the Hospital Clinico of Valencia from 2012 to 2017 and all have received a first line treatment with a platinum based chemotherapy combined with trastuzumab, as a standard of care according to international guidelines.

To verify if the activation of PIK3/AKT/mTOR/RPS6 pathway could be related with less effectivity of trastuzumab treatment, paraffin imbibed samples were studied. An IHC analyses of the downstream effector RPS6 was performed. We screened those previously mentioned patients, with an IHC of pRPS6. Finally, it was possible to evaluate only 18 patients, detecting 1 patient with IHC 1+; 5 patients with IHC 2+ and 12 IHC 3+. For the other patients, the analysis was not possible due to tissue availability. Patient characteristics are list in **table 1**.

Patients Characteristics	
Age	58,5
Gender	M: 11
	F: 7
Primary tumor site	Stomach: 55,5%
	EGJ: 44,45%
Lauren Classification	Intestinal 27,7%
	Diffuse 72,3%
Measurable tumour	100%
Metastatic site	liver 39%
	peritoneal 39%
	>2 sites: 16,6%
HER2 status	IHC 3+ 100%
IHC RPS6	IHC 1 +: 5,5%
	IHC 2+: 27,8%
	IHC 3+ : 66,6%

Table 1. Patients cha-racteristics. Retrospective analysis from dataset.

To evaluate the impact on time to progression to trastuzumab-based treatment, Progression free survival was evaluated only in the population included in the analysis of RPS6 by STATA. Patients were classified as high RPS6 (3+) and low RPS6 (1+ and 2+). In our series it was possible to observe a trend towards a less benefit for patients who expressed a IHC 3 + for RS6K (10.1 versus 5.8, p: 0.24; HR: 0.54). This analysis is not statistically significant due to the low number of patients studied (**Fig.1**)

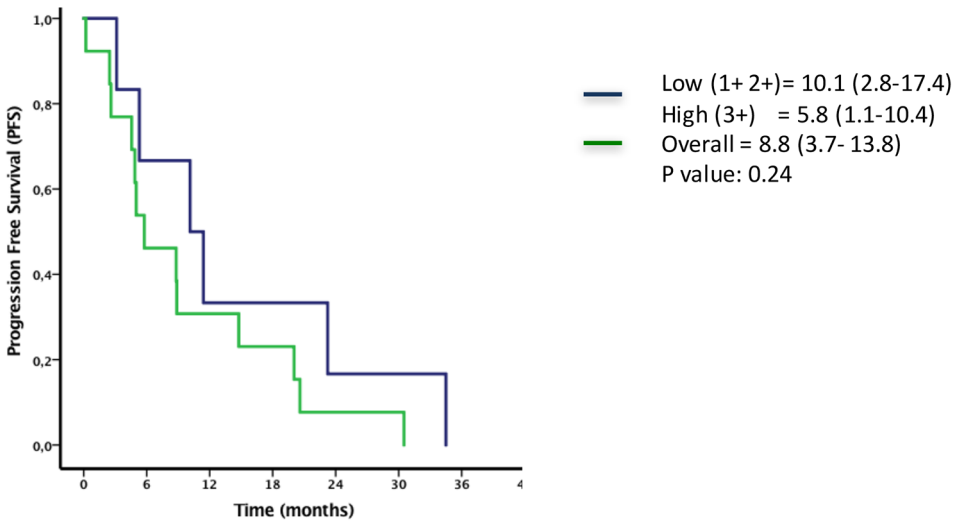

Figure 1. PFS low RPS6 vs high RPS6. All patients were treated with trastuzumab + platinum based chemotherapy.

In one case diagnosed with locally advanced HER2 amplified oesophageal gastric junction carcinoma, pre and post treatment biopsies were studied. This patient, a 75 years old female, was staged as cT3 cN+. A perioperative treatment with platinum based chemotherapy and trastuzumab was started within the INNOVATION trial (NCT02205047) and, after 4 cycles, according to the study protocol, the patient was newly evaluated and a surgical resection was performed. Impressively, no tumour regression was observed in the pathology assessment of the surgical specimen.

We decided to test this patient for pRPS6 and a very strong staining in the IHC both before and post treatment was detected. This may suggest that PI3K was strongly activated in her tumour, having a role in primary resistance to antiHER2 treatment. (**Fig.2**)

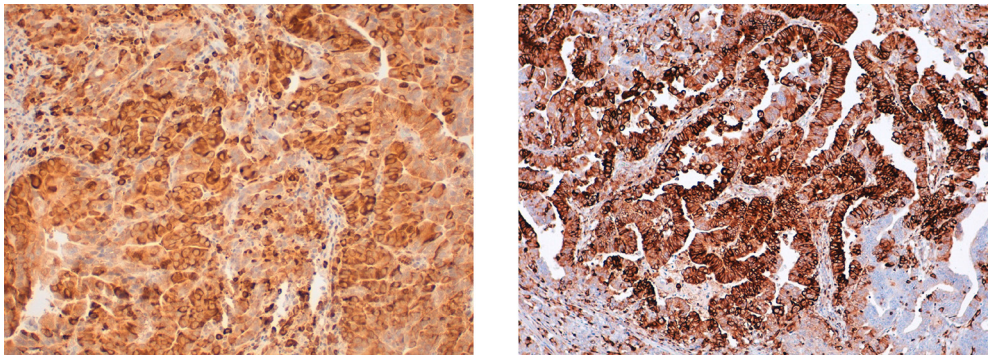

Figure 2. Immunostaining of RPS6 in a patient diagnosed with locally advanced HER2 positive EGJ tumour. Pre and post trastuzumab + platinum based chemotherapy treatment.

Discussion:

In HER2 positive gastric cancer patients the use of trastuzumab in combination with a platinum based chemotherapy is able to improve overall survival and response rate. Differently from what we can observe in HER2 positive breast cancer, the rate of primary resistance to antiHER2 treatment represents a relevant problem. Many patients experience a progression disease during treatment. Several causes have been proposed to justify the lack of response. The most relevant was the heterogeneity of HER2 expression in gastric tumours causing a serious bias in the selection of patients. Despite this phenomenon, many other molecular changes may be responsible for primary or acquired resistance. Recently, an elegant experiment has been published suggesting the possibility of de novo appearance of mutations of PIK3CA among patients treated with platinum based chemotherapy and trastuzumab, suggesting that the hyperactivation of such pathway causes resistance to treatment (17). In our experiment, we sought to identify the molecular mechanisms responsible for the resistance of gastric cancer to antiHER2 treatment. We demonstrated that

both trastuzumab and lapatinib induce the activation of the PI3K/AKT/mTOR/RPS6 signalling pathway, sustaining, in turn, tumor growth and a more aggressive phenotype. Recent studies have related the activation of PI3K to resistance to antiHER2 drugs in other HER2 positive solid tumors, such as breast cancer.

In our study, we demonstrated that PI3K/AKT/mTOR/RPS6 is hyperactivated in gastric cancer cell models generated in our laboratory. In pre-treatment formaline fixed paraffine imbibed biopsies it was also possible to observe that those patients who presented high grade of expression of RPS6 have a trend towards a worse time to progression to fist line chemotherapy based on a combination of platinum based chemotherapy and trastuzumab. Most importantly, we confirmed our finding by demonstrating the overexpression of pRPS6 in paired pre and post-treatment samples from a patient diagnosed with a locally advanced carcinoma of the esophagogastric junction who did not experience any downstaging from the combination of trastuzumab with platinum based chemotherapy.

This study, however, had some limitations. The xenograft tumor models used are limited and could not reproduce the histopathologic features of the human disease, thus, impairing the representativeness of the results observed in patients. The limited number of patient samples available and the potential heterogeneity in the primary tumour do represent additional limitations of this study.

CONCLUSIONS

Conclusions

1. PI3K/AKT/mTOR pathway activation is responsible for primary resistance to antiHER2 drugs in HER2 positive gastric cancer cells.

2. Four different models of acquired resistance were developed and characterised: LR1 OE19, LR2 OE 19 and LR NCI made resistant to lapatinib and TR NCI with resistance to trastuzumab.

3. PI3K/AKT/mTOR/RPS6 pathway, Ephitelial Mesenchymal Transition and NRF2 were identified as relevant component in acquired resistance to antiHER2 inhibition in our developed models.

4. Silencing PI3K downstream effectors, such RPS6, with both specific drug inhibitors or siRNAs restores sensitivity to anti HER2 inhibition in our acquired lapatinib and trastuzumab resistant models.

5. Both cell lines and developed clones could be established in SCID xenografts models showing consistent growth. Treatment with a PI3K/mTORC1/2 inhibitor blocked this pathway through the reduction of pRPS6 *in vivo*.

6. Patients with high Immuno-histochemical expression of pRPS6, may have a short progression free survival, suggesting that hyperactivation of the PI3K/AKT/mTOR/RPS6 pathway may make antiHER2 treatment less effective.

SUMMARY

Resumen

El cáncer gástrico (CG) cuando se diagnostica en estadio avanzado debe considerarse una enfermedad incurable, con una mediana de supervivencia global (OS) de 12 meses. La identificación de las características moleculares de CG ha llevado al descubrimiento de rutas intracelulares y genes que contribuyen a la carcinogénesis (1). Entre estas alteraciones, la amplificación de HER2, detectable en 7-14% de los casos (2), juega un papel clave en el crecimiento celular, en la supervivencia y en la diferenciación celular (3-4). Un ensayo fase III, demostró el beneficio derivado de añadir trastuzumab, anticuerpo monoclonal que se une de manera selectiva y eficiente al receptor HER2, a quimioterapia basada en platino. En dos estudios fase III, lapatinib, un inhibidor de la actividad tirosina quinasa del dímero HER1-HER2, no demostró un beneficio clínico estadisticamente significativo. A pesar de la identificación de HER2 como biomarcador, la mayoría de los pacientes tratados con trastuzumab desarrollan una resistencia al tratamiento, primaria o secundaria (5).

El presente trabajo se centra en la búsqueda de mecanismos moleculares implicados tanto en la resistencia primaria como en la resistencia adquirida a tratamientos anti HER2 en cáncer gástrico HER2 positivo. Para evaluar los posibles mecanismos de resistencia primaria se ha seleccionado un panel de líneas celulares comerciales que tienen amplificado el gen *HER2* (SNU216, NCI N87 y OE19) y líneas HER2-negativas (AGS, SNU484). Diferentes ensayos de viabilidad han permitido caracterizar la sensibilidad de las líneas HER2-positivas a trastuzumab y lapatinib. La línea NCI N87 destaca por ser la más sensible a los dos fármacos mientras que la línea OE19 es insensible a trastuzumab. SNU216 es insensible a ambos fármacos. Se ha realizado una caracterización molecular de estas líneas, basada en un análisis mutacional por Sequenom y un exhaustivo análisis de expresión de proteínas. Estos estudios han permitido identificar la hiperactivación de las vías de señalización PI3K/AKT/mTOR/RPS6 y MEK/MAPK, de una manera prevalente en las líneas celulares que presentan resistencia a tratamiento anti HER2. Ante las alteraciones observadas

se evaluó la viabilidad de todas las líneas tras el tratamiento con un inhibidor de MEK1/MEK2 (Pimasertib) y un inhibidor dual PI3K/TORC1/C2 (GSK458) solos o en combinación con trastuzumab o lapatinib. La combinación del inhibidor dual GSK 458 con trastuzumab o lapatinib disminuye de forma significativa la viabilidad celular en las líneas HER2 positivas, lo que permite concluir que la activación de PI3K/AKT/mTOR tiene un papel relevante en la resistencia primaria a tratamiento anti HER2.

Para el estudio de los mecanismos moleculares implicados en resistencia secundaria a tratamientos anti HER2 se han generado diferentes modelos de resistencia tanto a trastuzumab como a lapatinib. Para ello se seleccionaron aquellas líneas celulares que presentaban mayor sensibilidad a tratamiento antiHER2 y mayor expresión de HER2, NCI N87 y OE19. Este trabajo ha permitido generar una librería de líneas resistentes a lapatinib (8 derivadas de las OE19 y 5 derivadas de las NCI N87) y 11 líneas resistentes a trastuzumab derivadas de las NCI N87, mediante tratamiento a dosis crecientes durante 4-5 meses. Para estudios posteriores se seleccionaron tres líneas resistentes a lapatinib, dos derivadas de las OE y una derivada de las NCI N87 y una línea resistente a trastuzumab. Para analizar los mecanismos moleculares implicados en la resistencia secundaria se ha realizado una serie de estudios tanto a nivel genómico (sequenom), transcriptómico (microarray de expresión, RT-PCR), como proteómico (ELISA “Pathscan array”, “Western blot”, inmuno fluorescencia) en los modelos seleccionados.

Cuando se comparan las líneas parentales con las líneas resistentes derivadas, se observan cambios llamativos de expresión génica tanto a nivel de proteína como de mRNA, no observándose cambios genómicos relevantes. A nivel proteico se observa, en todos los modelos de resistencia generados, un aumento de SRC, RPS6, y STAT3 en mayor o menor medida. Los estudios funcionales, mediante ensayos de silenciamiento génico y ensayos de viabilidad tras el tratamiento con inhibidores, apuntan que PI3K/AKT/mTOR/RPS6 es una de las vías implicadas en

la resistencia adquirida a tratamiento anti HER2 en estos modelos. Por otro lado, se ha observado un aumento de expresión de diferentes miembros de la familia FGFR y efrinas, proteínas que se ha relacionado con la transición epitelio mesénquima (EMT) y el desarrollo de resistencia adquirida en otros modelos de tumores sólidos. Las líneas resistentes generadas efectivamente migran mas que sus parentales y expresan marcadores EMT. También debe destacarse que la línea resistente a trastuzumab presenta una mayor capacidad de formación de esferas en un cultivo 3D, característica típica de células madre de cáncer (CSCs). El análisis del transcriptoma de las OE19 y sus dos líneas derivadas, resistentes a lapatinib, ha permitido poner de relieve que 132 genes cambian su expresión de manera significativa y común en ambos modelos de resistencia. Mediante la anotación funcional de estos genes se demuestra que los procesos biológicos mas alterados en las líneas resistentes tienen que ver con el metabolismo celular, procesos de oxido-reducción, respuesta a drogas y regulación de la proliferación celular. Muchos de los genes alterados detectados en este trabajo se han asociado a mecanismos de resistencia a quimioterapia en otros modelos pero el papel en resistencia a fármacos anti diana no está tan estudiado. Un análisis detallado de los genes alterados indicó que muchos de estos genes tienen en su promotor secuencias ARE (Antioxidant Response Element), reconocidas por el factor de transcripción NRF2. Este factor induce la expresión de genes que codifican enzimas destoxificantes y antioxidantes y el aumento de su expresión/activación se ha relacionado con quimio resistencia en otros modelos. Análisis por western blot e inmunofluorescencia, demuestran un aumento de expresión y activación (translocación al núcleo) de NRF2 en todos nuestros modelos y por tanto su posible papel en la adquisición de resistencia a tratamientos anti HER2, cuestión que está siendo analizada en el laboratorio.

Por otro lado, se ha puesto a punto el establecimiento de tumores, en ratones inmunodeprimidos, de todas las líneas resistentes generadas y sus parentales. Con el objetivo de realizar análisis funcionales de las alteraciones identificadas *in vitro*, se ha realizado un experimento piloto donde se han optimizado las condiciones para

la inhibición de la vía PI3K/AKT/mTOR en los tumores implantados, observándose una clara disminución de la fosforilación de su efector RPS6 por inmunohistoquímica (IHC). Aunque por el número de ratones no es estadísticamente significativo también se ha observado un reducción del crecimiento tumoral por efecto del tratamiento.

Finalmente, ante la evidente relación de la activación de RPS6 con la resistencia, tanto primaria como adquirida, a tratamientos antiHER2 en líneas celulares, se planteó un ensayo retrospectivo en muestras de pacientes diagnosticados con CG HER2 positivos que habían recibido tratamiento con trastuzumab. Se practicó una IHC de RPS6 fosforilada (pRPS6) y se relacionó con la PFS (Progression Free Survival). Los resultados no alcanzan una significación estadística pero se evidencia una tendencia hacia un menor beneficio clínico en los pacientes tratados con trastuzumab que presentan un aumento de pRPS6. Fue posible además analizar a una paciente que se diagnosticó con un cáncer de unión esófago gástrica HER2 positivo en estadio localmente avanzado que recibió tratamiento basado en platino más trastuzumab como tratamiento perioperatorio. Tras 4 ciclos la paciente se volvió a evaluar y se intervino, siendo finalmente un pT3 pN2 sin evidencia de respuesta a tratamiento neo adyuvante. El análisis de RPS6 en las muestras pre y post cirugía evidenció un nivel alto de pRPS6, confirmando el posible papel de esta proteína en el desarrollo de resistencia. Claramente estos datos son solo exploratorios y necesitan de una confirmación prospectiva.

REFERENCES

References

1. Torre, L. A., Siegel, R. L., Ward, E. M., Global cancer incidence and mortality rates and trends — an update. Cancer Epidemiol. Biomarkers Prev. 25, 16–27 (2016).
2. Colquhoun, A. et al. Global patterns of cardia and non-cardia gastric cancer incidence in 2012. Gut 64, 1881–1888 (2015).
3. Deans, C. et al. Cancer of the gastric cardia is rising in incidence in an Asian population and is associated with adverse outcome. World J. Surg. 35, 617–624 (2011).
4. Akiba, S., Koriyama, C., Herrera Goepfert, R. & Eizuru, Y. Epstein–Barr virus associated gastric carcinoma: epidemiological and clinicopathological features. Cancer Sci. 99, 195–201 (2008).
5. Lordick F, Allum W, Carneiro F Unmet needs and challenges in gastric cancer: the way forward. Cancer Treat Rev. 2014 Jul;40(6):692-700.Epub 2014 Mar 13Review
6. Cervantes A, Roda D, Tarazona N, Current questions for the treatment of advanced gastric cancer. Cancer Treat Rev. 2013 Feb;39(1):60-7
7. Ajani, J. A. et al. Gastric adenocarcinoma. Nat. Rev. Dis. Primers 3, 17036 (2017).
8. Bang, YJ., Van Cutsem, E., Feyereislova, A., et al. Trastuzumab in combination with chemotherapy versus chemotherapy alone for treatment of HER2-positive advanced gastric or gastro-oesophageal junction cancer (ToGA): a phase 3, open-label, randomised controlled trial. Lancet. 376, 687-97 (2010).
9. Wilke, H., Muro, K., Van Cutsem, E., et al. Ramucirumab plus paclitaxel versus placebo plus paclitaxel in patients with previously treated advanced gastric or gastro-oesophageal junction adenocarcinoma (RAINBOW): a double-blind, randomised phase 3 trial. Lancet Oncol. 15, 1224-35 (2014).
10. Lauren, P. The two histological main types of gastric carcinoma: diffuse and so- called intestinal-type carcinoma. Acta Pathol Microbiol Scand. 64, 31-49 (1965).
11. Lauwers, G.Y., Carneiro, F., Graham, D.Y. Classification of Tumours of the Digestive System. IARC. (2010).
12. Deng, N., Goh, L.K., Wang, H., et al. A comprehensive survey of genomic alterations in gastric cancer reveals systematic patterns of molecular exclusivity and co-occurrence among distinct therapeutic targets. Gut. 61, 673-84 (2012).
13. The Cancer Genome Atlas Research N. Comprehensive molecular characterization of gastric adenocarcinoma. Nature. 513, 202-9 (2014).
14. Cristescu, R., Lee, J., Nebozhyn, M., et al. Molecular analysis of gastric cancer identifies subtypes associated with distinct clinical outcomes. Nat Med. 21, 449-56 (2015).
15. Tarazona N, Gambardella V, Huerta M, Personalised Treatment in Gastric Cancer: Myth or Reality?Curr Oncol Rep. 2016 Jul;18(7):41. Review.
16. HER2 Testing and Clinical Decision Making in Gastroesophageal Adenocarcinoma: Guideline From the College of American Pathologists,American Society for Clinical Pathology, and the American Society of Clinical Oncology. JCO Volume 35, Number 4 Feb 1, 2017
17. Pietrantonio, F., Fucà, G., Morano, F., Gloghini, A., Corso, S., Aprile,G., et al. Biomarkers of primary resistance to trastuzumab in HER2-positive metastatic gastric cancer patients: the AMNESIA case-control study. Clin Cancer Res, 2781 (2017).
18. Moasser,M.M.,The oncogene HER2; Its signaling and transforming functions and its role in human cancer pathogenesis. Oncogene. 26, 6469–6487 (2007)
19. Rubin, I., Yarden, Y., The basic biology of HER2. Ann Oncol. 2001;Neve
20. Heiser, L.M., Sadanandam, A., Kuo, W.L., Benz, S.C., Goldstein, T.C., et al. Subtype and pathway specific responses to anticancer compounds in breast cancer. Proceedings of the National Academy of Sciences of the United States of America. 109, 2724–2729 (2012).
21. Utermark, T., Rao, T., Cheng, H., Wang, Q., et al. The p110alpha and p110beta isoforms of PI3K play divergent roles in mammary gland development and tumorigenesis. Genes Dev. 26, 1573–1586 (2012).

22. Rexer, B.N., Arteaga, C.L. Optimal targeting of HER2-PI3K signaling in breast cancer: mechanistic insights and clinical implications. Cancer research. 73, 3817–3820 (2013).
23. Arteaga, C.L., Engelman, J.A. ERBB receptors: from oncogene discovery to basic science to mechanism-based cancertherapeutics. Cancer Cell. 25, 282-303 (2014).
24. Hecht, J.R., Bang, Y.J., Qin, S.K., Chung, H.C., et al. Lapatinib in Combination With Capecitabine Plus Oxaliplatin in Human Epidermal Growth Factor Receptor 2-Positive Advanced or Metastatic Gastric, Esophageal, or Gastroesophageal Adenocarcinoma: TRIO-013/LOGiC--A Randomized Phase III Trial. J Clin Oncol. 34, 443-51 (2016).
25. Tabernero, J., et al. Pertuzumab (P) + trastuzumab (H) + chemotherapy (CT) for HER2-positive metastatic gastric or gastro-oesophageal junction cancer (mGC/GEJC): Final analysis of a Phase III study (JACOB) Annals of Oncology. 28 (suppl_5), v209-v268 (2017).
26. Satoh, T., Xu, R.H., Chung, H.C. Lapatinib plus paclitaxel versus paclitaxel alone in the second-line treatment of HER2-amplified advanced gastric cancer in Asian populations: TyTAN--a randomized, phase III study. J Clin Oncol. 32, 2039-49 (2014).
27. Gatsby Thuss-Patience PC, Shah MA, Ohtsu A Trastuzumab emtansine versus taxane use for previously treated HER2-positive locally advanced or metastatic gastric or gastro-oesophageal junction adenocarcinoma (GATSBY): an international randomised, open-label, adaptive, phase 2/3 study. Lancet Oncol. 2017 May;18(5):640-653
28. Ross, J.S., Wang, K., Sheehan, C.E., Boguniewicz, A.B., Otto, G., Downing, S.R., Sun, J., He, J., Curran, J.A., Ali, S., et al. Relapsed classic E-cadherin (CDH1)-mutated invasive lobular breast cancer shows a high frequency of HER2 (ERBB2) gene mutations. Clin Cancer Res.19, 2668–267 (2013).
29. Matsuoka T, Yashiro M. Recent advances in the HER2 targeted therapy of gastric cancer. World Journal of Clinical Cases : WJCC. 2015;3(1):42-51.
30. Ma J, Lyu H, Huang J, Liu B. Targeting of erbB3 receptor to overcome resistance in cancer treatment. Molecular Cancer. 2014;13:105. doi:10.1186/1476-4598-13-105.)
31. Minuti, G., Cappuzzo, F., Duchnowska, R., Jassem, J., Fabi, A., O'Brien, T., et al. Increased MET and HGF gene copy numbers are associated with trastuzumab failure in HER2-positive metastatic breast cancer. British journal of cancer. 107, 793–799 (2012).
32. Ritter, C.A., Perez-Torres, M., Rinehart, C., Guix, M., Dugger, T., Engelman, J.A., Arteaga, C.L. Human breast cancer cells selected for resistance to trastuzumab in vivo overexpress epidermal growth factor receptor and ErbB ligands and remain dependent on the ErbB receptor network. Clinical cancer research. 13, 4909– 4919 (2007).
33. Wang, S.E., Xiang, B., Guix, M., Olivares, M.G., Parker, J., Chung, C.H., Pandiella, A., Arteaga, C.L. Transforming growth factor beta engages TACE and ErbB3 to activate phosphatidylinositol-3 kinase/Akt in ErbB2-overexpressing breast cancer and desensitizes cells to trastuzumab. Mol Cell Biol. 28, 5605-20 (2008).
34. Nahta, R., Yuan, L.X., Du, Y., Esteva, F.J. Lapatinib induces apoptosis in trastuzumab-resistant breast cancer cells: effects on insulin-like growth factor I signaling. Mol Cancer Ther. 6, 667–674 (2007).
35. Zhuang, G., Brantley-Sieders, D.M., Vaught, D., Yu, J., Xie, L., Wells, S., Jackson, D., Muraoka-Cook, R., Arteaga, C., Chen, J. Elevation of receptor tyrosine kinase EphA2 mediates resistance to trastuzumab therapy. Cancer research. 70, 299–308 (2010).
36. Zhang C, Duan X, Xu L, Ye J, Zhao J, Liu Y. Erythropoietin receptor expression and its relationship with trastuzumab response and resistance in HER2-positive breast cancer cells. Breast Cancer Res Treat. 2012 Dec;136(3):739-48
37. Zhang, Z., Lee, J.C., Lin, L., Olivas, V., Au, V., La Framboise, T., Abdel-Rahman, M., Wang, X., Levine, A.D., Rho, J.K. et al. Activation of the AXL kinase causes resistance to EGFR-targeted therapy in lung cancer. Nat Genet. 44, 852–860 (2012).
38. Zuo, Q. et al. Development of trastuzumab-resistant human gastric carcinoma cell lines and mechanisms of drug resistance. Sci. Rep. 5, 11634; doi: 10.1038/srep11634 (2015)

39. Laplante, M. and Sabatini, D. M. mTOR signaling in growth control and disease. Cell 149, 274-293 (2012).
40. Engelman, J.A. Targeting PI3K signalling in cancer: opportunities, challenges and limitations. Nat Rev Cancer. 9, 550–562 (2009).
41. Wang Y, Ding Q, Yen CJ, The crosstalk of mTOR/S6K1 and Hedgehog pathways.Cancer Cell. 2012 Mar 20;21(3):374-87
42. Chakrabarty, A., Rexer, B.N., Wang, S.E., Cook, R.S., Engelman, J.A., Arteaga, C.L. H1047R phosphatidylinositol 3-kinase mutant enhances HER2-mediated transformation by heregulin production and activation of HER3. Oncogene. 29, 5193-203 (2010).
43. Meloche, et al. The ERK1/2 Mitogen-Activated Protein Kinase Pathway as a Master Regulator of the G1- to S-Phase Transition. Oncogene. 26, 3227–3239 (2007).
44. Liang, K., Esteva, F.J., Albarracin, C., Stemke-Hale, K., Lu, Y., Bianchini, G., Yang, C.Y., Li, Y., Li, X., Chen, C.T. et al. Recombinant human erythropoietin antagonizes trastuzumab treatment of breast cancer cells via Jak2-mediated Src activation and PTEN inactivation. Cancer cell. 18, 423-35 (2010).
45. Hong YS, Kim J, Pectasides E, et al. Src Mutation Induces Acquired Lapatinib Resistance in ERBB2-Amplified Human Gastroesophageal Adenocarcinoma Models. Velasco G, ed. PLoS ONE. 2014;9(10):e109440
46. Chung SS, Giehl N, Wu Y, Vadgama JV STAT3 activation in HER2-overexpressing breast cancer promotes epithelial-mesenchymal transition and cancer stem cell traits. Int J Oncol. 2014 Feb;44(2):403-11
47. Shiyu Song, Zhonglan Su, Hui Xu Luteolin selectively kills STAT3 highly activated gastric cancer cells through enhancing the binding of STAT3 to SHP-1 Cell Death & Disease volume 8, page e2612 (2017)
48. Shi-Wei, Y., Zhi-gang, Z., Ying-Xue, H. HIF-1α induces the epithelial-mesenchymal transition in gastric cancer stem cells through the Snail pathway. Oncotarget. 8, 9535–9545 (2017).
49. Lamouille, S., Derynck, R. Cell size and invasion in TGF-beta-induced epithelial to mesenchymal transition is regulated by activation of the mTOR pathway. J Cell Biol. 178, 437–51 (2007).
50. Brabletz, T., Jung, A., Spaderna, S., Hlubek, F., Kirchner, T. Opinion: migrating cancer stem cells - an integrated concept of malignant tumour progression. Nat Rev Cancer. 5, 744–9 (2005).
51. Peinado H, Olmeda D, Cano A (2007). “Snail, Zeb and bHLH factors in tumour progression: an alliance against the epithelial phenotype?”. Nature Reviews Cancer. 7 (6): 415–428.)
52. Wu Y, Zhou BP. Snail: More than EMT.. The epithelial-mesenchymal transition (EMT) regulatory factor SLUG (SNAI2) is a downstream target of SPARC and AKT in promoting melanoma cell invasion Cell Adhesion & Migration. 2010;4(2):199-203; PLoS One. 2012;7(7):e40378
53. Fenouille N1, Tichet M, Dufies M, Pottier A, Mogha A, Soo JK, Rocchi S, Mallavialle A, Galibert MD, Khammari A, Lacour JP, Ballotti R, Deckert M, Tartare-Deckert S. HER2 mediated de novo production of TGFβ leads to SNAIL driven epithelial-to-mesenchymal transition and metastasis of breast cancer
54. Fink MY, Chipuk JE. Survival of HER2-Positive Breast Cancer Cells: Receptor Signaling to Apoptotic Control Centers. Genes & Cancer. 2013;4(5-6):187-195.
55. Chakrabarty, A., Bhola, N.E., Sutton, C., Ghosh, R., Kuba, M.G., Dave, B., Chang, J.C., Arteaga, C.L. Trastuzumab-resistant cells rely on a HER2-PI3K-FoxO-survivin axis and are sensitive to PI3K inhibitors. Cancer research. 73, 1190–1200 (2013).
56. Scaltriti, M., Eichhorn, P.J., Cortes, J., Prudkin, L., Aura, C., Jimenez, J., Chandarlapaty, S., Serra, V., Prat, A., Ibrahim, Y.H., et al. Cyclin E amplification/overexpression is a mechanism of trastuzumab resistance in HER2+ breast cancer patients. Proceedings of the National Academy of Sciences of the United States of America.108, 3761–3766 (2011).
57. Xiaowei Wang, Athanasia Spandidos, Huajun Wang and Brian Seed PrimerBank: a PCR primer database for quantitative gene expression analysis, 2012 update. Nucleic Acid Research

58. Maximilian L.WürstleMaike A.LaussmannMarkusRehm The central role of initiator caspase-9 in apoptosis signal transduction and the regulation of its activation and activity on the apoptosome Experimental Cell Research Volume 318, Issue 11, 1 July 2012, Pages 1213-1220
59. Li TJ, Jiang YM, Hu YF, Huang L, Yu J, Zhao LY, Deng HJ, Mou TY, Liu H, Yang Y, Zhang Q, Li GX. Interleukin-17-Producing Neutrophils Link Inflammatory Stimuli to Disease Progression by Promoting Angiogenesis in Gastric Cancer. Clin Cancer Res. 2017 Mar 15;23(6):1575-1585. doi: 10.1158/1078-0432.CCR-16-0617. Epub 2016 Sep 12
60. Eno MR1, El-Gendy Bel-D2, Cameron MD1.P450 3A-Catalyzed O-Dealkylation of Lapatinib Induces Mitochondrial Stress and Activates Nrf2 hem Res Toxicol. 2016 May 16;29(5):784-96. doi: 10.1021/acs.chemrestox.5b00524. Epub 2016 Apr 8.
61. Mitshishi, Y., Motohashi, H. & Yamamoto, M. The Keap1-Nrf2 system in cancers: stress response and anabolic metabolism. Front Oncol. 2, 200 (2012).
62. Bryan, H. K., Olayanju, A., Goldring, C. E. & Park, B. K. The Nrf2 cell defense pathway: Keap1-dependent and –independent mechanisms of regulation. Biochem Pharmacol. 85, 705–717 (2013).
63. Ma, Q. Role of Nrf2 in oxidative stress and toxicity. Annu Rev Pharmacol Toxicol 53, 401–426 (2013). Niture, S. K., Khatri, R. & Jaiswal, A. K. Regulation of Nrf2-an update. Free Radic Biol Med 66, 36–44 (2014).
64. Valabrega, G., Capellero, S., Cavalloni, G., Zaccarello, G., Petrelli, A., Migliardi, G. et al. HER2-positive breast cancer cells resistant to trastuzumab and lapatinib lose reliance upon HER2 and are sensitive to the multitargeted kinase inhibitor sorafenib. Breast Cancer Res Treat. 130, 29–40 (2011).
65. Kim SH, Jang YH, Chau GC, Pyo S, Um SH. Prognostic significance and function of phosphorylated ribosomal protein S6 in esophageal squamous cell carcinoma.Mod Pathol. 2013 Mar;26(3):327-35. Epub 2012 Sep 21.
66. Yu, C. L., Meyer, D. J., Campbell, G. S., Larner, A. C., Carter-Su, C., Schwartz, J., and Jove, R. Enhanced DNA-binding activity of a Stat3-related protein in cells transformed by the Src oncoprotein. Science. 269, 81– 83 (1995).
67. Peiró, G., Ortiz-Martínez, F., Gallardo, A., Pérez-Balaguer, A. et al. Src, a potential target for overcoming trastuzumab resistance in HER2-positive breast carcinoma British Journal of Cancer. 111, 689–695 (2014).
68. Touat, M., Ileana, E., Postel-Vinay, S., Andre, F., Soria, J.C. Targeting FGFR signaling in cancer. Clin Cancer Res. 21, 2684–94 (2015
69. Oliveras-Ferraros, C., Cufi, S., Queralt, B., Vazquez-Martin, A., Martin-Castillo, B., de Llorens, R. et al. Cross-suppression of EGFR ligands amphiregulin and epiregulin and de-repression of FGFR3 signalling contribute to cetuximab resistance in wild-type KRAS tumour cells. Br J Cancer. 106, 1406–14 (2012).
70. An FGFR3 Autocrine Loop Sustains Acquired Resistance to Trastuzumab in Gastric Cancer Patients Piro G,Carbone C, Cataldo V Clin Cancer Res December 15 2016 (22) (24) 6164-6175;
71. Azuma, K., Tsurutani, J., Sakai, K., Kaneda, H., Fujisaka, Y., Takeda, M. et al. Switching addictions between HER2 and FGFR2 in HER2-positive breast tumor cells: FGFR2 as a potential target for salvage after lapatinib failure. Biochem Biophys Res Commun. 407, 219–24 (2011).
72. Vermeer PD, Colbert PL, Wieking BG, Vermeer DW, Lee JH.Targeting ERBB receptors shifts their partners and triggers persistent ERK signaling through a novel ERBB/EFNB1 complex. Cancer Res. 2013 Sep 15;73(18):5787-97.
73. Mitsuishi Y, Taguchi K, Kawatani Y et al. Nrf2 redirects glucose and glutamine into anabolic pathways in metabolic reprogramming. Cancer Cell 2012; 22: 66–79].

SUPPLEMENTARY MATERIAL

Annex 1

El ensayo de Sequenom realizado en la Fundación Investigación H. U. Clínico Valencia - INCLIVA se basa en la detección puntual de un alelo en los exones "hotSpots" de los oncogenes seleccionados. El test se basa en la extensión alelo específica de un oligo.

Se tienen diseñados tres paneles:

A. El panel de ensayos diseñados por la propia empresa Sequenom-OncocartaV1.0 . Basado en el análisis de 238 mutaciones en 19 oncogenes.

B. el panel de ensayos diseñados por la Dr. Vivancos-H.Vall d'Hebron-CLIAv1.1: Esta basado en el análisis de 136 mutaciones en 13 oncogenes.

C. Panel adicional para los genes ERBB2/3 con 29 mutaciones adicionales. Diseñado en UCIM_U. Epigenetica.

Los tres paneles (A, B,C) analizan un total de 25 genes con un total de 287 mutaciones somáticas (algunas de ellas están repetidas en paneles independientes y sirven de validacion entre ellas). Este estudio no está validado a nivel clínico, y su objetivo es la investigación. El laboratorio de realización del test (U. Análisis de Epigenética- UCIM) ha sido certificado con ISO901.

ABL1	E17K, G173R, K179M, G250E, Q252H, Y253H,E255K/V, D276G, F311L, T315I, F317L,M351T, E355G, F359V, H396R,
AKT1	E17K, G175R, rs11555435(V461L), rs11555431(P388T), rs11555432(L357T), rs12881616(E319G), rs11555433(V767A), rs11555436 (Q43*), rs34409589(E17del),
AKT2	S302G, R371H
AKT3	E17K, G171R
BRAF	K601E/N, G464V/E, G466V/G/E/R, F468C, G469S/E/A/V/R, D594V/G, F595L, G596R, L597S/R/Q/V, L597R_1790TG, T599I, V600A/D/E/G/K/L/M/R, K601N/E
CDK	R24C/H
EGFR	R108K, T263P, A289V, G598V, E709K/H, E709A/G/V, G719S/C/A, M766_A767insAI, S768I, V769_D770insASV, V769_D770insCV, E746_T751del, I insD770_N771>AGG/V769_D770insASV/V769_D770insASV, D770_N771insG, N771_P772>SVDNR, P772_H773insV, H773>NPY, H773_V774insNPH/H773_V774insPH/H773_V774insH, V774_C775insHV, T790 M, L858R, L861Q, L747_T750del, P ins/E746_A750del, T751A, -E746_T751del, I ins/S752_I759del, L747_E749del, A750P, E746_A750del, L747_E749del, A750P, L747_S752del, P753S, E746_T751del/V ins, L747_S752del/Q ins, E746_T751del, S752D/SNP C2255T, D770_N771>AGG/V769_D770insASV/V769_D770insASV, D770_N771insG, L747_T750del/P ins, E746_A750del, L747_T751del, E746_A750del/ V ins, S752_I759del, L858M
ERBB2	G309A, S310Y,H470Q, R678Q, L755P, I767M, M774_A775insYVMA, A775_G776insYVMA, G776S/G776LC, G776VC, G776VC/G776VC, P780_Y781insGSP, S779_P780insVGS, V842I
ERBB3	M91*, F94L,V104L/M/*,P262S/H , G284R, D297Y, E332*,T355I/A, A378P, Y464C, V528F,R667L, L783V, L792V, Q809R, S846I,E928G,T1169P, E1261A
FGFR1	S125L, P252T
FGFR3	R248C, S249C, G370C, Y373C, A391E, K650Q/E/T/M
FLT3	I836del, D835H/Y
GNAQ	Q209H/L/P/R/Y
GNAS	Q227L/R, R201H
IDH1	R132C/G/H/L/S/V
IDH2	R172G/K/M/S/W
HRAS	G12V/D, G13C/R/S/V/D, Q61H/L/R/P/K
JAK2	V617F
KIT	D52N, Y503_F504insAY, K550_K558del,M552L, W557R/W557R/W557G, V559D/V559A/V559G/I, K558_V560del, V560D/V560G, Y568D, D579del,F584S, P585P, K642E, D816V/H/Y, V825A, E839K, P551_V555del, Y553_Q556del, Y553_Q556del
KRAS	G12V/A/D/C/S/R/F, G13C/S/V/D, A59T, Q61E/K/L/R/P/H, A146T/P/V
MET	N375S, N848S, R970C, R988C, T992I, T1010I, H1112L/R/Y, H1124D, Y1230C, Y1235D, Y1248C/H, M1250T,M Y1253D, M1268T
NRAS	G12R/S/C/V/A/D/P/N/Y, G13R/S/C/V/A/D/N/Y, Q61E/H/K/L/P/R , A18T,
PDGFRA	V561D, T674I, F808L, D846Y, N870S, D1071N, D842_H845del, I843_D846del, S566_E571>K, I843_S847>T, D842V
PIK3CA	R38H, Q60K, R88Q,E110K, N345K, S405F, E418K,C420R, P539R, E542K/Q/V/G, E453K, E545A/D/G/K/Q/V, Q546E/H/K/L/P/R, H701P, C901F, F909L, Y1021C/H/H, T1025A/S, M1043I/V,A1046V, H1047R/L/Y, G1049R/S,
RET	C634R/W/Y, E632_L633del, M918T, A664D

LEYENDA CODIGO COLOR:

NEGRO	PANEL ONCOCARTA
AZUL	CLIAV1.1
VERDE	EXTENDED-HOUSE: * CLIAv1(1) - ANA VIVANCOS - REDISEÑADOS
ROJO	REPETIDAS, VALIDACIÓN EN DOS PANELES INDEPENDIENTES (ONCOCARTA - CLIAV1.1)

Annex 2

Listado de 132 genes que varían en las dos líneas resistentes vs línea parental con un FDR (Fold Discovery rate) <0,05

Gene Symbol	RefSeq Transcript ID	Fold change (B6A vs. OE)	Fold change (C6A vs. OE)	Gene Symbol	RefSeq Transcript ID	Fold change (B6A vs. OE)	Fold change (C6A vs. OE)
SEZ6	hsa_circ_0000748	1,6	1,4	ATP2A3	NM_005173	-1,4	-1,4
CYP2B6	NM_000767	1,8	-1,5	VSIG2	NM_014312	-2,7	-2,1
CTPS2	NM_001144002	-2,1	-2,9	TMEM154	NM_152680	-2,1	-2,3
TCEA3	NM_003196	-1,9	-5,5	C7orf55-LUC7L2	NM_001244584	1,2	1,3
GCOM1	NM_001018090	-1,7	-1,9	SHOC2	NM_001269039	-1,4	-1,5
OLFM1	NM_001282611	1,9	1,5	CDKN1A	NM_000389	-1,5	-2,1
SEMA3E	NM_001178129	-2,5	-4,4	PRPF4	NM_001244926	1,3	1,4
HMGA1	NM_002131	1,3	1,3	STOML2	NM_001287031	1,3	1,3
ZDHHC1	NM_013304	-1,3	-2,4	ARHGAP33	NM_001172630	-1,2	-1,2
GABRR1	NM_001256703	-1,6	-2,1	AKR1C4	NM_001818	1,9	2,6
HS6ST2	NM_001077188	-2,8	-2,3	ACTR3B	NM_001040135	1,6	1,5
AKR1C1	NM_001353	2,0	2,1	MBD4	NM_001276270	1,2	1,2
PALLD	NM_001166108	3,6	3,7	ZAK	NM_016653	1,6	1,7
EPHX1	NM_000120	1,9	1,9	C20orf24	NM_001199534	1,3	1,2
CAPN9	NM_006615	-2,1	-2,6	IL17RE	NM_001193380	2,3	1,6
SIDT1	NM_001308350	-1,5	-1,8	CES1	NM_001025195	5,1	2,3
CYP4F3	NM_000896	1,8	1,6	LYAR	NM_001145725	1,4	1,4
SYTL2	NM_001162951	-1,4	-1,4	VSIG10L	NM_001163922	1,7	2,1
TXNRD1	NM_001093771	1,3	1,4	RPS27	NM_001030	-1,1	-1,1
APBB1IP	NM_019043	-2,9	-8,6	ST6GALNAC3	NM_001160011	-3,6	-3,8
ABCC5	NM_001023587	2,8	2,6	ABCB6	NM_005689	1,5	1,4
AKR1C2	NM_001135241	3,4	3,4	GRM8	NM_000845	-1,2	-1,2
TINAG	NM_014464	5,5	5,6	TNFAIP2	NM_006291	-1,9	-2,2
FOXN2	NM_002158	1,5	1,3	CCDC25	NM_001304529	1,2	1,3
PTGR1	NM_001146108	2,2	2,0	FGFR1OP	NM_001278690	1,4	1,3
ECHDC1	NM_001002030	-1,5	-2,2	MBOAT7	NM_024298	1,3	1,2
LPAR1	NM_001401	2,9	4,4	GSR	NM_000637	1,5	1,6
FBP1	NM_000507	-3,3	-3,4	CUTC	NM_015960	1,5	1,7
HSPA1A	NM_005345	1,5	1,5	CPA6	NM_020361	-1,3	-1,3
CYP4F11	NM_001128932	4,2	3,3	AGRN	NM_001305275	-1,3	-1,3
GCLM	NM_001308253	2,8	3,0	PRKCZ	NM_001033581	-1,4	-1,4
CREB3L1	NM_052854	-1,5	-1,9	CST1	NM_001898	-8,6	-9,1
RNASET2	NM_003730	-1,6	-1,6	PPAT	NM_002703	1,4	1,5
CYP4F2	NM_001082	1,9	1,7	CRIP2	NM_001270837	-2,1	-2,1
C7orf73	NM_001130929	1,2	1,3	PFKFB3	NM_001145443	1,3	1,4
MUC5B	NM_002458	-1,7	-2,4	CCDC84	ENST00000628294	1,6	1,7
ANXA1	NM_000700	1,7	1,7	PM20D2	NM_001010853	1,4	1,3
SRSF10	NM_001191005	1,2	1,1	EXOSC2	NM_001282708	1,5	1,7
PIGT	NM_001184728	-1,2	-1,2	LIMCH1	NM_001112717	-1,8	-2,0
LYPD6B	NM_177964	1,6	1,8	DCAF13	NM_015420	1,3	1,2
AQP5	NM_001651	-4,6	-5,3	OSBPL5	NM_001144063	-1,5	-1,5
UGDH	NM_001184700	1,7	1,9	DSCR3	NM_006052	1,4	1,3
TAAR3	NR_028511	1,3	1,7	CNGB3	NM_019098	-1,3	-1,3
HRASLS2	NM_017878	2,5	2,4	SMN1	OTTHUMT00000216805	1,4	1,4
PGC	NM_001166424	-7,0	-10,9	TMEM92	NM_001168215	1,8	1,7
RPL7A	ENST00000625669	1,4	1,5	ABCC2	NM_000392	6,2	5,1
REG1A	NM_002909	-1,7	-1,6	SGSM3	NM_001301849	-1,5	-1,3
NQO2	NM_000904	1,5	1,8	AKR1C3	NM_001253908	1,5	1,5
MEIS2	NM_001220482	-1,4	-1,6	IFITM2	NM_006435	-2,7	-2,4
DLG1	NM_001098424	1,1	1,1	ZCCHC17	NM_001282566	1,3	1,3
NPDC1	NM_015392	-1,4	-1,5	AKR1B10	NM_020299	2,0	2,1
FUT6	NM_000150	-1,6	-2,3	C21orf91	NM_001100420	1,8	1,9
GPAT3	NM_001256421	1,9	2,2	NUDT21	NM_007006	1,2	1,2
ARHGAP32	NM_001142685	-1,5	-1,5	SNX24	NM_014035	-1,7	-1,6
TRIM44	NM_017583	-1,7	-1,8	AKR1B15	NM_001080538	1,7	1,8
RPL41P2	OTTHUMT00000476227	-1,2	-1,1	TALDO1	NM_006755	1,7	1,5
FAM214A	NM_001286495	-1,6	-2,3	ZFR2	NM_001145640	-1,2	-1,1
THRAP3	hsa_circ_0004157	1,7	1,4	NUP35	NM_001287584	1,4	1,4
LGALS3	NM_001177388	-1,4	-1,9	TSEN34	NM_001282332	1,3	1,2
ABCA12	NM_015657	-3,4	-3,4	PGBD4	NM_152595	1,5	1,3
SCFD2	NM_152540	1,5	1,5	GLA	NM_000169	2,6	2,8
FOPNL	NM_001304497	1,4	1,4	SIPA1L1	NM_001284245	-2,2	-2,1
FBL	ENST00000629471	1,5	1,6	LDLRAP1	NM_015627	-1,4	-1,4
TMEM17	NM_198276	1,7	1,5	TP53AIP1	NM_001195194	-1,2	-1,2
AK8	NM_152572	4,9	3,8	FOSL1	NM_001300844	1,6	1,5
F5	NM_000130	-1,6	-1,9	SGPP1	NM_030791	-1,5	-1,5